AUTOTAXIN

BIOCHEMICAL AND FUNCTIONAL STUDIES

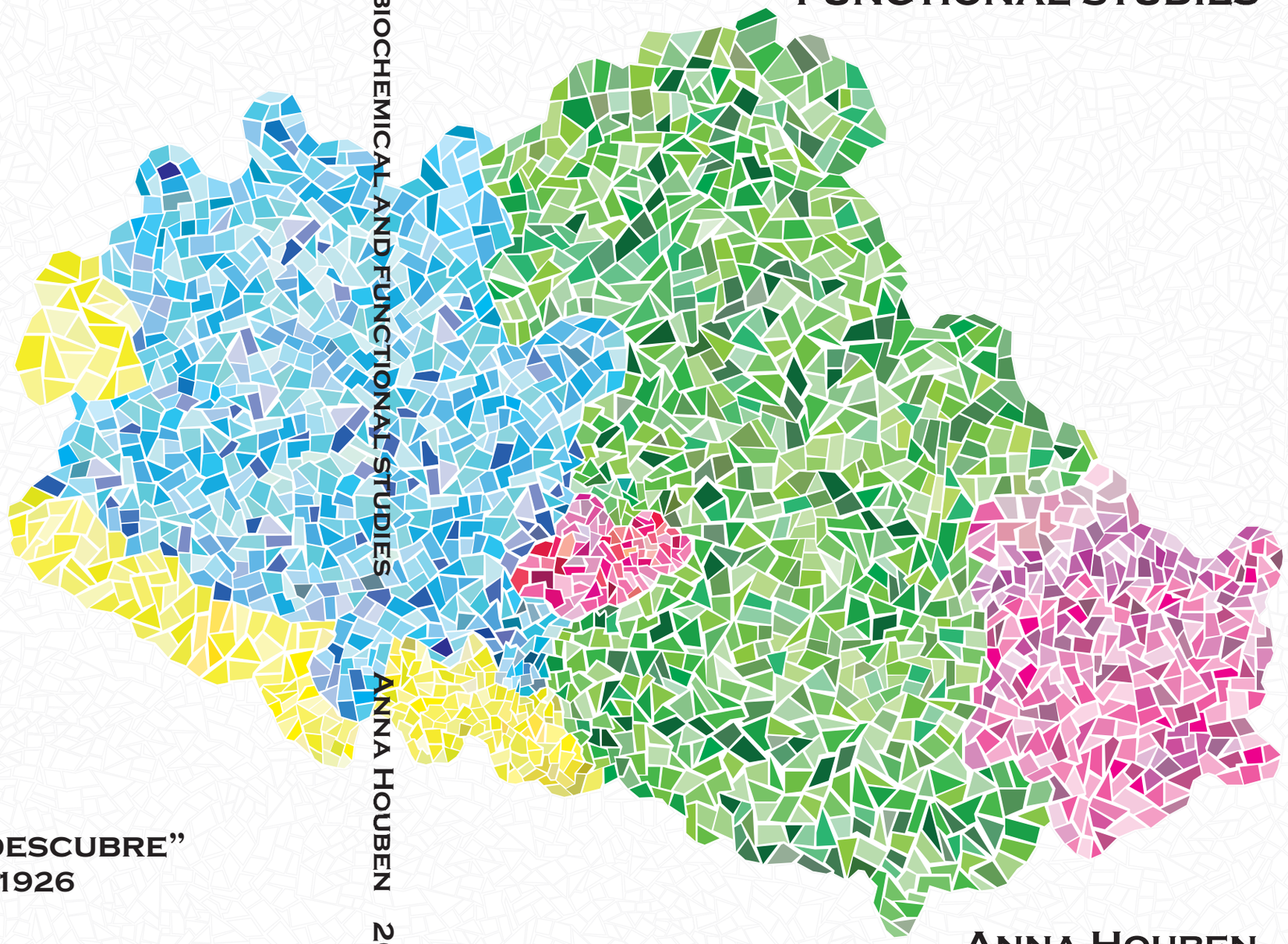

AUTOTAXIN BIOCHEMICAL AND FUNCTIONAL STUDIES ANNA HOUBEN 2012

"EL HOMBRE NO CREA: DESCUBRE"
ANTONI GAUDÍ 1852-1926

ANNA HOUBEN

AUTOTAXIN, BIOCHEMICAL AND FUNCTIONAL STUDIES

Anna Jacoba Sara Houben

ISBN: 978-94-6203-051-0

Front cover: Autotaxin Mosaic
Back cover: Quote of Antoni Gaudí
Picture design by Maikel Jongsma
Cover design by Anna J.S. Houben

Layout by Geert J. van Tetering and Anna J.S. Houben
Printed by Wöhrmann Print Service, Zutphen

The research described in this thesis was performed at the Division of Cell Biology I of the Netherlands Cancer Institute, Amsterdam, The Netherlands
Financial support was provided by the Dutch Cancer Society (KWF)

Publication of this thesis was financially supported by the Dutch Cancer Society (KWF) and the Netherlands Cancer Institute

AUTOTAXIN, BIOCHEMICAL AND FUNCTIONAL STUDIES

PROEFSCHRIFT

ter verkrijging van
de graad van Doctor aan de Universiteit Leiden,
op gezag van Rector Magnificus prof.mr. P.F. van der Heijden,
volgens besluit van het College voor Promoties
te verdedigen op dinsdag 25 september 2012
klokke 16.15 uur

door

Anna Jacoba Sara Houben
geboren te Roermond
in 1982

PROMOTIECOMMISSIE

Promotor:	Prof. Dr. W.H. Moolenaar
Overige leden:	Prof. Dr. J.J. Neefjes
	Prof. Dr. P. Peters *Technische Universiteit Delft*
	Dr. A. Perrakis *Nederlands Kanker Instituut*

CONTENTS

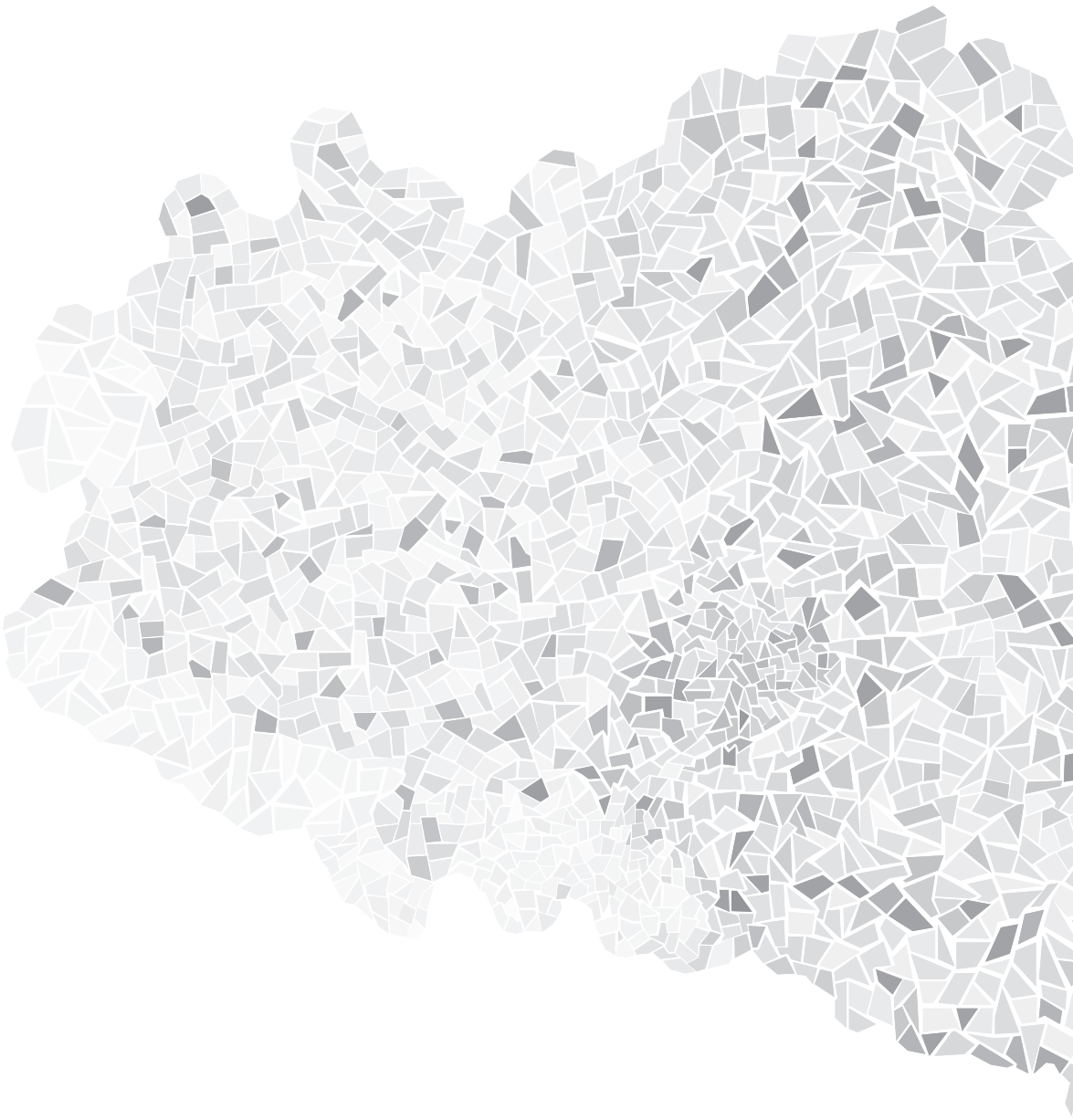

CHAPTER I

General Introduction

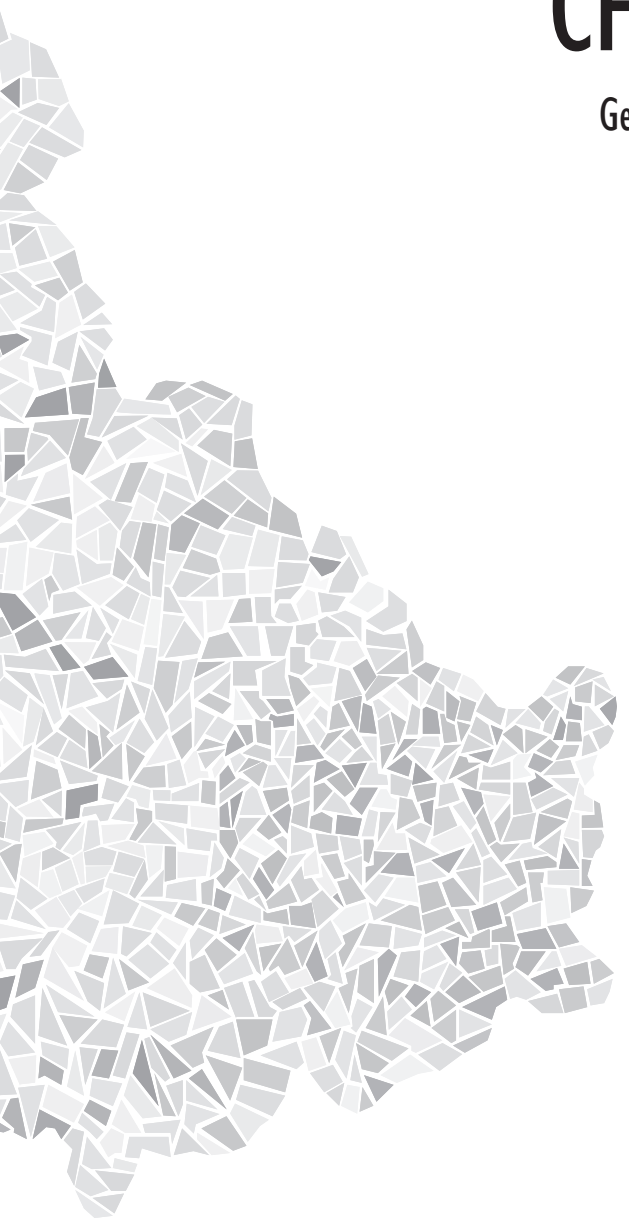

General Introduction

Anna J.S. Houben[1]
and Wouter H. Moolenaar[1]

[1]Division of Cell Biology,
The Netherlands Cancer Institute,
Amsterdam, The Netherlands

PREFACE

Lysophospholipids (LPLs) are lipid messengers that are present in the extracellular environment and play important roles in cell signaling. By binding to specific receptors, the effects of LPLs are translated into specific cellular responses. Lysophosphatidic acid (LPA) and sphingosine-1-phosphate (S1P) are LPLs that regulate a variety of signaling pathways implicated in both health and disease. As a consequence, LPLs, their receptors and the enzymes that generate or degrade them, are attractive drug targets for various diseases.

This thesis focuses on autotaxin (ATX), the main enzyme responsible for the production of LPA. The studies described in this thesis aim at characterizing the biochemical and functional properties of ATX, to advance our understanding of the molecular actions of ATX in (patho) physiology. This chapter introduces LPA production and signaling, elaborates on ATX processing, activity and regulation, and highlights the role of ATX-LPA receptor signaling in development and disease.

LYSOPHOSPHATIDIC ACID

LPA (monoacyl-*sn*-glycero-3-phosphate) is a structurally simple phospholipid, composed of a phosphate headgroup, a glycerol backbone and a fatty acyl chain (Fig. 1A). Originally, LPA was known as an intermediate in intracellular lipid metabolism, and only later recognized as an extracellular bioactive lipid mediator and major active component of serum. LPA has growth factor-like activities and stimulates a wide variety of cellular responses; including cell proliferation, survival, migration, morphological changes, wound healing, cytokine and chemokine secretion, increased endothelial permeability and inhibition of gap-junctional communication (1). More than a decade after the initial discovery of LPA as a bioactive lipid mediator, ATX was found to be identical to plasma lysophospholipase D (lysoPLD), the main enzyme responsible for producing bioactive LPA (2;3).

LPA Production

LPA is present in serum, plasma, saliva, follicular fluid, seminal plasma, mildly oxidized LDL (1) and malignant effusions, such as ascitic fluid from ovarian cancer patients (4;5). LPA is primarily produced in plasma, mainly via lysophospholipase D (lysoPLD) activity by hydrolyzing lysophosphatidylcholine (LPC) (6). LPC is a lysophospholipid composed of a choline head group, a phosphate group, a glycerol backbone and a fatty acyl chain (Fig. 1B). In the extracellular LPA production pathway, phospholipids are first converted to lysophospholipids by phospholipase A_1 (PLA_1) or A_2 (PLA_2) and subsequently these lysophospholipids are hydrolyzed by plasma lysoPLD/ATX to produce LPA (Fig. 1C). Next to this route, LPA can be produced intracellularly as well, via phospholipid hydrolysis by an intracellular PLD and subsequent hydrolysis of the product phosphatidic acid (PA) by PA-selective PLA (Fig. 1D). However, intracellular LPA is thought to be an intermediate for the synthesis of more complex phospholipids and it is unlikely to function as an extracellular mediator (7).

Extracellular Metabolism of LPA

LPA is a mixture of fatty acids that vary in the type of fatty acyl chain (length and saturation) and the linkage to the glycerol backbone (*sn-1* or *sn-2*). LPA species with saturated fatty acids (16:0, 18:0) and unsaturated fatty acids (16:1, 18:1, 18:2, 20:4) have been detected *in vivo* (8). In serum and plasma, LPA is bound to albumin (9). While human plasma LPA levels are low (10;11), serum LPA levels are significantly higher (9;12). For this reason it has been proposed that LPA in serum is produced by platelets as a result of blood coagulation. It is now clear that increased serum LPA levels upon platelet activation are not due to secretion of LPA from platelet granules. Instead, LPA is generated *de novo* by sequential actions of phospholipases. First, lysophospholipids (mainly LPC) are produced by activated platelets via PLAs and subsequently these lysophospholipids are hydrolyzed by ATX to produce LPA (13;14). In addition, LPA can be produced by hydrolysis of either PA, released by platelets, or LPC that is present on erythrocyte membranes. However, these two pathways make minor contributions to LPA production in blood (13).

Steady-state plasma LPC levels (>100 mM) are about 1000-fold higher than the levels of LPA, while ATX is constitutively active (12-14). This suggests a tightly controlled equilibrium between production, degradation and clearance. Indeed, LPA is rapidly degraded by membrane-bound phosphatases, mainly lipid phosphate phosphohydrolase type 1 (15), and ATX is cleared from the circulation within minutes (16). Moreover, the low plasma LPA levels

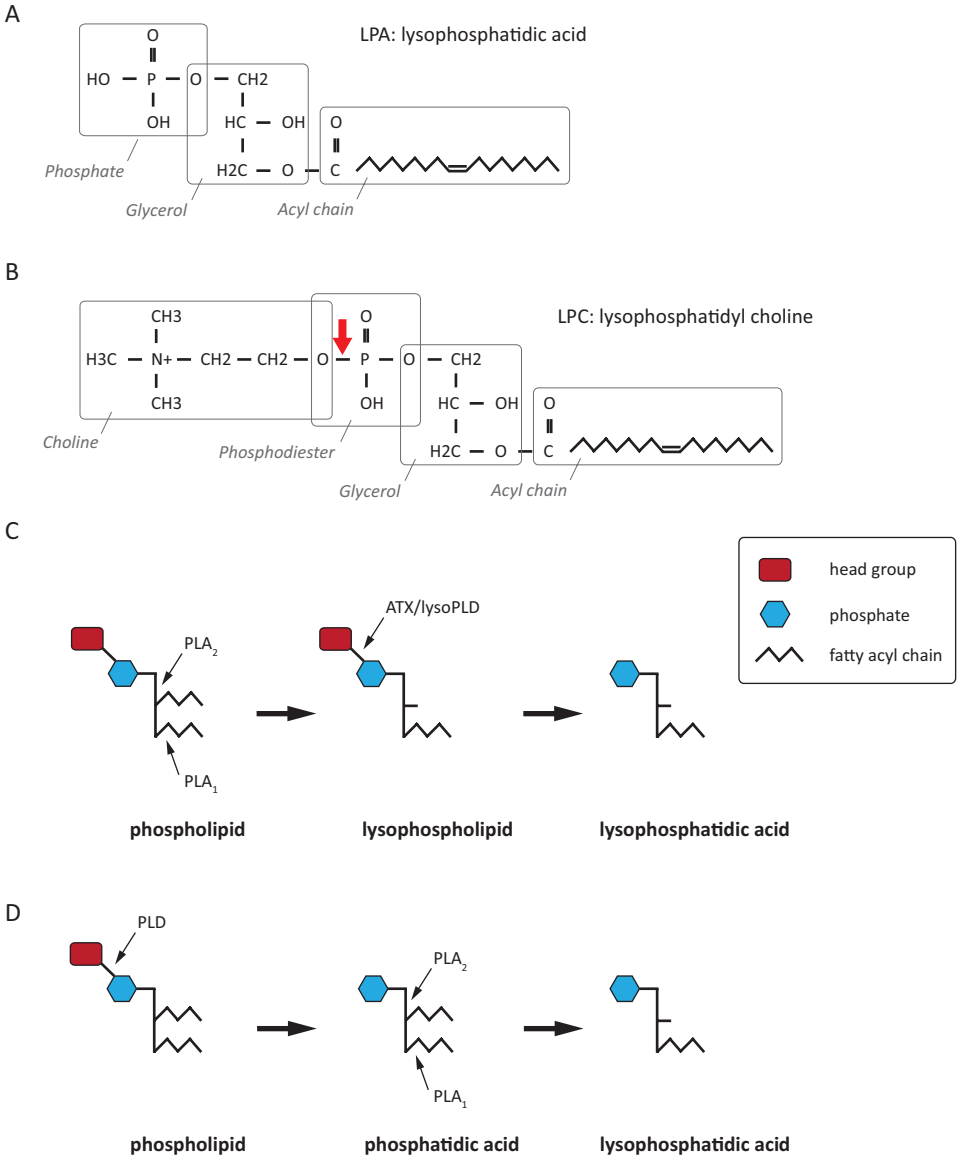

Figure 1: Structure and production of LPA. (A) Chemical structure of 1-acyl-2-hydroxy-*sn*-glycero-3-phosphate (LPA). In this example 1-oleoyl LPA (LPA 18:1) is shown. Note the presence of the fatty acyl chain on the *sn-1* position of the glycerol backbone, which is the most common form. (B) Chemical structure of 1-oleoyl-2-hydroxy-*sn*-glycero-3-phosphocholine (LPC). In this example 1-oleoyl LPC (LPC 18:1) is shown. The red arrow depicts where LPC will be hydrolyzed by ATX. (C), (D) LPA is produced via two major pathways: an extracellular (C) and intracellular (D) route. **Several LPA species can be produced via these pathways, depending on the length and saturation level of the fatty acyl chain of the phospholipids. Note that phospholipids contain two fatty acyl chains, while lysophospholipids only have a single fatty acyl chain. Examples of phospholipids are phosphatidylcholine, phosphatidylethanolamine and phosphatidylserine, which all have different head groups connected to the phosphate. This figure is adapted from (7).**

suggest high capacity of peripheral tissues to take up or metabolize circulating LPA (17). Together, these processes will contribute to the maintenance of low levels of circulating LPA.

LPA Receptors

LPA evokes a wide variety of cellular responses through binding to specific type I, rhodopsin-like G protein-coupled receptors (GPCRs), which are seven-transmembrane cell-surface receptors that signal via heterotrimeric G proteins. Subsequently, these G proteins can activate multiple signaling cascades (18). Until now, six LPA receptors have been identified and termed LPA_{1-6}, which can be subdivided into two subfamilies (Fig. 2A). The presence of two LPA receptor subfamilies suggests that LPA receptors have evolved from distinct ancestor genes. LPA_{1-3} belong to the "endothelial differentiation gene" (EDG) family and show about 50% amino acid homology. They are the "classical" LPA receptors and were formerly called EDG-2, EDG-4, EDG-7 respectively. The five additional members of the EDG-receptor subfamily are receptors specific for the bioactive lysophospholipid S1P, a small lipid similar to LPA but with a sphingosine instead of a glycerol backbone. The newly identified LPA receptors LPA_{4-6} (or P2Y9, GPR92, P2Y5, respectively) are more closely related to the purinergic (P2Y) receptors, sharing about 35% amino acid identity. They were previously thought to bind nucleotides like their purinergic receptor family members (19;20).

Biological Effects of LPA

LPA signaling through GPCRs activates a wide variety of signaling pathways, ranging from cell proliferation and migration to neurite remodeling and cytokine production (21;22). The effects include developmental and (patho) physiological processes and they involve basic cellular responses as well as multiple organ systems. LPA receptors show both overlapping and distinct signaling properties and tissue expression, with an outcome of LPA signaling depending on the LPA receptor expression profile in the cell (19;20). Some of the major biological effects of LPA are summarized in Table 1.

The main LPA-induced signaling pathways and there downstream effects are shown in Fig. 2B. They include: (i) cell proliferation via the G_i-linked Ras-MAPK (mitogen-activated protein kinase) pathway (23;24); (ii) cell survival via G_i-mediated activation of both the PI3K (phosphatidylinositol 3-kinase) - Akt/PKB (protein kinase B) pathway and the MAPK pathway (25;26); (iii) cytoskeletal remodeling and cell migration via the $G_{12/13}$-RhoA pathway (27;28) and G_i-mediated Rac activation (29); (iiii) G_q-mediated hydrolysis of PIP_2 (phosphatidylinositol-bisphosphate) by PLC (phospholipase C), with consequent calcium mobilization and PKC (protein kinase C) activation (30;31). Furthermore, LPA stimulation can induce changes in cAMP (cyclic adenosine monophosphate) levels via G_i or $G_{\beta\gamma}$ subunits and production of growth factors and cytokines (reviewed in (19)).

AUTOTAXIN

ATX was identified as an autocrine motility factor from A2058 melanoma cell-conditioned medium about two decades ago (32). Its mode of action was a mystery at the time and it took another decade until it was discovered that ATX was identical to plasma lysoPLD, responsible for the production of LPA (2;3). ATX, or NPP2, is a member of the ecto-nucleotide pyrophosphatase/phosphodiesterase ((E)NPP) family, consisting of seven structurally related ecto-enzymes. NPPs are usually present at the cell surface as type-I or type-II trans-

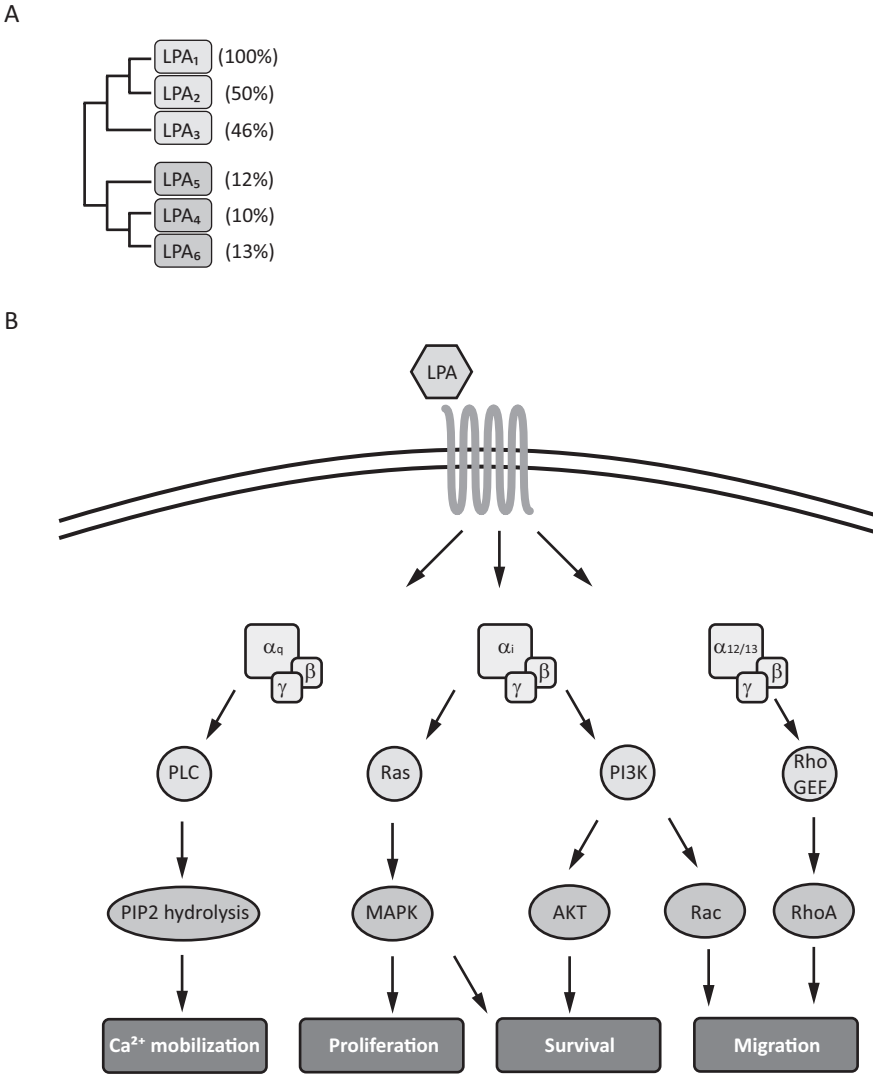

Figure 2: LPA receptor signaling. (A) Phylogenetic tree of human LPA receptors with indicated amino acid identity to LPA_1. The EDG family receptors are depicted in light grey and and the purinergic receptors in dark grey. This figure is adapted from (19). (B) Major signaling pathways of the LPA receptors, showing the distinct G proteins and their corresponding downstream effectors. G proteins are heterotrimeric proteins composed of 3 subunits: α, β and γ. RhoGEF: Rho-specific guanine nucleotide exchange factor. This figure is adapted from (19).

membrane proteins and are known to hydrolyze pyrophosphate or phosphodiester bonds in nucleotides and their derivatives. Despite their structurally related catalytic domain, each NPP enzyme has well-defined substrate specificity. Currently, it is widely accepted that ATX, although capable of hydrolyzing nucleotides *in vitro*, primarily functions as a lysoPLD *in vivo* and thus represents a unique family member. The closest relatives of ATX, NPP1 and

NPP3, convert adenosine triphosphate (ATP) into pyrophosphate (PP_i) and thereby regulate mineralization and calcification in bone. NPP6, as well as NPP7, is a choline-specific ectophospholipase C, probably serving catabolic functions. Activities of NPP4 and NPP5 are currently not defined (33).

ATX Processing

ATX is synthesized as a pre-pro-enzyme; the N-terminal signal peptide is removed by a signal peptidase, the protein is further trimmed by a furin-type protease, traffics along the classical export pathway and is subsequently secreted as an extracellular enzyme into the circulation (34-36). ATX is a heavily glycosylated protein and glycosylation of asparagine-residue 524 (Asn524) is essential for catalytic activity (37). ATX has a rapid turnover; it is cleared from the circulation within minutes and subsequently degraded in the liver. The constant levels of ATX and LPA in serum suggest a continuous synthesis of ATX (16). The cellular source of plasma ATX remains to be identified, but it is likely to originate from the abundant ATX-expressing lymphatic high endothelial venules (38) and/or adipose tissue (39). Indeed, adipose-ATX contributes significantly (though not completely) to circulating LPA levels, as demonstrated in adipose-specific ATX knockout mice that show around 40% reduction in plasma LPA levels (40).

	Physiological	Pathophysiological	
General	Proliferation (31) Survival (85) Migration (29) Invasion (86) Transformation (81) Wound healing (87)	Cancer	Tumor progression, invasion and angiogenesis (80;88;89)
		Pulmonary fibrosis	Fibroblast recruitment and vascular leakage (75)
Nervous system	Neurite retraction (90) Growth cone collapse or turning (90) Ion channel activity (91)	Neuropathic pain	Nerve demyelination and initiation of pain (74)
Vascular system	Platelet activation and aggregation (92) Vascular remodeling (93) Stabilization of embryonic vessels (62;63)	Atherosclerosis	Atherothrombogenesis in atherosclerotic plaques (94)
		Cancer	Stimulation of tumor angiogenesis (89)
Immune system	Cytokine production (95) Lymphocyte trafficking (38)	Atherosclerosis	Induction of atherosclerosis stimulating cytokine CXCL1 (96)
Adipose system	Adipocyte proliferation and migration control (97)	Obesity	Regulation of food intake (67)

Table 1: Major biological LPA signaling-mediated functions. Note that this list focuses on the main effects of LPA and is not complete. However, the remarkable diversity of effects points to the multifunctional signaling function of LPA. This table was adapted and adjusted from (19;21).

ATX Expression

Expression of ATX is most abundant in brain, placenta, ovary and small intestine; while intermediate expression levels are detected in kidney, prostate, testis, pancreas, colon and lung (41). During mouse development, ATX is first detectable at embryonic day 8.5 (E8.5) in the extra-embryonic yolk sac and at E9.5 in the floor plate of the neural tube (42). At later embryonic stages and in adulthood, high ATX expression is observed in choroid plexus epithelium (35;42-44). ATX has been detected in biological fluids, like cerebrospinal fluid (35;45), seminal fluid (46) and ascites (47).

Phosphodiesterase and LysoPLD Activity

ATX has both phosphodiesterase (PDE) and lysoPLD activity *in vitro*; it hydrolyzes nucleotide and lysophospholipid substrates, respectively, with threonine-residue 210 (Thr210) as the catalytic center for both activities. The PDE activity of ATX, however, does not seem to be of biological importance, as the apparent affinity for LPC is much higher than that for nucleotides (48). ATX has also been shown to hydrolyze sphingosylphosphorylcholine (SPC) and produce S1P *in vitro* (49). However, physiological significance is ambiguous due to a thousand-fold higher K_m of ATX for SPC than the normal SPC levels in plasma and serum (50). Thus, the biological roles of ATX are thought to be fully attributable to LPA production and subsequent signaling through LPA receptors.

ATX Crystal Structure

The recently obtained crystal structures of rat and mouse ATX identify a compact four domain-based architecture of two somatomedin B-like (SMB) domains, a central catalytic PDE domain and a nuclease-like (NUC) domain (Fig. 3A) (51;52). The PDE domain extensively interacts with the SMB-1 and SMB-2 domains on one side and with the NUC domain on the other side. A short loop is connecting the SMB and PDE domains and a long “lasso loop”, wrapped around the NUC domain, connects the PDE and NUC domains. The Asn524-linked glycan chain further reinforces the interdomain interactions, in agreement with the finding that this glycan is essential for catalytic activity (37).

The catalytic domain of ATX is similar to that of the bacterial *Xanthomonas axonopodis* NPP, a structural and evolutionary relative to alkaline phosphatase (AP). The crystal structure of ATX reveals the presence of two catalytic zinc ions coordinated by conserved residues, in close proximity to Thr210. As in *X. axonopodis* NPP and many other enzymes, the ions in this conserved bimetallo site participate in bond-breaking steps (51;53).

The catalytically inactive NUC domain has been thought to be involved in substrate binding and presentation (54). It is now clear that the rigid PDE-NUC domain interface merely functions to stabilize the thermodynamically unstable structure of the hydrophobic pocket of ATX, without directly contributing to the active site formation. Moreover, this stabilizing effect could be the reason why the hydrophobic lipid-binding pocket of ATX is always accessible, while most lipases have a closed pocket that only opens upon substrate binding (51;52).

Substrate Specificity

ATX hydrolyzes both nucleotide and phospholipid substrates *in vitro* (48). Substrate discrimination of ATX and the diverse substrate preferences of NPP family members have been a long time mystery. The ATX crystal structure reveals that both nucleotides and lipids partially

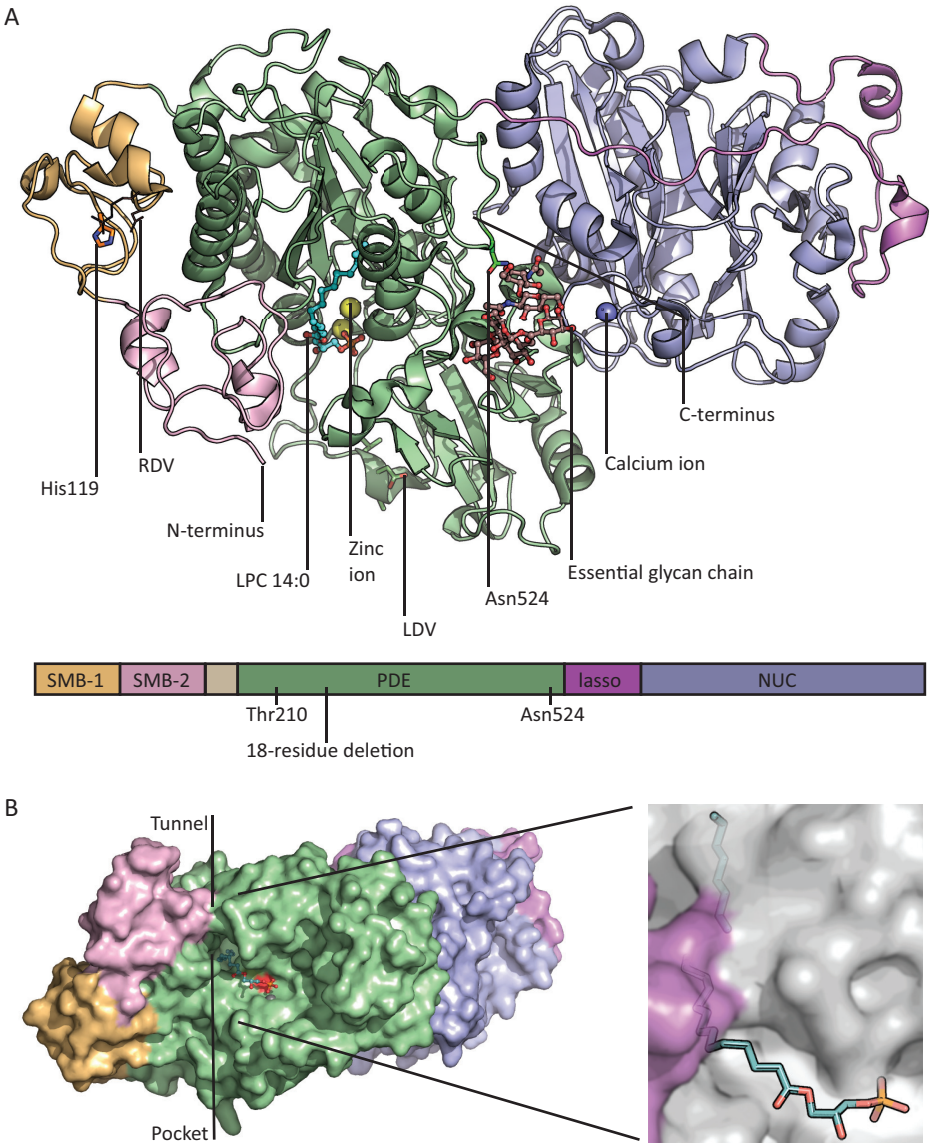

Figure 3: The structure of ATX. (A) The upper panel shows the crystal structure of ATX bound to LPC 14:0 with the N- and C-terminus, the zinc ions (yellow spheres) in the active site, the calcium ion (blue sphere) bound to the EF hand-like motif indicated. LPC, the essential glycan chain of Asn524, the integrin-interaction motifs LDV and His119 (close to the RGD motif) are depicted in a stick-and-sphere representation. The lower panel shows a schematic overview of the domain organization, with the active site residue Thr210, the 18-residue deletion (specific for ATX in the NPP family and responsible for formation of the lipid binding pocket) and Asn524 (containing the glycan chain essential for interdomain interactions between PDE and NUC). This figure was prepared using Pymol (www.pymol.org), adapted from (58). (B) Surface representation of ATX bound to LPC 14:0, with the acyl chain pointing into the viewing plane and the tunnel pointing upwards (left panel). LPC is shown in a sphere model. Domain colors are the same as in Fig. 3A. The right panel shows a zoom-in on the ATX active site showing LPA in the tunnel (again pointing upwards), which forms a T-junction with the substrate binding pocket containing LPC (with the phosphate group bound to the active site in the lower right corner and the acyl chain pointing inwards). The roof of the tunnel is partially made by residues of the SMB-1 domain, depicted in purple. This figure was prepared using Pymol (www.pymol.org), adapted from (58).

share the same binding pocket. The acyl chain of lipid substrates form additional hydrophobic contacts with ATX, suggesting that the product LPA has a higher affinity for ATX than nucleotide substrates and can only be displaced by lysophospholipid substrates like LPC. This would explain why LPA acts as an inhibitor of ATX activity against various artificial substrates (36) but not of LPC hydrolysis (55), determining LPA as a "substrate-specifying factor" (51).

The presence of an 18 amino acid insertion loop in all of the NPP family members, except ATX, is a major determinant for substrate specificity among the family. This insertion loop blocks the entry of the hydrophobic binding pocket, suggesting that the hydrophobic pocket is an extension of the nucleotide binding site. The absence of the loop in ATX enables the enzyme to accept both nucleotides and lysophospholipids as a substrate and to use the same catalytic site for both activities. Moreover, this pocket can only accommodate monoacyl but not diacyl phospholipids, providing substrate specificity for phospholipids with a single acyl chain and with an optimal length of 14 carbons (51;52).

Close to the hydrophobic pocket of ATX is a narrow tunnel, which is formed by the PDE and SMB-1 domains (Fig. 3B). An SMB-deletion mutant of ATX is ten-fold less sensitive to LPA inhibition, suggesting a role for the SMB domain and the tunnel in substrate recognition or product release (51). Indeed, Nishimasu and colleagues imply the presence of LPA in this hydrophobic tunnel, which suggests that the tunnel could function as a product exit route. Again, due to the presence of the insertion loop, the other NPP family members lack this tunnel. Another option would be that the tunnel serves as an entrance site for LPC substrates released from cells, which could function as a shuttle mechanism for substrate entrance versus product release to deliver LPA directly to LPA receptors on the cell membrane (52).

ATX Interactions

ATX has a flat molecular surface on the side of the tunnel, which is suggested to function as a cell membrane-binding platform to provide LPA directly to its receptors (52). Next to this model of direct binding, ATX has been suggested to bind to cells via interaction with integrins. T cells are able to interact with ATX in an integrin $\alpha_4\beta_1$-dependent manner, suggesting a model in which secretion of ATX and subsequent localized LPA production promotes lymphocyte motility. This interaction is thought to involve a Leu-Asp-Val (LDV) integrin-binding motif on the surface of the PDE domain of ATX (38). In addition to lymphocytes, ATX can bind to activated platelets in an integrin β_3-dependent manner, which could be mediated by an Arg-Gly-Asp (RGD) sequence motif present in ATX (56).

The ATX crystal structure revealed that the SMB domains are the primary mediators of the β_3-mediated ATX-integrin interaction. However, the binding mode is structurally distinct from the classical RGD-mediated integrin binding and involves a wider portion of the surface of the SMB-2 domain (51). Recently, platelets have been shown to bind ATX in an integrin-dependent manner with subsequent increase in local LPA production. Moreover, it is suggested that this ATX-integrin interaction even enhances LPA production, possibly by reorientation of the SMB domains to speed up catalysis or product release (57). Next to interactions with integrins, ATX is able to bind heparin. In chapter 5 we discuss our latest insight in ATX-heparin interactions and propose a third mechanism of localized LPA signaling by sequestering ATX to target cells via heparin sulphate proteoglycans. Together, these

models of ATX recruitment to the cell surface suggest that ATX not only drives the production of LPA, but also guides specificity of LPA signaling. Alternatively, the function of these interactions could be non-catalytic signaling of ATX via integrins (58).

ATX Isoforms

The human gene encoding ATX, *ENPP2*, is located on chromosome 8 and is organized in 27 exons. Alternative splicing of the *ENPP2* gene gives rise to three isoforms; ATXα, ATXβ and ATXγ. The originally isolated ATX isoform termed "autocrine motility factor", cloned from A2058 melanoma cells, was called ATX-melanoma or ATXα (32;59). Later, ATX-teratocarcinoma (ATXβ) was cloned from a teratocarcinoma cell line (41). This isoform is identical to plasma lysoPLD and currently the most widely studied isoform. A third, brain-specific isoform PD-Iα was identified and termed ATXγ (44;60). The ATXα and ATXγ isoform are characterized by the presence of exon 12 and 21, respectively. ATXα represents the longest isoform with a 52 amino acid insert in the PDE domain. ATXγ has an insert of 25 amino acids in the NUC domain. ATXβ was thought to be the shortest isoform, lacking both exon 12 and 21. Recently, two new isoforms have been identified: ATXδ and ATXε. ATXδ has a deletion of 4 amino acids in the lasso loop and ATXε is characterized by the 52 amino acid insert encoded by exon 12 together with the 4 amino acid deletion. Of all isoforms, ATXα represents the longest isoform and ATXδ the shortest (Fig. 4). ATXβ and ATXδ seem to be vastly expressed, ATXγ moderately, while ATXα and ATXε are much less abundant (61). The ATXα isoform is of special interest, since it contains a large insert in the heart of the catalytic domain. The unique biochemical properties of the ATXα isoform will be discussed in chapter 5.

ATX-LPA RECEPTOR SIGNALING IN DEVELOPMENT

ATX Knockout Mice

Gene targeting studies in mice show a crucial role for ATX in embryogenesis. *Enpp2* deficiency causes embryonic lethality at E9.5 due to vascular defects in both yolk sac and embryo. The vascular network normally present in the yolk sac is completely absent and replaced by blood patches, blood vessels in the embryo are enlarged and the neural tube is malformed.

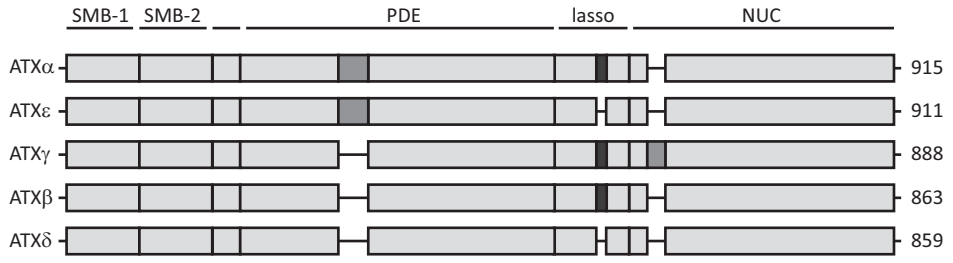

Figure 4: ATX isoforms. Protein structure of the five known isoforms of ATX ordered by length, with the longest isoform (ATXα) containing 915 residues and the shortest isoform (ATXδ) comprising 859 residues. The ATXα and ATXε isoforms are characterized by a 52 residue insert in the PDE domain (encoded by exon 12), ATXγ by a 25 residue insert in the NUC domain (encoded by exon 21), ATXδ and ATXε by a deletion of the first 4 amino acids of exon 19 in the lasso loop. ATXα, ATXβ and ATXγ all contain an intact exon 19. The domain architecture is depicted on top. This figure was adapted from (61).

Moreover, the heterozygous mice show half-normal plasma LPA levels, indicating that ATX is the main enzyme producing LPA in the circulation (62-64). Transgenic mice expressing the inactive mutant ATX-T210A display the same lethal phenotype, confirming that catalytic activity of ATX is crucial for vascular development (65).

LPA Receptor Knockout Mice

Loss of LPA_1 in mice results in 50% neonatal lethality and a reduced body size of surviving pups (66), which was attributed to defective suckling but has now been shown to be caused by a reduced food intake as well (67). In addition, LPA_1 has been implicated in neurogenesis, as a specific variant of the *Lpa*$_1$ KO strain shows defects in cortical development (68). *Lpa*$_2$ knockout mice are viable and without any phenotypic abnormalities, while *Lpa*$_1$*/Lpa*$_2$ double knockout mice do not show additional phenotypic abnormalities next to the defects found in the *Lpa*$_1$ single knockout mice. Thus, LPA_2 is not essential for mouse development, but rather acts redundantly with LPA_1 (69).

LPA_3 signaling, though, is crucial for embryo implantation and spacing. While *Lpa*$_3$ knockout mice appear normal, the *Lpa*$_3$-deficient females show a reduced litter size due to delayed embryo implantation and embryo crowding (70). *Lpa*$_1$*/Lpa*$_2$*/Lpa*$_3$ triple knockout mice show defects in male reproductive function, next to the phenotypes consistent with single receptor deletants (71). *Lpa*$_4$-deficient mice display abnormalities in the blood and lymphatic vascular system, causing partial lethality of embryos and newborn pups (72). The latter phenotype shows some similarities to, but is less severe than the *Enpp2* knockout mice.

ATX-LPA Receptor Signaling in Vascular Development

The vascular defects observed in *Enpp2*-deficient embryos have also been found in *G*$_{13}$ knockout mice (73). Absence of G_{13} does not influence the formation of endothelial cells, but affects the growth and sprouting of endothelial cells to form an organized vascular network (73). While initial blood vessel formation is not affected in the *Enpp2* deficient mice, newly formed blood vessels fail to mature in the absence of ATX (62;63). This suggests that ATX and LPA play a role in angiogenesis. However, ATX and LPA are suggested to function in stabilizing preformed blood vessels, rather than being angiogenic factors (63). Thus, loss of LPA-G_{13} signaling is likely to underlie the vascular defects of *Enpp2* knockout embryos, in particular defects in the formation and stabilization of blood vessels.

ATX-LPA RECEPTOR SIGNALING IN (PATHO)PHYSIOLOGY

ATX-LPA signaling has been implicated in a wide range of physiological and pathological processes, ranging from vascular and neural development (62-64), lymphocyte trafficking (38), neuropathic pain (74), fibrosis (75), hydrocephalus (76) and cholestatic pruritis (77) to tumor initiation and progression (78-81). ATX may function as a potential diagnostic marker since the serum or plasma levels are increased in some physiological and pathological conditions like chronic liver disease (82), obesity (39;40), cancer (83) and pregnancy (84). In addition, the implication of the ATX-LPA axis in diverse pathophysiological processes has put forward the identification of ATX as a valuable therapeutic target. The crystal structure has revealed a wealth of important information regarding substrate binding and selectivity, which will boost the design and optimization of effective ATX inhibitors in the near future.

A prominent area of research interest is the emerging role of ATX-LPA receptor signaling in cancer. With its growth-factor like activities, LPA stimulates multiple signaling pathways that could contribute to tumor initiation and progression as well as metastasis. Indeed, LPA receptor expression and signaling, aberrant LPA production and ATX expression have all been linked to cancer (1). As discussed above, most evidence is pointing to a role of the ATX-LPA signaling axis *in vivo* in the vascular system. This raises the question if ATX could contribute to the progression of tumors by stabilizing blood vessels in tumors or the tumor microenvironment, in addition to its effect on proliferation and migration. Additional studies such as deletion of non-EDG LPA receptors (LPA_{4-6}) and their combinations, as well as tissue specific or inducible deletion of both ATX and/or LPA receptors, are awaited to sort out the mechanism of the ATX-LPA signaling axis and its role in development and pathology. Details about the role of ATX-LPA receptor signaling in cancer will be further discussed in chapter 2.

THESIS OUTLINE

The ATX-LPA receptor axis has a wide implication in health and disease. The studies described in this thesis focus on the biochemical and functional properties of ATX to increase our understanding of its molecular actions. **Chapter 2** reviews the latest insights of ATX and LPA receptor signaling in cancer. The prognostic value of ATX protein expression in breast cancer is explored in **chapter 3**. **Chapter 4** describes the development and optimization of a first-generation ATX activity-based probe for *in vivo* screening of ATX activity. Next, the specific characteristics of the ATXα isoform have been studied: intradomain cleavage of ATXα and high-affinity binding to heparin are discussed in **chapter 5**, and the SH3 domain-mediated protein-interaction capacity of ATXα is described in the **chapter 6**. In **chapter 7**, all results presented in this thesis are summarized and discussed.

REFERENCES

1. Mills, G. B. and Moolenaar, W. H. (2003) *Nat Rev Cancer* 3, 582-591
2. Tokumura, A., Majima, E., Kariya, Y., Tominaga, K., Kogure, K., Yasuda, K., and Fukuzawa, K. (2002) *J Biol Chem* 277, 39436-39442
3. Umezu-Goto, M., Kishi, Y., Taira, A., Hama, K., Dohmae, N., Takio, K., Yamori, T., Mills, G. B., Inoue, K., Aoki, J., and Arai, H. (2002) *J Cell Biol* 158, 227-233
4. Mills, G. B., May, C., Hill, M., Campbell, S., Shaw, P., and Marks, A. (1990) *J Clin Invest* 86, 851-855
5. Westermann, A. M., Havik, E., Postma, F. R., Beijnen, J. H., Dalesio, O., Moolenaar, W. H., and Rodenhuis, S. (1998) *Ann Oncol* 9, 437-442
6. Tokumura, A., Harada, K., Fukuzawa, K., and Tsukatani, H. (1986) *Biochim Biophys Acta* 875, 31-38
7. Okudaira, S., Yukiura, H., and Aoki, J. (2010) *Biochimie* 92, 698-706
8. Aoki, J., Inoue, A., and Okudaira, S. (2008) *Biochim Biophys Acta* 1781, 513-518
9. Tigyi, G. and Miledi, R. (1992) *J Biol Chem* 267, 21360-21367
10. Baker, D. L., Morrison, P., Miller, B., Riely, C. A., Tolley, B., Westermann, A. M., Bonfrer, J. M., Bais, E., Moolenaar, W. H., and Tigyi, G. (2002) *JAMA* 287, 3081-3082
11. Xu, Y., Shen, Z., Wiper, D. W., Wu, M., Morton, R. E., Elson, P., Kennedy, A. W., Belinson, J., Markman, M., and Casey, G. (1998) *JAMA* 280, 719-723
12. Baker, D. L., Desiderio, D. M., Miller, D. D., Tolley, B., and Tigyi, G. J. (2001) *Anal Biochem* 292, 287-295
13. Aoki, J., Taira, A., Takanezawa, Y., Kishi, Y., Hama, K., Kishimoto, T., Mizuno, K., Saku, K., Taguchi, R., and Arai, H. (2002) *J Biol Chem* 277, 48737-48744
14. Sano, T., Baker, D., Virag, T., Wada, A., Yatomi, Y., Kobayashi, T., Igarashi, Y., and Tigyi, G. (2002) *J Biol Chem* 277, 21197-21206
15. Tomsig, J. L., Snyder, A. H., Berdyshev, E. V., Skobeleva, A., Mataya, C., Natarajan, V., Brindley, D. N., and Lynch, K. R. (2009) *Biochem J* 419, 611-618
16. Jansen, S., Andries, M., Vekemans, K., Vanbilloen, H., Verbruggen, A., and Bollen, M. (2009) *Cancer Lett* 284, 216-221
17. Tokumura, A. (2002) *Biochim. Biophys. Acta* 1582, 18-25
18. Pierce, K. L., Premont, R. T., and Lefkowitz, R. J. (2002) *Nat Rev Mol Cell Biol* 3, 639-650
19. Choi, J. W., Herr, D. R., Noguchi, K., Yung, Y. C., Lee, C. W., Mutoh, T., Lin, M. E., Teo, S. T., Park, K. E., Mosley, A. N., and Chun, J. (2010) *Annu Rev Pharmacol Toxicol* 50, 157-186
20. Chun, J., Hla, T., Lynch, K. R., Spiegel, S., and Moolenaar, W. H. (2010) *Pharmacol Rev* 62, 579-587
21. van Meeteren, L. A. and Moolenaar, W. H. (2007) *Prog Lipid Res* 46, 145-160
22. Moolenaar, W. H., van Meeteren, L. A., and Giepmans, B. N. (2004) *Bioessays* 26, 870-881
23. van Corven, E. J., Hordijk, P. L., Medema, R. H., Bos, J. L., and Moolenaar, W. H. (1993) *Proc Natl Acad Sci U S A* 90, 1257-1261
24. Kranenburg, O. and Moolenaar, W. H. (2001) *Oncogene* 20, 1540-1546
25. Fang, X., Yu, S., Lapushin, R., Lu, Y., Furui, T., Penn, L. Z., Stokoe, D., Erickson, J. R., Bast, R. C., Jr., and Mills, G. B. (2000) *Biochem. J.* 352 Pt 1, 135-143
26. Roche, S., Downward, J., Raynal, P., and Courtneidge, S. A. (1998) *Mol. Cell Biol.* 18, 7119-7129
27. Kranenburg, O., Poland, M., van Horck, F. P., Drechsel, D., Hall, A., and Moolenaar, W. H. (1999) *Mol Biol Cell* 10, 1851-1857
28. Stam, J. C., Michiels, F., van der Kammen, R. A., Moolenaar, W. H., and Collard, J. G. (1998) *EMBO J* 17, 4066-4074
29. Van Leeuwen, F. N., Olivo, C., Grivell, S., Giepmans, B. N., Collard, J. G., and Moolenaar, W. H. (2003) *J. Biol. Chem.* 278, 400-406
30. Jalink, K., van Corven, E. J., and Moolenaar, W. H. (1990) *J. Biol. Chem.* 265, 12232-12239
31. van Corven, E. J., Groenink, A., Jalink, K., Eichholtz, T., and Moolenaar, W. H. (1989) *Cell* 59, 45-54
32. Stracke, M. L., Krutzsch, H. C., Unsworth, E. J., Arestad, A., Cioce, V., Schiffmann, E., and Liotta, L. A. (1992) *J Biol Chem* 267, 2524-2529
33. Stefan, C., Jansen, S., and Bollen, M. (2005) *Trends Biochem Sci* 30, 542-550
34. Jansen, S., Stefan, C., Creemers, J. W., Waelkens, E., Van Eynde, A., Stalmans, W., and Bollen, M. (2005) *J Cell Sci* 118, 3081-3089
35. Koike, S., Keino-Masu, K., Ohto, T., and Masu, M. (2006) *Genes Cells* 11, 133-142
36. van Meeteren, L. A., Ruurs, P., Christodoulou, E., Goding, J. W., Takakusa, H., Kikuchi, K., Perrakis, A., Nagano, T., and Moolenaar, W. H. (2005) *J Biol Chem* 280, 21155-21161
37. Jansen, S., Callewaert, N., Dewerte, I., Andries, M., Ceulemans, H., and Bollen, M. (2007) *J Biol Chem* 282, 11084-11091
38. Kanda, H., Newton, R., Klein, R., Morita, Y., Gunn, M. D., and Rosen, S. D. (2008) *Nat Im-*

munol 9, 415-423
39. Ferry, G., Tellier, E., Try, A., Gres, S., Naime, I., Simon, M. F., Rodriguez, M., Boucher, J., Tack, I., Gesta, S., Chomarat, P., Dieu, M., Raes, M., Galizzi, J. P., Valet, P., Boutin, J. A., and Saulnier-Blache, J. S. (2003) *J Biol Chem* 278, 18162-18169
40. Dusaulcy, R., Rancoule, C., Gres, S., Wanecq, E., Colom, A., Guigne, C., van Meeteren, L. A., Moolenaar, W. H., Valet, P., and Saulnier-Blache, J. S. (2011) *J Lipid Res*
41. Lee, H. Y., Murata, J., Clair, T., Polymeropoulos, M. H., Torres, R., Manrow, R. E., Liotta, L. A., and Stracke, M. L. (1996) *Biochem Biophys Res Commun* 218, 714-719
42. Bachner, D., Ahrens, M., Betat, N., Schroder, D., and Gross, G. (1999) *Mech Dev* 84, 121-125
43. Fuss, B., Baba, H., Phan, T., Tuohy, V. K., and Macklin, W. B. (1997) *J Neurosci* 17, 9095-9103
44. Narita, M., Goji, J., Nakamura, H., and Sano, K. (1994) *J Biol Chem* 269, 28235-28242
45. Sato, K., Malchinkhuu, E., Muraki, T., Ishikawa, K., Hayashi, K., Tosaka, M., Mochiduki, A., Inoue, K., Tomura, H., Mogi, C., Nochi, H., Tamoto, K., and Okajima, F. (2005) *J Neurochem* 92, 904-914
46. Tanaka, M., Kishi, Y., Takanezawa, Y., Kakehi, Y., Aoki, J., and Arai, H. (2004) *FEBS Lett* 571, 197-204
47. Tokumura, A., Kume, T., Fukuzawa, K., Tahara, M., Tasaka, K., Aoki, J., Arai, H., Yasuda, K., and Kanzaki, H. (2007) *Life Sci* 80, 1641-1649
48. Gijsbers, R., Aoki, J., Arai, H., and Bollen, M. (2003) *FEBS Lett* 538, 60-64
49. Clair, T., Aoki, J., Koh, E., Bandle, R. W., Nam, S. W., Ptaszynska, M. M., Mills, G. B., Schiffmann, E., Liotta, L. A., and Stracke, M. L. (2003) *Cancer Res* 63, 5446-5453
50. Liliom, K., Sun, G., Bunemann, M., Virag, T., Nusser, N., Baker, D. L., Wang, D. A., Fabian, M. J., Brandts, B., Bender, K., Eickel, A., Malik, K. U., Miller, D. D., Desiderio, D. M., Tigyi, G., and Pott, L. (2001) *Biochem J* 355, 189-197
51. Hausmann, J., Kamtekar, S., Christodoulou, E., Day, J. E., Wu, T., Fulkerson, Z., Albers, H. M., van Meeteren, L. A., Houben, A. J., van Zeijl, L., Jansen, S., Andries, M., Hall, T., Pegg, L. E., Benson, T. E., Kasiem, M., Harlos, K., Kooi, C. W., Smyth, S. S., Ovaa, H., Bollen, M., Morris, A. J., Moolenaar, W. H., and Perrakis, A. (2011) *Nat Struct Mol Biol* 18, 198-204
52. Nishimasu, H., Okudaira, S., Hama, K., Mihara, E., Dohmae, N., Inoue, A., Ishitani, R., Takagi, J., Aoki, J., and Nureki, O. (2011) *Nat Struct Mol Biol* 18, 205-212
53. Zalatan, J. G., Fenn, T. D., Brunger, A. T., and Herschlag, D. (2006) *Biochemistry* 45, 9788-9803
54. Jansen, S., Andries, M., Derua, R., Waelkens, E., and Bollen, M. (2009) *J Biol Chem* 284, 14296-14302
55. Albers, H. M., van Meeteren, L. A., Egan, D. A., van Tilburg, E. W., Moolenaar, W. H., and Ovaa, H. (2010) *J Med Chem* 53, 4958-4967
56. Pamuklar, Z., Federico, L., Liu, S., Umezu-Goto, M., Dong, A., Panchatcharam, M., Fulkerson, Z., Berdyshev, E., Natarajan, V., Fang, X., van Meeteren, L. A., Moolenaar, W. H., Mills, G. B., Morris, A. J., and Smyth, S. S. (2009) *J Biol Chem* 284, 7385-7394
57. Fulkerson, Z., Wu, T., Sunakura, M., Vander Kooi, C., Morris, A. J., and Smyth, S. S. (2011) *J Biol Chem*
58. Moolenaar, W. H. and Perrakis, A. (2011) *Nat Rev Mol Cell Biol*
59. Murata, J., Lee, H. Y., Clair, T., Krutzsch, H. C., Arestad, A. A., Sobel, M. E., Liotta, L. A., and Stracke, M. L. (1994) *J Biol Chem* 269, 30479-30484
60. Kawagoe, H., Soma, O., Goji, J., Nishimura, N., Narita, M., Inazawa, J., Nakamura, H., and Sano, K. (1995) *Genomics* 30, 380-384
61. Hashimoto, T., Okudaira, S., Igarashi, K., Hama, K., Yatomi, Y., and Aoki, J. (2012) *J. Biochem.* 151, 89-97
62. van Meeteren, L. A., Ruurs, P., Stortelers, C., Bouwman, P., van Rooijen, M. A., Pradere, J. P., Pettit, T. R., Wakelam, M. J., Saulnier-Blache, J. S., Mummery, C. L., Moolenaar, W. H., and Jonkers, J. (2006) *Mol Cell Biol* 26, 5015-5022
63. Tanaka, M., Okudaira, S., Kishi, Y., Ohkawa, R., Iseki, S., Ota, M., Noji, S., Yatomi, Y., Aoki, J., and Arai, H. (2006) *J Biol Chem* 281, 25822-25830
64. Fotopoulou, S., Oikonomou, N., Grigorieva, E., Nikitopoulou, I., Paparountas, T., Thanassopoulou, A., Zhao, Z., Xu, Y., Kontoyiannis, D. L., Remboutsika, E., and Aidinis, V. (2010) *Dev Biol* 339, 451-464
65. Ferry, G., Giganti, A., Coge, F., Bertaux, F., Thiam, K., and Boutin, J. A. (2007) *FEBS Lett* 581, 3572-3578
66. Contos, J. J., Fukushima, N., Weiner, J. A., Kaushal, D., and Chun, J. (2000) *Proc Natl Acad Sci U S A* 97, 13384-13389
67. Dusaulcy, R., Daviaud, D., Pradere, J. P., Gres, S., Valet, P., and Saulnier-Blache, J. S. (2009) *J. Physiol Biochem.* 65, 345-350
68. Estivill-Torrus, G., Llebrez-Zayas, P., Matas-Rico, E., Santin, L., Pedraza, C., De, D., I, Del, A., I, Fernandez-Llebrez, P., Chun, J., and De Fonseca, F. R. (2008) *Cereb. Cortex* 18, 938-950
69. Contos, J. J., Ishii, I., Fukushima, N., Kingsbury, M. A., Ye, X., Kawamura, S., Brown, J. H., and Chun, J. (2002) *Mol Cell Biol* 22, 6921-6929

70. Ye, X., Hama, K., Contos, J. J., Anliker, B., Inoue, A., Skinner, M. K., Suzuki, H., Amano, T., Kennedy, G., Arai, H., Aoki, J., and Chun, J. (2005) *Nature* 435, 104-108
71. Ye, X., Skinner, M. K., Kennedy, G., and Chun, J. (2008) *Biol. Reprod.* 79, 328-336
72. Sumida, H., Noguchi, K., Kihara, Y., Abe, M., Yanagida, K., Hamano, F., Sato, S., Tamaki, K., Morishita, Y., Kano, M. R., Iwata, C., Miyazono, K., Sakimura, K., Shimizu, T., and Ishii, S. (2010) *Blood* 116, 5060-5070
73. Offermanns, S., Mancino, V., Revel, J. P., and Simon, M. I. (1997) *Science* 275, 533-536
74. Inoue, M., Rashid, M. H., Fujita, R., Contos, J. J., Chun, J., and Ueda, H. (2004) *Nat. Med.* 10, 712-718
75. Tager, A. M., LaCamera, P., Shea, B. S., Campanella, G. S., Selman, M., Zhao, Z., Polosukhin, V., Wain, J., Karimi-Shah, B. A., Kim, N. D., Hart, W. K., Pardo, A., Blackwell, T. S., Xu, Y., Chun, J., and Luster, A. D. (2008) *Nat Med* 14, 45-54
76. Yung, Y. C., Mutoh, T., Lin, M. E., Noguchi, K., Rivera, R. R., Choi, J. W., Kingsbury, M. A., and Chun, J. (2011) *Sci Transl Med* 3, 99ra87
77. Kremer, A. E., Martens, J. J., Kulik, W., Rueff, F., Kuiper, E. M., van Buuren, H. R., van Erpecum, K. J., Kondrackiene, J., Prieto, J., Rust, C., Geenes, V. L., Williamson, C., Moolenaar, W. H., Beuers, U., and Oude Elferink, R. P. (2010) *Gastroenterology* 139, 1008-18, 1018
78. David, M., Wannecq, E., Descotes, F., Jansen, S., Deux, B., Ribeiro, J., Serre, C. M., Gres, S., Bendriss-Vermare, N., Bollen, M., Saez, S., Aoki, J., Saulnier-Blache, J. S., Clezardin, P., and Peyruchaud, O. (2010) *PLoS One* 5, e9741
79. Lin, S., Wang, D., Iyer, S., Ghaleb, A. M., Shim, H., Yang, V. W., Chun, J., and Yun, C. C. (2009) *Gastroenterology* 136, 1711-1720
80. Liu, S., Umezu-Goto, M., Murph, M., Lu, Y., Liu, W., Zhang, F., Yu, S., Stephens, L. C., Cui, X., Murrow, G., Coombes, K., Muller, W., Hung, M. C., Perou, C. M., Lee, A. V., Fang, X., and Mills, G. B. (2009) *Cancer Cell* 15, 539-550
81. Taghavi, P., Verhoeven, E., Jacobs, J. J., Lambooij, J. P., Stortelers, C., Tanger, E., Moolenaar, W. H., and van Lohuizen, M. (2008) *Oncogene* 27, 6806-6816
82. Nakamura, K., Igarashi, K., Ide, K., Ohkawa, R., Okubo, S., Yokota, H., Masuda, A., Oshima, N., Takeuchi, T., Nangaku, M., Okudaira, S., Arai, H., Ikeda, H., Aoki, J., and Yatomi, Y. (2008) *Clin Chim Acta* 388, 51-58
83. Masuda, A., Nakamura, K., Izutsu, K., Igarashi, K., Ohkawa, R., Jona, M., Higashi, K., Yokota, H., Okudaira, S., Kishimoto, T., Watanabe, T., Koike, Y., Ikeda, H., Kozai, Y., Kurokawa, M., Aoki, J., and Yatomi, Y. (2008) *Br J Haematol* 143, 60-70
84. Tokumura, A., Kanaya, Y., Miyake, M., Yamano, S., Irahara, M., and Fukuzawa, K. (2002) *Biol. Reprod.* 67, 1386-1392
85. Weiner, J. A. and Chun, J. (1999) *Proc. Natl. Acad. Sci. U. S. A* 96, 5233-5238
86. Imamura, F., Horai, T., Mukai, M., Shinkai, K., Sawada, M., and Akedo, H. (1993) *Biochem. Biophys. Res. Commun.* 193, 497-503
87. Balazs, L., Okolicany, J., Ferrebee, M., Tolley, B., and Tigyi, G. (2001) *Am. J. Physiol Regul. Integr. Comp Physiol* 280, R466-R472
88. Nam, S. W., Clair, T., Campo, C. K., Lee, H. Y., Liotta, L. A., and Stracke, M. L. (2000) *Oncogene* 19, 241-247
89. Nam, S. W., Clair, T., Kim, Y. S., McMarlin, A., Schiffmann, E., Liotta, L. A., and Stracke, M. L. (2001) *Cancer Res* 61, 6938-6944
90. Jalink, K., Eichholtz, T., Postma, F. R., van Corven, E. J., and Moolenaar, W. H. (1993) *Cell Growth Differ.* 4, 247-255
91. Postma, F. R., Jalink, K., Hengeveld, T., Bot, A. G., Alblas, J., de Jonge, H. R., and Moolenaar, W. H. (1996) *EMBO J.* 15, 63-72
92. Rother, E., Brandl, R., Baker, D. L., Goyal, P., Gebhard, H., Tigyi, G., and Siess, W. (2003) *Circulation* 108, 741-747
93. Yoshida, K., Nishida, W., Hayashi, K., Ohkawa, Y., Ogawa, A., Aoki, J., Arai, H., and Sobue, K. (2003) *Circulation* 108, 1746-1752
94. Siess, W., Zangl, K. J., Essler, M., Bauer, M., Brandl, R., Corrinth, C., Bittman, R., Tigyi, G., and Aepfelbacher, M. (1999) *Proc. Natl. Acad. Sci. U. S. A* 96, 6931-6936
95. Stortelers, C., Kerkhoven, R., and Moolenaar, W. H. (2008) *BMC Genomics* 9, 387
96. Zhou, Z., Subramanian, P., Sevilmis, G., Globke, B., Soehnlein, O., Karshovska, E., Megens, R., Heyll, K., Chun, J., Saulnier-Blache, J. S., Reinholz, M., van, Z. M., Weber, C., and Schober, A. (2011) *Cell Metab* 13, 592-600
97. Pages, C., Daviaud, D., An, S., Krief, S., Lafontan, M., Valet, P., and Saulnier-Blache, J. S. (2001) *J. Biol. Chem.* 276, 11599-11605

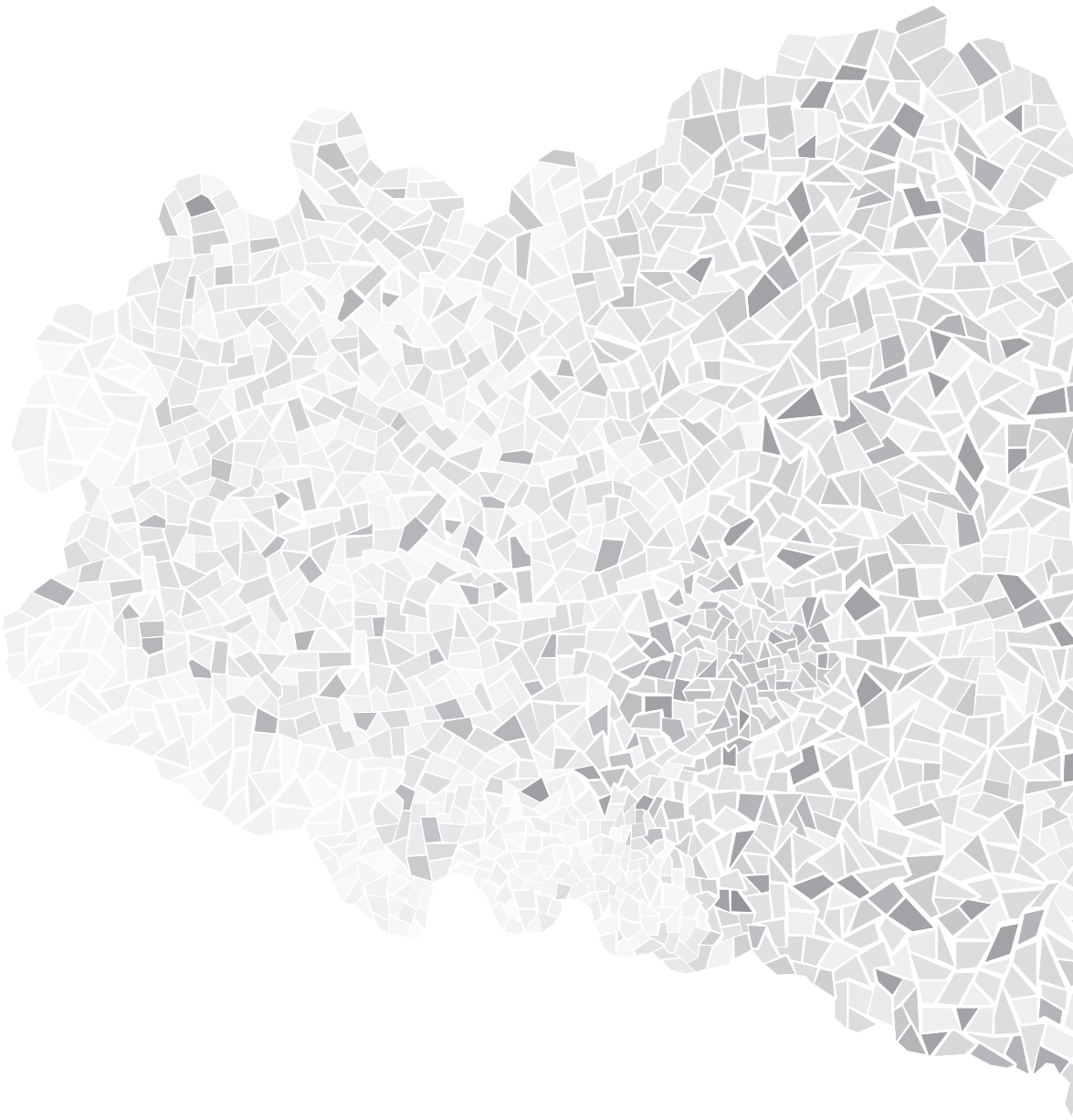

CHAPTER 2

Autotaxin and LPA receptor signaling in cancer

Cancer and Metastasis Reviews 2011

Autotaxin and LPA receptor signaling in cancer

Anna J.S. Houben[1]
and Wouter H. Moolenaar[1]

[1]Division of Cell Biology,
The Netherlands Cancer Institute,
Amsterdam, The Netherlands

ABSTRACT

Lysophosphatidic acid (LPA; monoacyl-glycerol-3-phosphate) is a lipid mediator that functions as a mitogen and motility factor for many cell types. LPA signals through six specific G protein-coupled receptors, named $LPA_{1–6}$, which trigger both overlapping and distinct signaling pathways. LPA is produced from extracellular lysophosphatidylcholine by a secreted lysophospholipase D, named autotaxin (ATX), originally identified as an "autocrine motility factor" for tumor cells. ATX-LPA signaling is vital for embryonic development and promotes tumor formation, angiogenesis, and experimental metastasis in mice. Elevated expression of ATX and/or aberrant expression of LPA receptors are found in several human malignancies, while loss of LPA_6 function has been implicated in bladder cancer. In this review, we summarize our present understanding of ATX and LPA receptor signaling in cancer.

INTRODUCTION

The impact of the tumor microenvironment on tumor progression is mediated, in large part, by growth factors, motility factors and proangiogenic factors that are produced by the tumor cells themselves as well as the surrounding stroma. One such factor is lysophosphatidic acid (LPA; monoacyl-glycerol-3-phosphate), a multifunctional lipid mediator best known for its ability to stimulate proliferation, migration and survival of many cell types, both normal and malignant. However, the list of biological responses to LPA is quite diverse, as it ranges from growth factor-like activities to neurite remodeling and modulation of ion channel activity (1;2). Bioactive LPA is produced extracellularly from lysophosphatidylcholine (LPC, an abundant plasma lipid) by a secreted lysophospholipase D (lysoPLD) (3;4), known as autotaxin (ATX), named after its first discovered activity as an "autocrine motility factor" for melanoma cells (5). LPA acts through six known G protein-coupled receptors (GPCRs), termed LPA_{1-6}, which are differentially expressed and show both overlapping and distinct signaling properties (1;6). A schematic representation of the ATX-LPA receptor signaling axis is shown in Fig. 1.

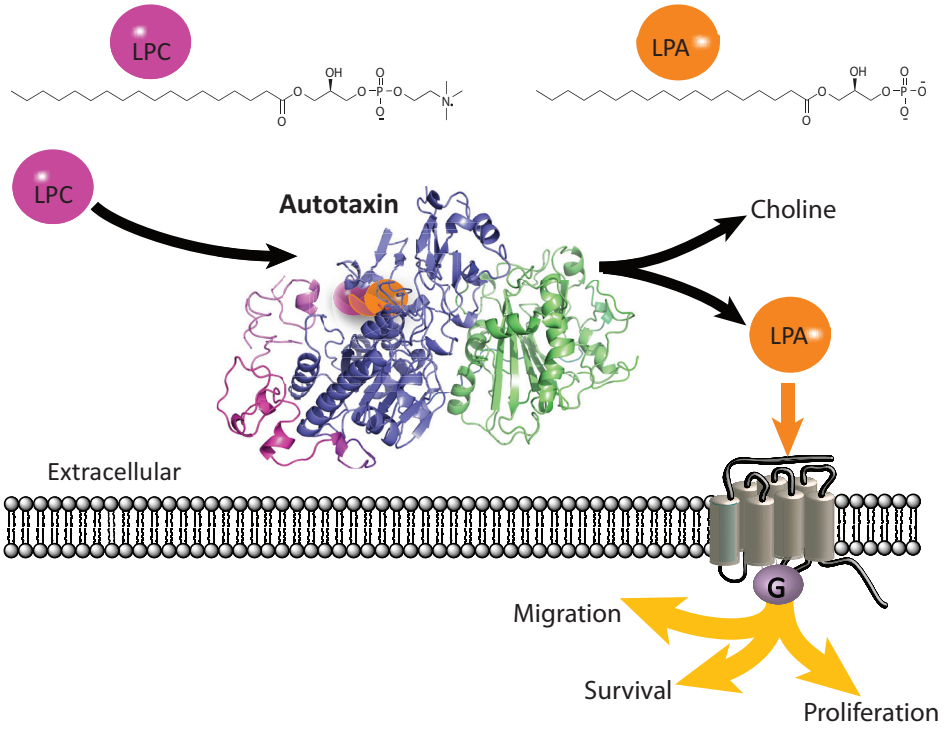

Fig. 1. Autotaxin-LPA receptor signaling. Autotaxin is a secreted lysophospholipase D that hydrolyzes extracellular LPC (an abundant plasma phospholipid) into bioactive LPA. LPA acts through specific G protein-coupled receptors and stimulates cell proliferation, migration, and survival. ATX is a multidomain enzyme; the colors refer to the specific domains (for structural details, see references (24;25)).

Increasing evidence points to an important role for ATX and LPA receptor signaling in cancer (7), as will be discussed below. In brief: (1) elevated or aberrant expression of ATX and LPA receptors is found in several human malignancies; (2) overexpression of ATX or individual LPA receptors promotes tumor formation and metastasis in mouse models, whereas knockdown has the opposite effect; and (3) LPA_2 knockout mice show reduced colon carcinogenesis. Moreover, loss of function of LPA_6 has been implicated in bladder cancer development, suggesting that LPA_6 is a candidate tumor suppressor. In this review, we summarize the evidence for a role of ATX-LPA signaling in cancer and also discuss recent developments in targeting ATX by pharmacological inhibitors.

LPA RECEPTOR SIGNALING

LPA receptors can be divided in two subfamilies. The classical LPA_{1-3} receptors belong to the so-called endothelial differentiation gene (Edg) family, whereas three additional LPA receptors (LPA_{4-6}) are more closely related to the purinergic receptor family (1;6). Depending on receptor subtype, LPA stimulation results in: (1) activation of the mitogenic $G\alpha_i$-linked Ras-Raf-MEK-ERK pathway (8;9), (2) $G\alpha_i$-mediated activation of phosphoinositide 3-kinase-beta (10), which promotes cell survival and many other cellular functions, (3) cytoskeletal remodeling, cell migration and invasion via the $G\alpha_{12/13}$-linked RhoA pathway acting in concert with the $G\alpha_i$-mediated Rac activation pathway (11-13); and (4) $G\alpha_q$-linked activation of phospholipase C with consequent production of second messengers (14;15). In addition, LPA stimulation often leads to changes in cAMP levels via either $G\alpha_i$ or $G\beta\gamma$ subunits (for review, see (1;2)). LPA stimulation also promotes the production of growth factors and cytokines via multiple pathways (16). For a given LPA receptor, the net outcome of these synergizing signaling pathways strongly depends on cellular context. For example, depending on the cell system used, LPA_4 receptor signaling may either enhance (17) or inhibit (18) tumor cell migration and invasiveness.

LPA PRODUCTION BY AUTOTAXIN, A SECRETED LYSO-PLD

LPA is produced by autotaxin (ATX or ENPP2), a member of the ecto-nucleotide pyrophosphatase/phosphodiesterase (ENPP) family. The ENPP family consists of seven structurally related ectoenzymes that hydrolyze pyrophosphate and phosphodiester bonds in nucleotides and their derivatives (19). ATX hydrolyzes LPC into LPA (plus free choline) and is the only lysoPLD in the ENPP family. ATX is synthesized as a preproenzyme, processed by a furin-type protease and secreted along the classical secretory route as a glycosylated protein into the extracellular milieu (reviewed in (20)). ATX is widely expressed and present in plasma. The origin of plasma ATX remains to be determined, but likely sources are the lymphatic high endothelial venules (21) and adipose tissue, which express and secrete ATX at high levels. Indeed, adipose-specific deletion of *Enpp2* leads to reduced plasma LPA levels (22).

ATX is a multidomain protein consisting of two N-terminal somatomedin B (SMB)-like domains, a central catalytic phosphodiesterase domain, and an N-terminal nuclease-like domain (19;20). Although ATX is capable of hydrolyzing nucleotides *in vitro*, the apparent affinity of ATX for LPC is some 10-fold higher than for nucleotides (23) and, furthermore, extracellular nucleotide levels are normally very low. Therefore, all biological effects of ATX are thought to be attributable to LPA production and subsequent receptor stimula-

tion (20). Formally, however, additional noncatalytic functions of ATX cannot be excluded at present. Recent structural studies (24;25) have revealed how the different domains of ATX are organized and interact (Fig. 1) and shed light on what makes ATX a unique lysoPLD, namely a deep hydrophobic lipid-binding pocket in the catalytic domain. The ATX structure further suggests that the SMB domains could be involved in regulating catalytic activity (24).

ATX INTERACTION WITH THE CELL SURFACE

To ensure efficient delivery of LPA to its receptors, ATX must communicate with target cells in a locally restricted manner. One mechanism by which ATX interacts with target cells is via integrins. ATX binds to activated lymphocytes via $\alpha_4\beta_1$ integrins (21) and to activated platelets via integrin β_3 (26). The SMB domains of ATX appear to be the primary mediators of integrin β_3 binding (24). Injection of enzymatically inactive ("dominant-negative") ATX in mice attenuates the homing of T cells to secondary lymphoid organs, presumably by competing with endogenous ATX for binding to integrins (21). Since ATX is abundantly expressed in lymphatic high endothelial venules (HEVs), this suggests a model in which secretion of ATX by HEVs promotes the entry of lymphocytes into lymphoid organs. In this model, ATX is secreted into the lumen of HEVs and binds to adherent lymphocytes through activated integrins. Subsequently, the lymphocyte-bound ATX may produce a high local concentration of LPA to activate LPA receptors on the lymphocytes and promote their transendothelial migration (21). In support of this scenario, LPA induces invasion of T lymphoma cells across a monolayer of normal fibroblasts (12). Thus, ATX/LPA could use a similar strategy to stimulate the extravasation of circulating tumor cells, a hallmark of the metastatic cascade.

Since ATX is a heparin-binding protein (as it can be purified using heparin affinity chromatography), binding to heparan sulfate proteoglycans (HSPs) on the cell surface could be an alternative or additional way by which ATX ensures local delivery of LPA to its cognate receptors. Thus, diverse scenarios for localized LPA production and signaling can be envisioned in which ATX is recruited to target cells via specific cell-surface molecules such as integrins and HSPs.

ATX AND LPA RECEPTORS IN EMBRYONIC DEVELOPMENT

Gene targeting studies in mice have revealed a vital role for ATX during embryogenesis, as *Enpp2* knockout causes embryonic lethality at midgestation (around E9.5) due to severe vascular defects in both yolk sac and the embryo proper (27;28). The vascular network normally present in the yolk sac is completely absent and replaced by blood patches, while blood vessels in the embryo are enlarged; furthermore, the neural tube is malformed (28;29). Heterozygous *Enpp2* knockout mice show half-normal plasma LPA levels, consistent with ATX being the major LPA-producing enzyme in the circulation. The phenotype of *Enpp2*-knockout mice is strongly reminiscent of that of the $G\alpha_{13}$ knockout, suggesting that the observed defects in *Enpp2*-null embryos can be explained by loss of migratory G_{13}-RhoA signaling through multiple LPA receptors (28;30).

The phenotype of individual LPA receptor knockouts is much less severe than that of the *Enpp2* knockout. Thus far, LPA receptor knockout studies in mice have uncovered normal physiological roles for LPA signaling in such diverse processes as neurogenesis (31) and bone

formation (32) (LPA_1), embryo implantation (LPA_3) (33), and formation of blood and lymphatic vessels (LPA_4) (34). *Lpa*$_2$-knockout mice show no abnormalities (35), while the *Lpa*$_5$- and *Lpa*$_6$-deficient phenotypes remain to be described.

ATX-LPA RECEPTOR SIGNALING IN CANCER

Since the discovery of ATX as an autocrine motility factor for melanoma cells, many subsequent studies have implicated a role for ATX-LPA signaling in tumor formation and metastasis.

Studies in vitro

High expression of ATX is found in a number of tumor cell types, including neuroblastoma (36), hepatocellular carcinoma (37), breast cancer (38), renal cell carcinoma (39), glioblastoma (40), non-small cell lung cancer (NSCLC) (41), B cell lymphomas (42;43), and thyroid carcinoma (44). Expression of ATX is found both in the tumor core as well as in the invasive cells of glioblastomas (40), and in NSCLC the highest expression is detected in poorly differentiated tumors (41). This argues that ATX is able to augment cellular characteristics necessary for tumor aggressiveness.

ATX expression is regulated by various growth factors, cytokines, and (proto-)oncogenes, which will differ per cell type and thus cause diverse outcomes. For example, EGF, bFGF, TGFβ, and other factors induce up- or down-regulation of ATX mRNA depending on cell type (44;45). v-Jun-transformed fibroblasts show strongly upregulated ATX expression (46), while ATX is upregulated in Wilms' tumors harboring oncogenic β-catenin mutations (47) and in mammary epithelial cells stimulated by Wnt-1 (48). Downregulation of ATX is observed following retinoic acid treatment of Wilms' tumor cells and N-Myc-overexpressing neuroblastoma cells (49;50).

In Hodgkin lymphoma cells, Epstein-Barr virus infection leads to strong induction of ATX expression, with subsequent generation of LPA and enhanced cell growth and survival (42). Specific downregulation of ATX decreased LPA levels and reduced cell growth and viability in these cells. Furthermore, ATX expression is strongly induced upon forced expression of integrin $\alpha_6\beta_4$ in MDA-MB-435 tumor cells, an effect mediated by the transcription factor NFAT1 (51). This provides a possible explanation for the stimulatory effect of integrin $\alpha_6\beta_4$ on tumor cell migration and invasion.

INSIGHTS FROM MOUSE STUDIES

Xenograft models

The first evidence for a tumorigenic role of ATX *in vivo* came from studies using ATX-overexpressing, Ras-transformed NIH3T3 cells. ATX overexpression resulted in increased tumor growth, aggressiveness, and angiogenesis, whereas the inactive mutant ATX(T210A) did not (45;52). Subsequent studies have shown a role for both ATX and LPA receptor signaling in tumor progression and metastasis. LPA_1 overexpression in MDA-MB-231 breast cancer cells promotes increased skeletal tumor growth and tumor-induced bone destruction in xenografted mice. The tumor cells do not express ATX, but they stimulate the production of LPA by activated platelets, thereby promoting tumor cell proliferation and cytokine-mediated

bone destruction (53). Silencing or pharmacological inhibition of LPA_1 reduced both tumor growth and bone metastasis progression (54). Furthermore, ATX overexpression in mammary carcinoma cells promotes metastasis to bone, while silencing of endogenous ATX expression inhibited metastasis, with little effect on primary tumor growth (55).

Forced overexpression of LPA_1, LPA_2, or LPA_3 in ovarian cancer cells enhances tumor growth in nude mice, showing increased growth factor production, ascites formation, and organ invasion (56). In another study, overexpressed LPA_1, LPA_2, and LPA_4 were found to collaborate with c-Myc and Tbx2 (a transcriptional repressor of p19Arf) to transform mouse embryo fibroblasts (MEFs) both *in vitro* and in xenografts. In this case, LPA-mediated cell transformation is mediated by the G_i-linked MAPK and PI3K pathways. Overexpression of individual LPA receptors in naïve MEFs had no transforming effect, indicating that LPA signaling needs to collaborate with other pro-oncogenic events to induce cell transformation (57).

Genetic models

Unfortunately, the embryonic lethality of *Enpp2*-deficient mice has hampered studies on the importance of ATX in cancer progression. However, important insights have been gained from studies in transgenic and LPA receptor-knockout mice. MMTV-driven overexpression of ATX or individual LPA receptors (LPA_{1-3}) in mouse mammary gland leads to late-onset invasive and metastatic mammary carcinomas and cancer-associated inflammation. The transgene expression influenced several signaling pathways, including PI3K-Akt and MAPK pathways, as well as Wnt pathway components and E-cadherin. The ATX and LPA receptor-driven tumors do not form a distinct cluster, as would be expected due to the fact that each of the receptors links to particular pathways and functional outcomes (58). This reinforces the notion that transgenic overexpression of ATX and LPA receptors allows accumulation of secondary mutations leading to mammary cancers, possibly by increasing cell viability upon LPA signaling and thus increasing the likelihood of acquiring (pro-)oncogenic mutations.

Of the known LPA receptors, LPA_2 has been implicated in intestinal cancer. In a model of chemically induced colon carcinogenesis, *Lpa*$_2$-knockout mice (which show a wild-type phenotype) display a remarkably reduced tumor incidence and progression. This is accompanied by a decrease in both cell proliferation and chemokine expression, in particular the proinflammatory factors MCP-1 and MIF which are associated with colorectal cancer. Reduced colon tumorigenesis in the *Lpa*$_2$-null animals correlated with reduced infiltration by macrophages, a predominant stromal cell type known to contribute to tumor progression. Furthermore, LPA treatment increased tumor incidence in *Apc*$^{min/+}$ mice, a model for spontaneous intestinal cancer (59). Conversely, loss of LPA_2 dramatically reduced tumor incidence in *Apc*$^{min/+}$ mice, accompanied by reduced expression levels of cell cycle regulators such as KLF5, c-Myc and cyclin D1 (60). These studies show that LPA_2, in combination with loss of the tumor suppressor APC, is capable of promoting tumorigenesis in the colon. It thus appears that, again, LPA signaling increases the susceptibility to accelerate cancer progression when other genetic factors are present. The results from the various *in vivo* studies are summarized in Table 1.

CLINICAL IMPLICATIONS

To what extent do the findings obtained in mouse models bear relevance to the human disease? Cancer-specific gain-of-function mutations in ATX or LPA receptors have not been reported to date; in contrast, loss-of-function mutations have been reported for LPA_6 in bladder cancer (see below). Analysis of multiple microarray datasets (www.oncomine.org)

		Model	System	Remarks	Phenotype	Refs.
ATX overexpression		Xenograft	NIH3T3 cells (Ras transformed)	v-Ras dependent	Increased tumorigenesis, metastasis and angiogenesis	45, 52
		Xenograft	Human breast cancer (MDA-MB231 metastatic subclone)		Enhanced tumor growth and metastasis to bone	55
		Transgene	Mammary gland	MMTV driven	Induction of invasive and metastatic mammary cancer	58
ATX knockdown		Xenograft	Mouse mammary tumor cells (4T1)		Reduced bone metastasis (unaffected primary tumor growth)	55
LPA receptor overexpression	LPA_{1-3}	Xenograft	Ovarian cancer cells		Increased tumor growth, invasion, cytokine production and ascites formation	56
	$LPA_{1,2,4}$	Xenograft	Mouse embryonic fibroblasts	Myc dependent	Induction of tumor formation	57
	LPA_1	Xenograft	Human breast cancer cells (MDA-MB231 metastatic subclone)	Involvement of platelets	Enhanced tumor formation and metastasis to bone	53, 54
	LPA_{1-3}	Transgene	Mammary gland	MMTV driven	Induction of invasive and metastatic mammary cancer	58
LPA receptor knockdown	LPA_1	Xenograft	Human breast cancer cells (MDA-MB231 metastatic subclone)	Reproduced by LPA_1 antagonist Ki16425	Reduced tumor growth and metastasis to bone	54
LPA receptor knockout	LPA_2	Knockout	Chemically induced colon cancer model		Reduced tumor incidence; less macrophage infiltration	59
	LPA_2	Knockout	$APC^{min/+}$ intestinal cancer model		Reduced tumor incidence	60

Table 1. In vivo ATX and LPA receptor cancer models.

reveals strongly elevated ATX expression in certain human cancers, especially B cell lymphomas, renal carcinoma, liver cancer, and pancreatic cancer. Also, individual LPA receptors are found overexpressed in several cancers when compared to the corresponding normal tissues (www.oncomine.org, see also (7)).

In follicular lymphoma, serum ATX levels correlate with tumor burden and clinical course, suggesting that ATX may serve as a biomarker in follicular lymphoma (43). Furthermore, an increase in serum ATX activity has been reported in pancreatic cancer patients (61) and *ENPP2* is one of the genes in a 64-gene signature that predicts poor survival of patients with stage I NSCLC (62). As a word of caution, it should be realized that high ATX expression by itself does not necessarily imply elevated LPA levels and enhanced receptor signaling, since substrate (LPC) availability and LPA degradation by cell-associated lipid phosphate phosphatases are additional determinants of bioactive LPA levels in the cellular microenvironment (20). Ultimately, it is the LPA receptor expression profile on both the tumor and surrounding stromal cells that will determine the outcome of enhanced ATX expression. One area of future research is to establish to what extent aberrant ATX and/or LPA receptor expression patterns are associated with clinical outcome.

LPA_6: a candidate tumor suppressor in bladder cancer

The LPA_6 receptor, previously known as orphan receptor P2Y5 (or 6H1), deserves special mention because it has been associated with familial bladder cancer (63) as well as genetic hair growth abnormalities (64). LPA_6/P2Y5 is known to couple to the G_{13}-RhoA signaling pathway, which regulates the actin cytoskeleton, but it does not mediate changes in cytosolic calcium or cAMP (65). *P2RY5* is an inducible gene: its expression is rapidly induced upon T cell activation (66) and in LPA-stimulated fibroblasts (16).

The LPA_6-encoding gene, *P2RY5,* is located inside the retinoblastoma tumor suppressor gene *RB1* (intron 17) in the reverse orientation. In bladder cancer, a segment around *RB1* is characterized by a loss of polymorphism associated with the initial expansion of neoplasia (63;67). This segment contains several so-called forerunner genes that may contribute to such expansion, and *P2RY5* is one of these genes. Homozygous mutational inactivation of *P2RY5* precedes the loss of *RB* during tumor development, while nucleotide substitutions in *P2RY5* represent a cancer-predisposing factor, particularly in combination with tobacco smoking (63;67). Reintroduction of *P2RY5* into bladder cancer cells that lacked it resulted in cell cycle arrest and apoptosis, consistent with *P2RY5* being a candidate tumor suppressor. One family with an inherited risk of cancer, including breast, colon, lung, prostate, and uterus, carried a germline mutation in *P2RY5*. The most frequent polymorphism results in a W307C mutation in the LPA_6 cytoplasmic tail. This could affect LPA_6 interaction with G proteins (63;67) and hence compromise LPA signaling, but this needs to be tested. Interestingly, a single nucleotide polymorphism within the same genomic locus that is predicted to downregulate *P2RY5* expression is a potential risk factor for developing invasive ovarian cancer (68).

Loss of P2RY5 function has also been implicated in genetic hair growth disorders (64). LPA_6 is detected in the inner root sheath of hair follicles. However, human hair follicles do not express ATX but, instead, an LPA-producing phospholipase A1 encoded by *LIPH* (69); mutations in *LIPH* induce the same abnormal hair growth phenotype as mutations in *LPA_6*. This

raises the question of whether LPA_6 in other tissues, such as bladder epithelium, is normally stimulated via ATX- or LIPH-mediated LPA production. Given the very restricted tissue distribution of LIPH, however, ATX is the more attractive candidate. In conclusion, LPA_6 provides a new paradigm for cancer development and may represent an early detection and risk marker in bladder cancer (70). It is now important that the biological function and signaling properties of LPA_6 and its mutant versions be elucidated in further detail.

ATX AS DRUG TARGET

As a secreted phosphodiesterase, ATX is an attractive and easily "druggable" therapeutic target. Several ATX inhibitors have been based on the seminal finding that LPA and sphingosine 1-phosphate (S1P) inhibits ATX activity against nucleotides and artificial substrates (K_i about 100 nM) (23). Several LPA analogs have been described as ATX inhibitors, some with an effect on melanoma cell metastasis (71;72) and breast tumor growth in mice (73). Yet, the potency of LPA analogs is rather low (and even very poor when tested in ATX-mediated LPC hydrolysis assays), and it is not clear whether the reported *in vivo* effects are attributable to ATX inhibition. Most LPA-based ATX inhibitors lack an *in vivo* pharmacodynamic proof of principle in that they have not shown to lower circulating LPA levels. Furthermore, there are concerns about their potential agonistic effect on LPA receptors. FTY720, a structural analogue of sphingosine, is an immunomodulator for patients with relapsing multiple sclerosis. The active form, FTY720-phosphate (FTY-P) is an S1P mimetic and acts on S1P receptors with high potency. At higher concentrations, FTY-P (like S1P) is a competitive inhibitor of ATX and reduces plasma LPA levels when injected into mice (74). It remains to be seen, however, whether ATX inhibition underlies the reported anticancer effects of high doses FTY720 (74). Lipid phosphonate analogs that inhibit ATX activity against artificial substrates show a reducing effect on plasma LPA levels and B16 melanoma metastasis; however, their potency is relatively low (75).

Nonlipid, small-molecule inhibitors clearly hold more promise. High-throughput screening identified thiazolidinedione-based compounds as a new class of ATX inhibitors (76). Their potency is increased dramatically by introduction of a boronic acid moiety, designed to target the catalytic Thr residue in ATX. The most potent analogs show IC_{50} values <10 nM in LPC hydrolysis assays. Injection of these compounds into mice results in a rapid fall in circulating LPA levels, consistent with LPA being rapidly produced and degraded *in vivo* (76;77). The crystal structure of ATX in complex with a boronic acid inhibitor reveals that it forms a reversibly covalent bond with the Thr210 nucleophile in the hydrophobic lipid-binding pocket of ATX (24). Another small-molecule inhibitor of ATX, PF-8380, shows adequate oral bioavailability and *in vivo* potency in reducing LPA levels in plasma and at sites of inflammation, indicating that ATX is a major source of LPA during inflammation. Furthermore, a close pharmacokinetic/pharmacodynamic relationship was observed (78). Compounds like PF-8380 and thiazolidinediones can serve as useful tools for elucidating the role of ATX in tumor progression in mice.

CONCLUDING REMARKS

Given its mitogenic and chemotactic properties, together with the wide distribution of LPA receptors, it is not surprising that LPA, when produced in the tumor-stroma microenvironment, can enhance cancer progression. Although the clinical consequences of enhanced or aberrant LPA production and signaling remain to be determined, studies in mice have provided strong evidence that the ATX-LPA receptor signaling axis contributes to tumor formation, angiogenesis, and metastasis. The *in vivo* studies also indicate that distinct oncogenic events, such as H-Ras or c-Myc activation, must collaborate with LPA signaling to promote tumor progression. The LPA_2 receptor provides perhaps the strongest case for a link between LPA signaling and cancer, since *Lpa*$_2$-knockout mice show a marked decrease in colon tumor incidence. Additional evidence is provided by the study on transgenic overexpression of ATX and LPA receptors in mouse mammary gland. To more broadly assess the importance of LPA signaling in tumor maintenance and progression, a logical approach would be to crossbreed LPA receptor-null mice with genetically engineered mouse tumor models, in which cancer is initiated by *Cre*-recombinase-mediated activation of oncogenic mutations in specific tissues.

The LPA_6 receptor represents an interesting case, since it may function as a tumor suppressor in familial bladder cancer and loss of function mutations have been detected in patients; nucleotide substitutions in the LPA_6-encoding gene (*P2RY5*) are considered a cancer-predisposing factor. Obviously, these intriguing findings require further validation and investigation. *Lpa*$_6$ knockout mice will provide a powerful tool to examine the suspected tumor-suppressing function of LPA_6.

Hopefully, the knowledge on ATX-LPA signaling gleaned in academic labs can now be applied toward the development of new drugs for cancer treatment in the foreseeable future. That ATX is an extracellular enzyme and GPCRs, such as those for LPA, are highly druggable will add to their attractiveness as targets. Potent small-molecule inhibitors that target ATX *in vivo* have already been described. Now that the crystal structure of ATX has been determined, drug development efforts will undoubtedly get a further boost.

ACKNOWLEDGEMENTS

Work related to this review is supported by grants from the Dutch Cancer Society and the Netherlands Organization of Pure Research. We thank Anastassis Perrakis for designing Fig. 1.

REFERENCES

1. Choi, J. W., Herr, D. R., Noguchi, K., Yung, Y. C., Lee, C. W., Mutoh, T., Lin, M. E., Teo, S. T., Park, K. E., Mosley, A. N., and Chun, J. (2010) *Annu. Rev. Pharmacol. Toxicol.* 50, 157-186
2. Moolenaar, W. H., van Meeteren, L. A., and Giepmans, B. N. (2004) *Bioessays* 26, 870-881
3. Tokumura, A., Majima, E., Kariya, Y., Tominaga, K., Kogure, K., Yasuda, K., and Fukuzawa, K. (2002) *J. Biol. Chem.* 277, 39436-39442
4. Umezu-Goto, M., Kishi, Y., Taira, A., Hama, K., Dohmae, N., Takio, K., Yamori, T., Mills, G. B., Inoue, K., Aoki, J., and Arai, H. (2002) *J. Cell Biol.* 158, 227-233
5. Stracke, M. L., Krutzsch, H. C., Unsworth, E. J., Arestad, A., Cioce, V., Schiffmann, E., and Liotta, L. A. (1992) *J. Biol. Chem.* 267, 2524-2529
6. Chun, J., Hla, T., Lynch, K. R., Spiegel, S., and Moolenaar, W. H. (2010) *Pharmacol. Rev.* 62, 579-587
7. Mills, G. B. and Moolenaar, W. H. (2003) *Nat. Rev. Cancer* 3, 582-591
8. Kranenburg, O. and Moolenaar, W. H. (2001) *Oncogene* 20, 1540-1546
9. van Corven, E. J., Hordijk, P. L., Medema, R. H., Bos, J. L., and Moolenaar, W. H. (1993) *Proc. Natl. Acad. Sci. U. S. A* 90, 1257-1261
10. Guillermet-Guibert, J., Bjorklof, K., Salpekar, A., Gonella, C., Ramadani, F., Bilancio, A., Meek, S., Smith, A. J., Okkenhaug, K., and Vanhaesebroeck, B. (2008) *Proc. Natl. Acad. Sci. U. S. A* 105, 8292-8297
11. Kranenburg, O., Poland, M., van Horck, F. P., Drechsel, D., Hall, A., and Moolenaar, W. H. (1999) *Mol. Biol. Cell* 10, 1851-1857
12. Stam, J. C., Michiels, F., van der Kammen, R. A., Moolenaar, W. H., and Collard, J. G. (1998) *EMBO J.* 17, 4066-4074
13. van Leeuwen, F. N., Olivo, C., Grivell, S., Giepmans, B. N., Collard, J. G., and Moolenaar, W. H. (2003) *J. Biol. Chem.* 278, 400-406
14. Jalink, K., van Corven, E. J., and Moolenaar, W. H. (1990) *J. Biol. Chem.* 265, 12232-12239
15. van Corven, E. J., Groenink, A., Jalink, K., Eichholtz, T., and Moolenaar, W. H. (1989) *Cell* 59, 45-54
16. Stortelers, C., Kerkhoven, R., and Moolenaar, W. H. (2008) *BMC. Genomics* 9, 387
17. Harper, K., Arsenault, D., Boulay-Jean, S., Lauzier, A., Lucien, F., and Dubois, C. M. (2010) *Cancer Res.* 70, 4634-4643
18. Lee, Z., Cheng, C. T., Zhang, H., Subler, M. A., Wu, J., Mukherjee, A., Windle, J. J., Chen, C. K., and Fang, X. (2008) *Mol. Biol. Cell* 19, 5435-5445
19. Stefan, C., Jansen, S., and Bollen, M. (2005) *Trends Biochem. Sci.* 30, 542-550
20. van Meeteren, L. A. and Moolenaar, W. H. (2007) *Prog. Lipid Res.* 46, 145-160
21. Kanda, H., Newton, R., Klein, R., Morita, Y., Gunn, M. D., and Rosen, S. D. (2008) *Nat. Immunol.* 9, 415-423
22. Dusaulcy, R., Rancoule, C., Gres, S., Wanecq, E., Colom, A., Guigne, C., van Meeteren, L. A., Moolenaar, W. H., Valet, P., and Saulnier-Blache, J. S. (2011) *J. Lipid Res.* 52, 1247-1255
23. van Meeteren, L. A., Ruurs, P., Christodoulou, E., Goding, J. W., Takakusa, H., Kikuchi, K., Perrakis, A., Nagano, T., and Moolenaar, W. H. (2005) *J. Biol. Chem.* 280, 21155-21161
24. Hausmann, J., Kamtekar, S., Christodoulou, E., Day, J. E., Wu, T., Fulkerson, Z., Albers, H. M., van Meeteren, L. A., Houben, A. J., van, Z. L., Jansen, S., Andries, M., Hall, T., Pegg, L. E., Benson, T. E., Kasiem, M., Harlos, K., Kooi, C. W., Smyth, S. S., Ovaa, H., Bollen, M., Morris, A. J., Moolenaar, W. H., and Perrakis, A. (2011) *Nat. Struct. Mol. Biol.* 18, 198-204
25. Nishimasu, H., Okudaira, S., Hama, K., Mihara, E., Dohmae, N., Inoue, A., Ishitani, R., Takagi, J., Aoki, J., and Nureki, O. (2011) *Nat. Struct. Mol. Biol.* 18, 205-212
26. Pamuklar, Z., Federico, L., Liu, S., Umezu-Goto, M., Dong, A., Panchatcharam, M., Fulkerson, Z., Berdyshev, E., Natarajan, V., Fang, X., van Meeteren, L. A., Moolenaar, W. H., Mills, G. B., Morris, A. J., and Smyth, S. S. (2009) *J. Biol. Chem.* 284, 7385-7394
27. Tanaka, M., Okudaira, S., Kishi, Y., Ohkawa, R., Iseki, S., Ota, M., Noji, S., Yatomi, Y., Aoki, J., and Arai, H. (2006) *J Biol Chem* 281, 25822-25830
28. van Meeteren, L. A., Ruurs, P., Stortelers, C., Bouwman, P., van Rooijen, M. A., Pradere, J. P., Pettit, T. R., Wakelam, M. J., Saulnier-Blache, J. S., Mummery, C. L., Moolenaar, W. H., and Jonkers, J. (2006) *Mol Cell Biol* 26, 5015-5022
29. Fotopoulou, S., Oikonomou, N., Grigorieva, E., Nikitopoulou, I., Paparountas, T., Thanassopoulou, A., Zhao, Z., Xu, Y., Kontoyiannis, D. L., Remboutsika, E., and Aidinis, V. (2010) *Dev. Biol.* 339, 451-464
30. Koike, S., Keino-Masu, K., and Masu, M. (2010) *Biochem Biophys Res Commun* 400, 66-71
31. Matas-Rico, E., Garcia-Diaz, B., Llebrez-Zayas, P., Lopez-Barroso, D., Santín, L., Pedraza, C., Smith-Fernandez, A., Fernandez-Llebrez, P., Tellez, T., Redondo, M., Chun, J., De Fonseca, F. R., and Estivill-Torrus, G. (2008) *Mol. Cell Neurosci.* 39, 342-355
32. Gennero, I., Laurencin-Dalicieux, S., Conte-Au-

riol, F., Briand-Mesange, F., Laurencin, D., Rue, J., Beton, N., Malet, N., Mus, M., Tokumura, A., Bourin, P., Vico, L., Brunel, G., Oreffo, R. O., Chun, J., and Salles, J. P. (2011) *Bone* 49, 395-403

33. Ye, X., Hama, K., Contos, J. J., Anliker, B., Inoue, A., Skinner, M. K., Suzuki, H., Amano, T., Kennedy, G., Arai, H., Aoki, J., and Chun, J. (2005) *Nature* 435, 104-108
34. Sumida, H., Noguchi, K., Kihara, Y., Abe, M., Yanagida, K., Hamano, F., Sato, S., Tamaki, K., Morishita, Y., Kano, M. R., Iwata, C., Miyazono, K., Sakimura, K., Shimizu, T., and Ishii, S. (2010) *Blood* 116, 5060-5070
35. Contos, J. J., Ishii, I., Fukushima, N., Kingsbury, M. A., Ye, X., Kawamura, S., Brown, J. H., and Chun, J. (2002) *Mol Cell Biol* 22, 6921-6929
36. Kawagoe, H., Stracke, M. L., Nakamura, H., and Sano, K. (1997) *Cancer Res.* 57, 2516-2521
37. Zhang, G., Zhao, Z., Xu, S., Ni, L., and Wang, X. (1999) *Chin Med. J. (Engl.)* 112, 330-332
38. Yang, S. Y., Lee, J., Park, C. G., Kim, S., Hong, S., Chung, H. C., Min, S. K., Han, J. W., Lee, H. W., and Lee, H. Y. (2002) *Clin. Exp. Metastasis* 19, 603-608
39. Stassar, M. J., Devitt, G., Brosius, M., Rinnab, L., Prang, J., Schradin, T., Simon, J., Petersen, S., Kopp-Schneider, A., and Zoller, M. (2001) *Br. J. Cancer* 85, 1372-1382
40. Hoelzinger, D. B., Mariani, L., Weis, J., Woyke, T., Berens, T. J., McDonough, W. S., Sloan, A., Coons, S. W., and Berens, M. E. (2005) *Neoplasia.* 7, 7-16
41. Yang, Y., Mou, L., Liu, N., and Tsao, M. S. (1999) *Am. J. Respir. Cell Mol. Biol.* 21, 216-222
42. Baumforth, K. R., Flavell, J. R., Reynolds, G. M., Davies, G., Pettit, T. R., Wei, W., Morgan, S., Stankovic, T., Kishi, Y., Arai, H., Nowakova, M., Pratt, G., Aoki, J., Wakelam, M. J., Young, L. S., and Murray, P. G. (2005) *Blood* 106, 2138-2146
43. Masuda, A., Nakamura, K., Izutsu, K., Igarashi, K., Ohkawa, R., Jona, M., Higashi, K., Yokota, H., Okudaira, S., Kishimoto, T., Watanabe, T., Koike, Y., Ikeda, H., Kozai, Y., Kurokawa, M., Aoki, J., and Yatomi, Y. (2008) *Br. J. Haematol.* 143, 60-70
44. Kehlen, A., Englert, N., Seifert, A., Klonisch, T., Dralle, H., Langner, J., and Hoang-Vu, C. (2004) *Int. J. Cancer* 109, 833-838
45. Nam, S. W., Clair, T., Kim, Y. S., McMarlin, A., Schiffmann, E., Liotta, L. A., and Stracke, M. L. (2001) *Cancer Res* 61, 6938-6944
46. Black, E. J., Clair, T., Delrow, J., Neiman, P., and Gillespie, D. A. (2004) *Oncogene* 23, 2357-2366
47. Zirn, B., Samans, B., Wittmann, S., Pietsch, T., Leuschner, I., Graf, N., and Gessler, M. (2006) *Genes Chromosomes. Cancer* 45, 565-574
48. Tice, D. A., Szeto, W., Soloviev, I., Rubinfeld, B., Fong, S. E., Dugger, D. L., Winer, J., Williams, P. M., Wieand, D., Smith, V., Schwall, R. H., Pennica, D., and Polakis, P. (2002) *J. Biol. Chem.* 277, 14329-14335
49. Dufner-Beattie, J., Lemons, R. S., and Thorburn, A. (2001) *Mol. Carcinog.* 30, 181-189
50. Zirn, B., Samans, B., Spangenberg, C., Graf, N., Eilers, M., and Gessler, M. (2005) *Oncogene* 24, 5246-5251
51. Chen, M. and O'Connor, K. L. (2005) *Oncogene* 24, 5125-5130
52. Nam, S. W., Clair, T., Campo, C. K., Lee, H. Y., Liotta, L. A., and Stracke, M. L. (2000) *Oncogene* 19, 241-247
53. Boucharaba, A., Serre, C. M., Gres, S., Saulnier-Blache, J. S., Bordet, J. C., Guglielmi, J., Clezardin, P., and Peyruchaud, O. (2004) *J Clin Invest* 114, 1714-1725
54. Boucharaba, A., Serre, C. M., Guglielmi, J., Bordet, J. C., Clezardin, P., and Peyruchaud, O. (2006) *Proc Natl Acad Sci U S A* 103, 9643-9648
55. David, M., Wannecq, E., Descotes, F., Jansen, S., Deux, B., Ribeiro, J., Serre, C. M., Gres, S., Bendriss-Vermare, N., Bollen, M., Saez, S., Aoki, J., Saulnier-Blache, J. S., Clezardin, P., and Peyruchaud, O. (2010) *PLoS One* 5, e9741
56. Yu, S., Murph, M. M., Lu, Y., Liu, S., Hall, H. S., Liu, J., Stephens, C., Fang, X., and Mills, G. B. (2008) *J. Natl. Cancer Inst.* 100, 1630-1642
57. Taghavi, P., Verhoeven, E., Jacobs, J. J., Lambooij, J. P., Stortelers, C., Tanger, E., Moolenaar, W. H., and van Lohuizen, M. (2008) *Oncogene* 27, 6806-6816
58. Liu, S., Umezu-Goto, M., Murph, M., Lu, Y., Liu, W., Zhang, F., Yu, S., Stephens, L. C., Cui, X., Murrow, G., Coombes, K., Muller, W., Hung, M. C., Perou, C. M., Lee, A. V., Fang, X., and Mills, G. B. (2009) *Cancer Cell* 15, 539-550
59. Lin, S., Wang, D., Iyer, S., Ghaleb, A. M., Shim, H., Yang, V. W., Chun, J., and Yun, C. C. (2009) *Gastroenterology* 136, 1711-1720
60. Lin, S., Lee, S. J., Shim, H., Chun, J., and Yun, C. C. (2010) *Am. J. Physiol Gastrointest. Liver Physiol* 299, G1128-G1138
61. Nakai, Y., Ikeda, H., Nakamura, K., Kume, Y., Fujishiro, M., Sasahira, N., Hirano, K., Isayama, H., Tada, M., Kawabe, T., Komatsu, Y., Omata, M., Aoki, J., Koike, K., and Yatomi, Y. (2011) *Clin. Biochem.* 44, 576-581
62. Lu, Y., Lemon, W., Liu, P. Y., Yi, Y., Morrison, C., Yang, P., Sun, Z., Szoke, J., Gerald, W. L., Watson,

M., Govindan, R., and You, M. (2006) *PLoS. Med.* 3, e467
63. Lee, S., Jeong, J., Majewski, T., Scherer, S. E., Kim, M. S., Tuziak, T., Tang, K. S., Baggerly, K., Grossman, H. B., Zhou, J. H., Shen, L., Bondaruk, J., Ahmed, S. S., Samanta, S., Spiess, P., Wu, X., Filipek, S., McConkey, D., Bar-Eli, M., Issa, J. P., Benedict, W. F., and Czerniak, B. (2007) *Proc. Natl. Acad. Sci. U. S. A* 104, 13732-13737
64. Pasternack, S. M., von, K., I, Aboud, K. A., Lee, Y. A., Ruschendorf, F., Voss, K., Hillmer, A. M., Molderings, G. J., Franz, T., Ramirez, A., Nurnberg, P., Nothen, M. M., and Betz, R. C. (2008) *Nat. Genet.* 40, 329-334
65. Yanagida, K., Masago, K., Nakanishi, H., Kihara, Y., Hamano, F., Tajima, Y., Taguchi, R., Shimizu, T., and Ishii, S. (2009) *J. Biol. Chem.* 284, 17731-17741
66. Kaplan, M. H., Smith, D. I., and Sundick, R. S. (1993) *J. Immunol.* 151, 628-636
67. Majewski, T., Lee, S., Jeong, J., Yoon, D. S., Kram, A., Kim, M. S., Tuziak, T., Bondaruk, J., Lee, S., Park, W. S., Tang, K. S., Chung, W., Shen, L., Ahmed, S. S., Johnston, D. A., Grossman, H. B., Dinney, C. P., Zhou, J. H., Harris, R. A., Snyder, C., Filipek, S., Narod, S. A., Watson, P., Lynch, H. T., Gazdar, A., Bar-Eli, M., Wu, X. F., McConkey, D. J., Baggerly, K., Issa, J. P., Benedict, W. F., Scherer, S. E., and Czerniak, B. (2008) *Lab Invest* 88, 694-721
68. Song, H., Ramus, S. J., Shadforth, D., Quaye, L., Kjaer, S. K., DiCioccio, R. A., Dunning, A. M., Hogdall, E., Hogdall, C., Whittemore, A. S., McGuire, V., Lesueur, F., Easton, D. F., Jacobs, I. J., Ponder, B. A., Gayther, S. A., and Pharoah, P. D. (2006) *Cancer Res.* 66, 10220-10226
69. Kazantseva, A., Goltsov, A., Zinchenko, R., Grigorenko, A. P., Abrukova, A. V., Moliaka, Y. K., Kirillov, A. G., Guo, Z., Lyle, S., Ginter, E. K., and Rogaev, E. I. (2006) *Science* 314, 982-985
70. Crawford, J. M. (2008) *Lab Invest* 88, 686-693
71. Baker, D. L., Fujiwara, Y., Pigg, K. R., Tsukahara, R., Kobayashi, S., Murofushi, H., Uchiyama, A., Murakami-Murofushi, K., Koh, E., Bandle, R. W., Byun, H. S., Bittman, R., Fan, D., Murph, M., Mills, G. B., and Tigyi, G. (2006) *J. Biol. Chem.* 281, 22786-22793
72. Durgam, G. G., Virag, T., Walker, M. D., Tsukahara, R., Yasuda, S., Liliom, K., van Meeteren, L. A., Moolenaar, W. H., Wilke, N., Siess, W., Tigyi, G., and Miller, D. D. (2005) *J. Med. Chem.* 48, 4919-4930
73. Zhang, H., Xu, X., Gajewiak, J., Tsukahara, R., Fujiwara, Y., Liu, J., Fells, J. I., Perygin, D., Parrill, A. L., Tigyi, G., and Prestwich, G. D. (2009) *Cancer Res.* 69, 5441-5449
74. van Meeteren, L. A., Brinkmann, V., Saulnier-Blache, J. S., Lynch, K. R., and Moolenaar, W. H. (2008) *Cancer Lett.* 266, 203-208
75. Gupte, R., Patil, R., Liu, J., Wang, Y., Lee, S. C., Fujiwara, Y., Fells, J., Bolen, A. L., Emmons-Thompson, K., Yates, C. R., Siddam, A., Panupinthu, N., Pham, T. C., Baker, D. L., Parrill, A. L., Mills, G. B., Tigyi, G., and Miller, D. D. (2011) *ChemMedChem.* 6, 922-935
76. Albers, H. M., Dong, A., van Meeteren, L. A., Egan, D. A., Sunkara, M., van Tilburg, E. W., Schuurman, K., van, T. O., Morris, A. J., Smyth, S. S., Moolenaar, W. H., and Ovaa, H. (2010) *Proc. Natl. Acad. Sci. U. S. A* 107, 7257-7262
77. Albers, H. M., van Meeteren, L. A., Egan, D. A., van Tilburg, E. W., Moolenaar, W. H., and Ovaa, H. (2010) *J. Med. Chem.* 53, 4958-4967
78. Gierse, J., Thorarensen, A., Beltey, K., Bradshaw-Pierce, E., Cortes-Burgos, L., Hall, T., Johnston, A., Murphy, M., Nemirovskiy, O., Ogawa, S., Pegg, L., Pelc, M., Prinsen, M., Schnute, M., Wendling, J., Wene, S., Weinberg, R., Wittwer, A., Zweifel, B., and Masferrer, J. (2010) *J. Pharmacol. Exp. Ther.* 334, 310-317

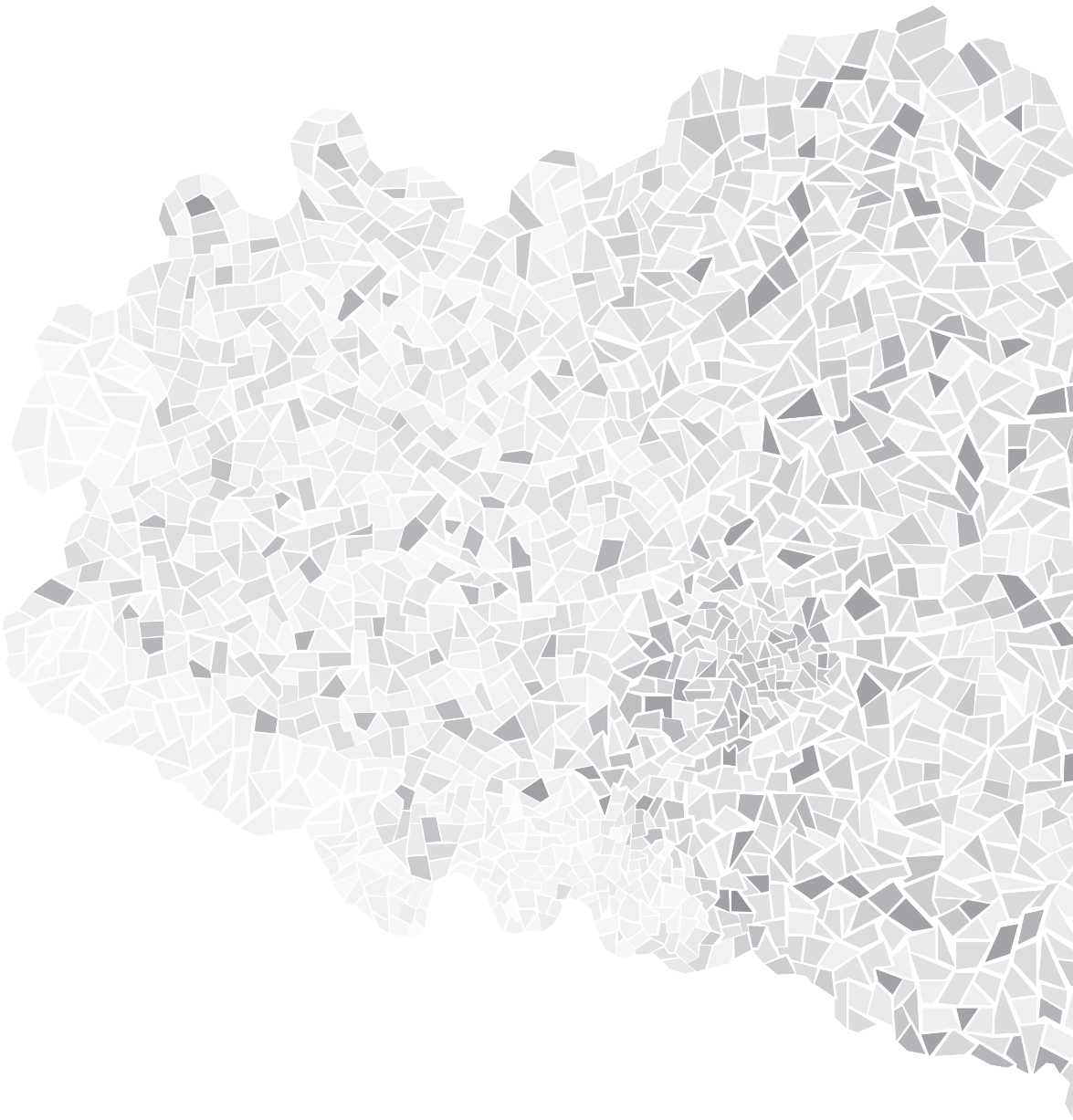

CHAPTER 3

Autotaxin expression profiling in human breast cancer

Autotaxin expression profiling in human breast cancer

Anna J.S. Houben[1],
Hugo M. Horlings[2,3],
Jelle Wesseling[2]
and Wouter H. Moolenaar[1]

[1]Division of Cell Biology,
The Netherlands Cancer Institute,
Amsterdam, The Netherlands
[2]Division of Medical Oncology,
The Netherlands Cancer Institute,
Amsterdam, The Netherlands
[3]Present address:
Department of Pathology,
Academic Medical Center,
Amsterdam, The Netherlands

ABSTRACT

Autotaxin (ATX) is a secreted phosphodiesterase that produces the lipid mediator LPA, a mitogen and motility factor for many cell types. ATX is essential for embryonic development, while excessive ATX-LPA signaling promotes tumor formation, angiogenesis and experimental metastasis. In particular, overexpression of ATX in mouse mammary glands promotes late-onset, invasive mammary cancer. However, little is known about ATX expression in human breast cancer. Here, ATX immunohistochemistry was performed in 193 breast cancer samples, and associations between ATX expression, clinico-pathological characteristics and survival were evaluated. Virtually all carcinoma samples were ATX-positive, regardless of tumor size, grade or lymph node status, while the surrounding stroma showed little or no ATX expression. Despite the high amount of ATX-immunoreactivity, there was no significant correlation between ATX protein and mRNA expression and clinical parameters. We conclude that, although breast cancer cells express ATX and are known to be LPA-responsive, the ATX expression profile by itself is not significantly correlated with clinical outcome.

INTRODUCTION

Lysophosphatidic acid (LPA) signaling is implicated in both physiological as well as pathological processes by inducing proliferation, migration and many other cellular functions (reviewed in (1)). LPA acts on specific G protein-coupled receptors, which are expressed in virtually every cell type (2). Autotaxin (ATX) is a secreted phosphodiesterase that hydrolyzes lysophosphatidylcholine into the lipid mediator lysophosphatidic acid (LPA) (3). ATX was originally identified as an autocrine motility factor for human melanoma cells (4) and later found to be identical to plasma lysophospholipase D, the main enzyme accounting for LPA production in the circulation (5;6)

ATX is essential for embryonic development (7;8) and, when overexpressed in mice, it is an effector of tumor formation, angiogenesis and metastasis (reviewed in (9)). Of particular interest, transgenic expression of ATX or individual LPA receptors (LPA_{1-3}) in mouse mammary glands induces late-onset, invasive mammary cancer (10). Furthermore, injection of ATX-expressing mammary carcinoma cells into nude mice enhances the formation of osteolytic bone metastasis (11).

In human malignancies, high ATX expression has been implicated in development and progression of prostate cancer (12), early-stage colorectal cancer (13) and Hodgkin lymphoma

A

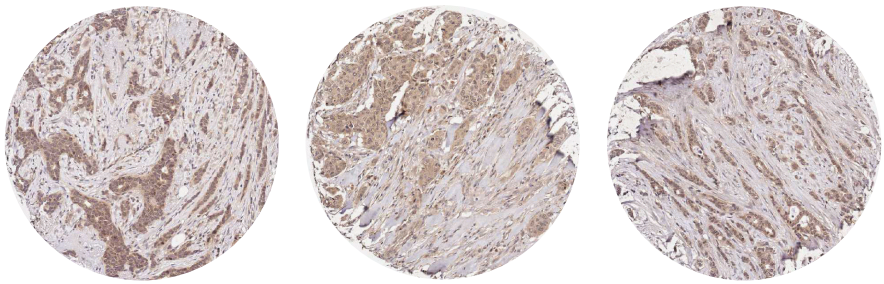

B

ATX IHC score	Number
negative	3
faint	23
moderate	93
strong	74

C

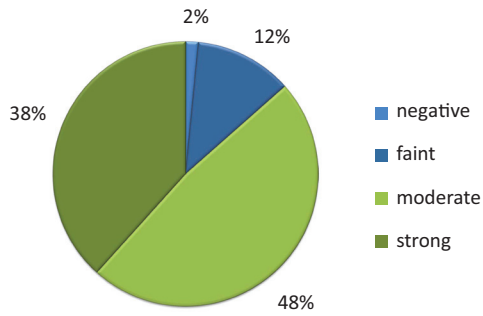

Figure 1. ATX expression in primary breast tumors. Tissue microarrays of primary breast tumors were analyzed for cytoplasmic ATX expression by IHC, using anti-ATX monoclonal antibody 4F1. (A) Representative tumors with high ATX expression levels. (B) Distribution of IHC scores in 193 breast tumors. (C) Pie chart showing relative ATX expression (n=193).

(14). Thus far, ATX expression patterns in breast cancer patients have not been adequately analyzed. In the present study, we examined ATX expression by immunohistochemical (IHC) analysis on tissue microarrays derived of 193 mammary carcinomas, and explored possible correlations with clinico-pathological and prognostic characteristics.

RESULTS

We analyzed ATX protein expression in a series of primary tumors by IHC on tissue microarray sections using anti-ATX monoclonal antibody 4F1 (16). Specificity and reactivity of the 4F1 antibody in tissue sections has been assessed previously (12;17). ATX IHC staining was observed specifically in carcinoma cells, with little or no ATX expression detectable in the surrounding stroma (Fig. 1A). Positive staining was found in the majority of tumors, with moderate to strong staining (scores 2 and 3) in 86% of all cases, while only very few tumors were ATX negative (Fig. 1B and Fig. 1C). Thus, ATX expression is a common feature of primary breast cancer, suggesting that ATX-LPA receptor signaling might play a role in mammary tumorigenesis and progression.

Using the known gene expression data of this patient cohort (15), we analyzed the correlation between ATX mRNA and protein expression. Unexpectedly, the IHC scores did not correlate with the mRNA expression pattern (p=0.28). Whereas the ATX IHC profile showed clear differences among patients, the mRNA expression pattern did not show much variability (Fig. 2). It should be noted that ATX mRNA expression levels represent the sum of intracellular and secreted ATX, while IHC analysis only detects the intracellular pool representing newly synthesized ATX. It is currently not clear how intracellular ATX levels relate to the secreted, LPA-generating, ATX pool. It seems likely that intracellular and extracellular levels are closely correlated. However, future analysis is needed to test this hypothesis.

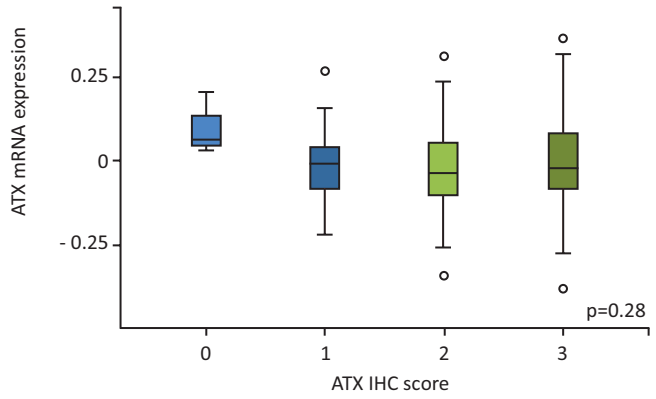

Figure 2. Correlation between ATX mRNA and protein expression. Boxplot showing the ATX mRNA expression per group of ATX IHC score (n=193). There is no clear correlation between ATX mRNA and protein expression (p=0.28, Kruskall Wallis test, n=193).

	ER positive			ER negative		
Characteristic	ATX low	ATX high	p-value	ATX low	ATX high	p-value
Age			0.63[$]			0.08
< 50 years	72 (77.4)	49 (89.1)		23 (88.5)	18 (94.7)	
≥ 50 years	21 (22.6)	6 (10.9)		3 (11.5)	1 (5.3)	
Tumor size			0.17			0.88
≤ 2 cm	45 (48.4)	33 (60)		9 (34.6)	7 (36.8)	
> 2 cm	48 (51.6)	22 (40)		17 (65.4)	12 (63.2)	
Lymph node status			0.89			0.71
negative	40 (43)	23 (41.8)		15 (57.7)	12 (63.2)	
positive	53 (57)	32 (58.2)		11 (42.3)	7 (36.8)	
Histological grade			0.27[#]			0.31
I (good)	30 (32.3)	19 (34.5)		2 (7.7)	0 (0)	
II (intermediate)	33 (35.5)	25 (45.5)		5 (19.2)	2 (10.5)	
III (poor)	30 (32.3)	11 (20)		19 (73.1)	17 (89.5)	
Her2 status			0.56			0.29
negative	76 (81.7)	47 (85.5)		19 (73.1)	11 (57.9)	
positive	17 (18.3)	8 (14.5)		7 (26.9)	8 (42.1)	
PR status			0.61			0.69[$]
negative	22 (23.7)	11 (20)		23 (88.5)	16 (84.2)	
positive	71 (76.3)	44 (80)		3 (11.5)	3 (15.8)	
Chemotherapy			0.32			0.90
no	54 (58.1)	31 (56.4)		14 (53.8)	13 (68.4)	
yes	39 (41.9)	24 (43.6)		12 (46.2)	6 (31.6)	
Hormonal therapy			0.50			0.84
no	77 (82.8)	46 (83.6)		24 (92.3)	19 (100)	
yes	16 (17.2)	9 (16.4)		2 (7.7)	0 (0)	

Table 1. Association of ATX protein expression with clinico-pathological variables in primary breast tumors. The number of patients is indicated, with the column percentage between brackets. The p-values were calculated with the use of Chi square test, unless indicated otherwise. ATX low is defined as ATX IHC score 0-2; ATX high is defined as ATX IHC score 3; Her2: Her2 receptor (expression determined by IHC); PR: progesterone receptor (expression determined by microarray analysis); chemo- and hormonal therapy: adjuvant therapy. [$] Fisher exact test; [#] Chi square test for trend; n=193.

Next, we examined the association of ATX immunoreactivity with patient and tumor characteristics, including age, tumor size, differentiation grade as well as lymph node, Her2 and progesterone receptor status. Breast cancer is a heterogeneous disease with different histological and molecular subtypes (18). Due to the known distinct behavior of ER positive breast cancer versus ER negative breast cancer, we analyzed these subgroups separately. As summarized in Table 1, no association between ATX expression and clinico-pathological parameters could be demonstrated. In addition, Kaplan-Meier analyses showed no significant correlation between ATX IHC score and patient survival (Fig. 3A). The ER-negative patient group showed a trend towards better survival, although this difference was not statistically

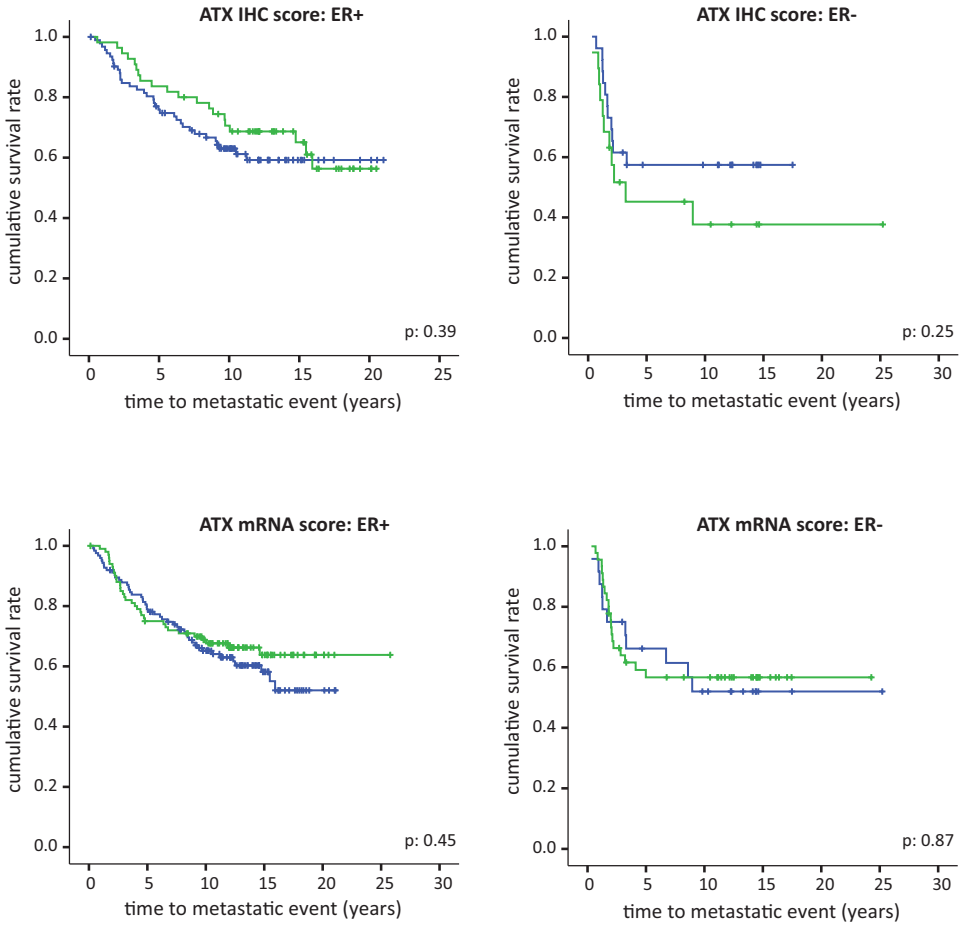

Figure 3. ATX expression and metastasis-free survival in human breast cancer. Kaplan-Meier survival analyses of patient survival, defined as time to any metastatic event, versus (A) ATX IHC score in two groups: ATX low is defined as ATX IHC score 0-2, ATX high is defined as ATX IHC score 3; and (B) ATX mRNA expression in two groups: ATX low versus ATX high. For panels A and B, patients were divided in ER positive (left graph) and ER negative (right graph) groups. There is no significant correlation between ATX expression and survival in either data set. Blue line: ATX low group, green line: ATX high group. Censored data are depicted with a vertical line. The p-values were calculated using the Log Rank Mantel-Cox test (n=193).

significant (univariate Cox regression for ER-positive group: hazard ratio (HR) 0.79, p=0.39, and for ER-negative group: HR 1.6, p=0.25; multivariate Cox regression for ER-positive group: HR 0.78, p=0.38, and for ER-negative group: HR 1.6, p=0.29). Similar as for the IHC scores, ATX mRNA expression profiles also failed to show a correlation with patient outcome (Fig. 3B). In line with our results, a recent study reported absence of a correlation between ATX mRNA levels and classical prognostic parameters in breast cancer patients (11). Thus, we conclude that ATX expression profiles are not significantly correlated with clinical outcome in human primary breast cancer.

FUTURE PROSPECTS

Mammary carcinoma cells are highly responsive to LPA, particularly with respect to cell migration (19), and a causal link between ATX-LPA receptor signaling and mammary cancer has been reported in a transgenic mouse model (10). This suggests that excessive ATX-LPA signaling is sufficient for tumor initiation and progression in mice. We thus hypothesized that ATX would play a role in human breast cancer, and might serve as a prognostic factor. However, the results of our tissue microarray analysis show that ATX expression in breast cancer does not correlate with clinical and prognostic characteristics. Of note, high ATX expression does not necessarily imply enhanced LPA signaling, as the interplay between substrate availability, product degradation and the LPA receptor expression profile together will determine the outcome of ATX action. A previous study showed that LPA_2 expression is linked to invasive ductal breast carcinoma (20). It will be interesting to examine how LPA receptor expression profiles, either by itself or in combination with ATX expression, correlate with clinical outcome in human breast cancer.

EXPERIMENTAL PROCEDURES

Patients

This study was carried out using tumor samples from a breast cancer patient cohort of the fresh-frozen tissue bank of the Netherlands Cancer Institute (15). All patients were younger than 53 years and were diagnosed with stage I or II breast cancer, lymph node negative or positive, containing both estrogen receptor (ER) negative and ER positive tumors. The median duration of follow-up (defined as time to any metastatic event) among all patients was 9.9 years, with 12.1 years for the patients without a metastasis event and 2.9 years for the patients with a metastasis event. All patients had been treated by breast conserving or ablative therapy followed by radiotherapy and/or adjuvant chemotherapy and/or hormonal therapy. The study was approved by the medical ethics committee of the Netherlands Cancer Institute.

Immunohistochemistry

Blocks of formalin-fixed, paraffin-embedded primary breast cancer tissue were prepared using a tissue arrayer. For immunohistochemistry, sections were heated at 75°C for 30 min., deparrafinized in xylene and rehydrated via a series of graded alcohols. After washing with TBS (J.T. Baker BV) for 5 min., sections were boiled for 15 min. in citrate buffer pH 6 (trinatrium-citrate-dihydrate 8.2 mM, citric acid 0.18 mM) for antigen retrieval and cooled down for 1 hour. Sections were then incubated with peroxidase blocking solution (Immunovision Technologies) for 10 min., washed with TBS for 5 min. and incubated overnight with rat monoclonal antibody 4F1 raised against a human ATX polypeptide (amino acid 58-182) (16), 1:50 dilution at 4°C. Next, sections were washed for 5 min. with TBS, incubated with post-antibody blocking/polymer penetration enhancer solution (Immunovision Technologies) for 15 min., washed, incubated with polymerized HRP-anti-mouse/rabbit IgG (Immunovision Technologies), washed, and incubated with DAB and hematoxyline. ATX staining in the tumor sections was scored by a consultant breast pathologist (JW) as 0, 1, 2, 3 corresponding respectively to negative, faint, moderate, strong staining intensity. The highest score out of three cores from the same tumor was used for analysis. If one or two cores out of three failed, the highest value of the remaining core(s) was included. Only the tumor component

was considered when judging staining and sections containing stromal tissue without carcinoma cells were discarded from the analysis. This resulted in a total number of 193 patient samples that were scored for ATX expression.

Statistical analysis

Time to metastasis for two ATX groups (IHC score 0-2 versus 3) was estimated according to the Kaplan-Meier method. In addition, we tested for trend, using the significance of the coefficient for the continuous ATX IHC score 0-3. The association between ATX IHC score (4 groups: score 0, 1, 2 and 3) and ATX mRNA expression was tested using the Kruskall Wallis test. Associations between ATX IHC score and clinico-pathological variables were evaluated by a Chi square test, unless otherwise indicated.

ACKNOWLEDGEMENTS

We gratefully thank Junken Aoki for the generous gift of the anti-ATX monoclonal antibody 4F1; Karin Beelen for the regression and survival analyses; Mark Opdam, Abderrahim Ajouaou and Elisa Matas for help with immunohistochemistry protocols and Jorma de Ronde for statistical advice.

REFERENCES

1. Mills, G. B. and Moolenaar, W. H. (2003) *Nat Rev Cancer* 3, 582-591
2. Chun, J., Hla, T., Lynch, K. R., Spiegel, S., and Moolenaar, W. H. (2010) *Pharmacol Rev* 62, 579-587
3. Moolenaar, W. H. and Perrakis, A. (2011) *Nat Rev Mol Cell Biol*
4. Stracke, M. L., Krutzsch, H. C., Unsworth, E. J., Arestad, A., Cioce, V., Schiffmann, E., and Liotta, L. A. (1992) *J Biol Chem* 267, 2524-2529
5. Tokumura, A., Majima, E., Kariya, Y., Tominaga, K., Kogure, K., Yasuda, K., and Fukuzawa, K. (2002) *J Biol Chem* 277, 39436-39442
6. Umezu-Goto, M., Kishi, Y., Taira, A., Hama, K., Dohmae, N., Takio, K., Yamori, T., Mills, G. B., Inoue, K., Aoki, J., and Arai, H. (2002) *J Cell Biol* 158, 227-233
7. Tanaka, M., Okudaira, S., Kishi, Y., Ohkawa, R., Iseki, S., Ota, M., Noji, S., Yatomi, Y., Aoki, J., and Arai, H. (2006) *J Biol Chem* 281, 25822-25830
8. van Meeteren, L. A., Ruurs, P., Stortelers, C., Bouwman, P., van Rooijen, M. A., Pradere, J. P., Pettit, T. R., Wakelam, M. J., Saulnier-Blache, J. S., Mummery, C. L., Moolenaar, W. H., and Jonkers, J. (2006) *Mol Cell Biol* 26, 5015-5022
9. Houben, A. J. and Moolenaar, W. H. (2011) *Cancer Metastasis Rev.*
10. Liu, S., Umezu-Goto, M., Murph, M., Lu, Y., Liu, W., Zhang, F., Yu, S., Stephens, L. C., Cui, X., Murrow, G., Coombes, K., Muller, W., Hung, M. C., Perou, C. M., Lee, A. V., Fang, X., and Mills, G. B. (2009) *Cancer Cell* 15, 539-550
11. David, M., Wannecq, E., Descotes, F., Jansen, S., Deux, B., Ribeiro, J., Serre, C. M., Gres, S., Bendriss-Vermare, N., Bollen, M., Saez, S., Aoki, J., Saulnier-Blache, J. S., Clezardin, P., and Peyruchaud, O. (2010) *PLoS One* 5, e9741
12. Nouh, M. A., Wu, X. X., Okazoe, H., Tsunemori, H., Haba, R., bou-Zeid, A. M., Saleem, M. D., Inui, M., Sugimoto, M., Aoki, J., and Kakehi, Y. (2009) *Cancer Sci.* 100, 1631-1638
13. Kazama, S., Kitayama, J., Aoki, J., Mori, K., and Nagawa, H. (2011) *J. Gastrointest. Cancer* 42, 204-211
14. Baumforth, K. R., Flavell, J. R., Reynolds, G. M., Davies, G., Pettit, T. R., Wei, W., Morgan, S., Stankovic, T., Kishi, Y., Arai, H., Nowakova, M., Pratt, G., Aoki, J., Wakelam, M. J., Young, L. S., and Murray, P. G. (2005) *Blood* 106, 2138-2146
15. van de Vijver, M. J., He, Y. D., van't Veer, L. J., Dai, H., Hart, A. A., Voskuil, D. W., Schreiber, G. J., Peterse, J. L., Roberts, C., Marton, M. J., Parrish, M., Atsma, D., Witteveen, A., Glas, A., Delahaye, L., van der Velde, T., Bartelink, H., Rodenhuis, S., Rutgers, E. T., Friend, S. H., and Bernards, R. (2002) *N Engl J Med* 347, 1999-2009
16. Tanaka, M., Kishi, Y., Takanezawa, Y., Kakehi, Y., Aoki, J., and Arai, H. (2004) *FEBS Lett* 571, 197-204
17. Savaskan, N. E., Rocha, L., Kotter, M. R., Baer, A., Lubec, G., van Meeteren, L. A., Kishi, Y., Aoki, J., Moolenaar, W. H., Nitsch, R., and Brauer, A. U. (2007) *Cell Mol. Life Sci.* 64, 230-243
18. Polyak, K. (2011) *J. Clin. Invest* 121, 3786-3788
19. Chen, M., Towers, L. N., and O'Connor, K. L. (2007) *Am. J. Physiol Cell Physiol* 292, C1927-C1933
20. Kitayama, J., Shida, D., Sako, A., Ishikawa, M., Hama, K., Aoki, J., Arai, H., and Nagawa, H. (2004) *Breast Cancer Res.* 6, R640-R646

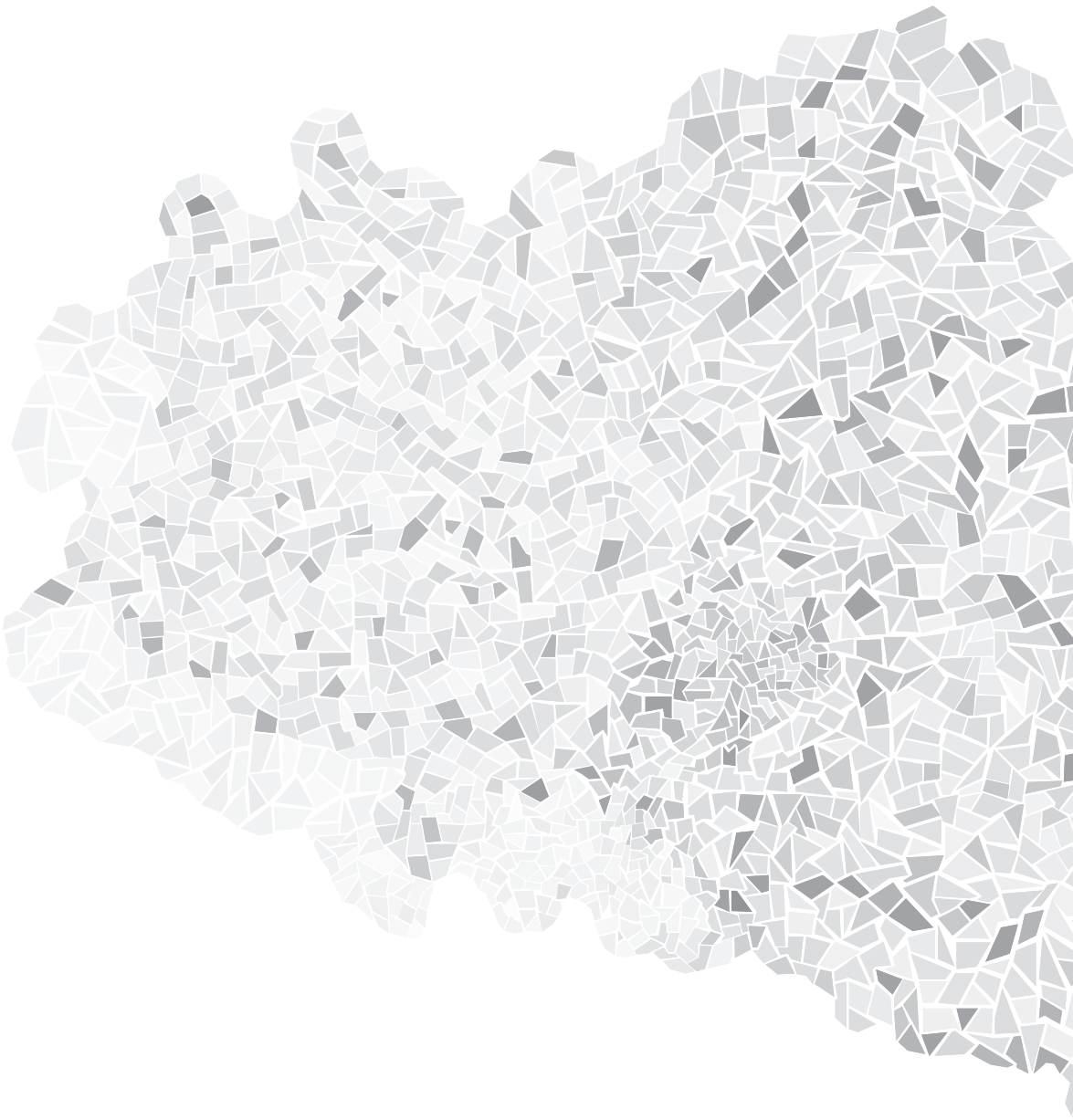

CHAPTER 4

Development of an activity-based probe for autotaxin

ChemBioChem 2010

Development of an activity-based probe for autotaxin

Anna J.S. Houben[a] *,
Silvia Cavalli[a,b] *,
Harald M.H.G. Albers[a,c],
Erica W. van Tilburg[a,d],
Arnoud de Ru[e],
Junken Aoki[f],
Peter van Veelen[e],
Wouter H. Moolenaar[a,g]
and Huib Ovaa[a,c]

[a]Division of Cell Biology,
The Netherlands Cancer Institute,
Amsterdam, The Netherlands.
[b]Networking Centre on
Bioengineering,
Biomaterials & Nanomedicine,
CIBER-BBN,
Institute for Research in Biomedicine,
Barcelona, Spain.
[c]The Netherlands Proteomics Centre.
[d]Department of Nuclear Medicine,
Erasmus Medical Center,
Rotterdam, The Netherlands.
[e]Division of Immunohematology and
Blood Transfusion,
Leiden University Medical Center,
Leiden, The Netherlands.
[f]Graduate School of Pharmaceutical
Sciences,
Tohoku University Aobayama,
Aoba-ku, Sendai, Japan.
[g]Centre for Biomedical Genetics

* These authors contributed equally to this work

ABSTRACT

Autotaxin (ATX), or ecto-nucleotide pyrophosphatase/phosphodiesterase 2 (ENPP2), is a secreted lysophospholipase D that hydrolyzes lysophosphatidylcholine into the lipid mediator lysophosphatidic acid (LPA), a mitogen and chemoattractant for many cell types. ATX has been implicated in tumor progression and inflammation, and might serve as a biomarker. Here we describe the development of a fluorescent activity-based probe that covalently binds to the active site of ATX. The probe consists of a lysophospholipid-based backbone linked to a trapping moiety that becomes reactive after phosphate ester hydrolysis, and a Cy5 fluorescent dye to allow visualization of active ATX. The probe reacts specifically with the three known isoforms of ATX, it competes with small-molecule inhibitors for binding to ATX, and allows ATX activity in plasma to be determined. Our activity-based reporter will be useful for monitoring ATX activity in biological fluids and for inhibitor screening.

INTRODUCTION

Autotaxin (ATX), also known as ENPP2 (ecto-nucleotide pyrophosphatase/phosphodiesterase 2), is a secreted glycoprotein (~120 kDa) that functions as a lysophospholipase D to hydrolyze lysophosphatidylcholine (LPC) into the lipid mediator lysophosphatidic acid (LPA) (1;2). LPA acts on specific G protein-coupled receptors and thereby evokes a great variety of cellular responses, including cell proliferation, migration and survival (3). ATX is a multi-domain protein and uses a single catalytic site at residue T210, which harbors the active-site nucleophile (Fig. 1) (4).

ATX was originally identified as an autocrine motility factor for melanoma cells (5) and was later found to enhance experimental metastasis of Ras-transformed NIH3T3 cells (6). Since then, many studies have shown a role for ATX-LPA signaling in tumor progression (7-9), and gene knockout studies have uncovered a vital role for ATX in vascular development (10;11). ATX is expressed and secreted by diverse tissues and is present in the circulation; virtually every cell type expresses functional LPA receptors. The ATX-LPA receptor axis has been implicated not only in tumor progression but also in chronic inflammation (12), fibrotic disease (13) and neurological disorders (14;15), making it an attractive target for therapy. We and others have developed potent small-molecule inhibitors of ATX that lower circulating LPA levels in mice (16-18).

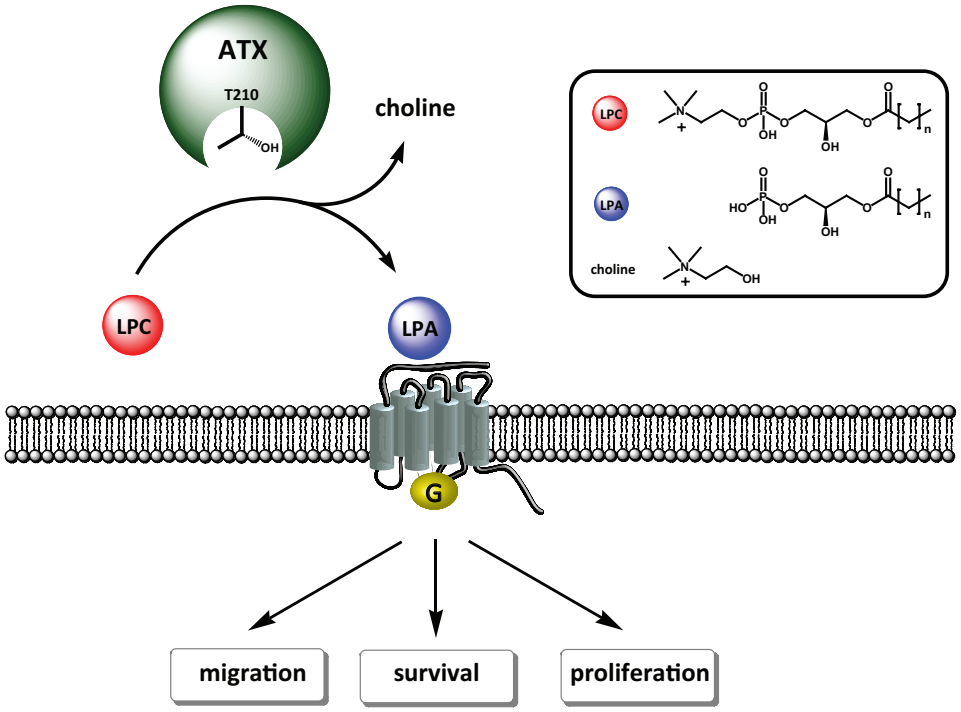

Figure 1: The ATX-LPA receptor signaling axis. Secreted ATX converts LPC to LPA in the extracellular environment. LPA binds to specific G protein-coupled receptors leading to the activation of downstream signaling cascades that trigger cell migration, proliferation and survival.

Several studies indicate that secreted ATX might serve as a biomarker. In particular, serum ATX levels are significantly elevated in patients with follicular lymphoma (FL) and correlate with tumor burden (19). Furthermore, ATX/lysoPLD activity is enhanced in serum from patients with chronic liver disease (20) and in malignant effusions from ovarian cancer patients (9). Therefore it will be useful to develop activity-based probes (ABPs) to monitor ATX activity in body fluids. ABPs are reagents that contain key recognition and reporter elements that allow the study of target enzymes based on catalytic activity instead of expression levels (21). ABPs have proved useful for monitoring enzyme function in complex biological systems, for the discovery of biomarkers, and for inhibitor profiling (21;22).

Here, we report the design, synthesis and characterization of a fluorescent ABP for ATX. By using recombinant ATX and inhibitor competition experiments, we validate the ability of this reagent to label the ATX active site. In particular, our ABP can label ATX activity in serum and plasma. Our study shows that ATX-specific ABPs have the potential to be developed into diagnostic reagents.

RESULTS

Probe design

The ATX activity-based probe (**ATX-ABP**) consists of four major components: a recognition element, a trapping device, a linker, and a reporter group (Scheme 1A). The lysophospholipid-based recognition element defines the specificity of the target protein. The latent trapping device functions as a chemical tool for covalent binding upon activation and generates a reactive intermediate upon phosphate ester hydrolysis, thereby covalently reacting with ATX in an activity-dependent manner (Scheme 1B). This trapping device has previously been used to probe protein tyrosine phosphatase activity (23-27). Upon ATX-mediated cleavage of the phosphodiester bond in the probe, the released intermediate undergoes rapid 1,6-elimination of the fluoride and generates a reactive quinone methide species that, in turn, traps nearby nucleophiles in the ATX active site; this results in covalent labeling of ATX in an activity-dependent manner. Incorporation of a fluorescent dye allows visualization of active ATX. Sulfoindocyanine Cy5 was chosen as a marker because of its good solubility in aqueous solutions and its compatibility with most fluorimetric equipment. The dye was connected to the trapping device through a hydrophilic (ethylenedioxy)diethylamine linker.

Chemical synthesis

ATX-ABP was prepared via a convergent synthetic approach as shown in Scheme 2. In brief, 4-hydroxymandelic acid was condensed with Boc-2,2'-(ethylenedioxy)diethylamine (**1**, EDC/HOBt/DMF) to give compound **2** in 90% yield. The 2-*O*-methoxymethyl (MOM)-protected lipid building block **3** was prepared by using previously reported protocols with minor modifications (Scheme 3) (27;28). The two building blocks were connected by phosphoramidite chemistry. Lipid building block **3** was treated with chloro(diisopropylamino)methoxy phosphine and subsequently building block **2** was added to the phosphine intermediate. After oxidation with *tert*-butyl hydroperoxide, the phosphodiester product **4** was obtained in a 37% overall yield (three steps). The benzylic fluoride functionality was introduced by treating **4** with diethylaminosulfur trifluoride (DAST). The fluorinated product **5** was obtained in 68% yield. Removal of MOM and methyl ester was achieved simultaneously with TMSBr and the crude product **6** was subsequently treated with TFA in dichloromethane to remove the

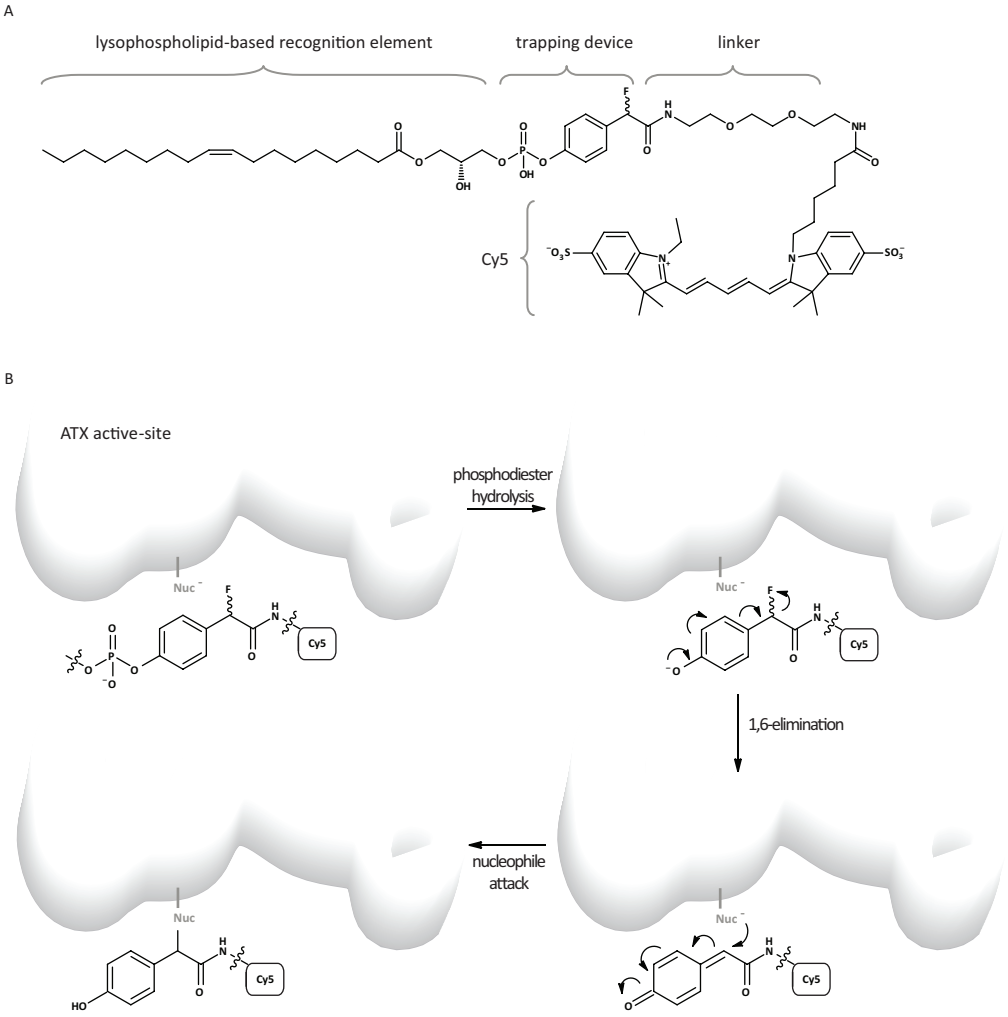

Scheme 1: Chemical structure of the fluorescent activity-based probe for ATX (ATX-ABP) and the labeling reaction. (A) The fluorescent activity probe (**ATX-ABP**) has four structural components: a lysophospholipid-based backbone as a recognition element, a latent trapping device reactive unit (derived from *p*-hydroxymandelic acid), a linker and the sulfoindocyanine Cy5 dye as fluorescent tag. (B) Reaction mechanism of ATX labeling with **ATX-ABP**; only one of the potential products resulting from cross-linking is shown. Nuc: nucleophile.

Boc group (**7**). Crude TFA salt **7** was coupled with Cy5-NHS ester to afford **ATX-ABP** in 8% yield after purification.

Activity labeling of recombinant ATX

ATX-ABP was tested for its ability to label recombinant ATX *in vitro*. Increasing concentrations of **ATX-ABP** (up to 100 µM) were incubated with purified recombinant ATX with or without bovine serum albumin (BSA). Proteins were separated by SDS-PAGE, and protein labeling was analyzed by in-gel fluorescence measurements. At 1 µM of **ATX-ABP**, a fluores-

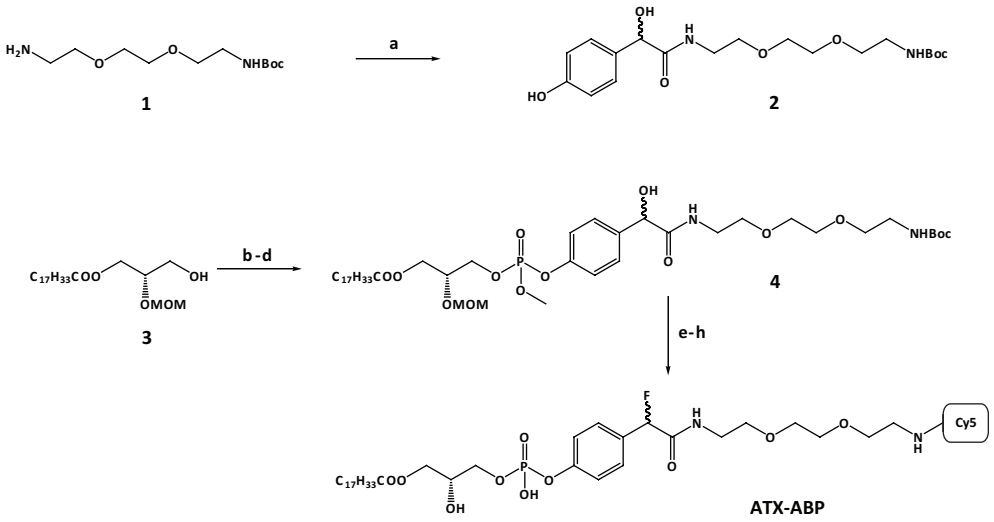

Scheme 2: Synthetic scheme of the fluorescent activity-based probe (ATX-ABP).
(a) 4-hydroxymandelic acid, HOBt, EDC, DMF, RT, overnight (90% yield); (b) Chloro(diisopropylamino)methoxy phosphine, iPr_2EtN, CH_2Cl_2, argon atmosphere, RT, 1 h; (c) **2**, 0.45 M 1*H*-tetrazole in MeCN, CH_2Cl_2, RT, 4 h; (d), *tert*-butyl hydroperoxide (70 wt% in H_2O), CH_2Cl_2, -70°C to RT, 4 h (37% yield, three steps); (e) DAST, CH_2Cl_2, -70°C to RT, 2 h (68% yield); (f) TMSBr (10 equiv.), CH_2Cl_2, 0°C, 4 h, 0°C to RT, 1 h; (g), TFA/CH_2Cl_2 (1:1, *v/v*), RT, 1 h; (h) Cy5-NHS ester dye, iPr_2EtN, DMF, RT, overnight. Steps (f) and (g) were performed without purification of the products. The final product (**ATX-ABP**) was purified by reversed-phase HPLC (8% yield).

cent signal became apparent, and more intense labeling was measured at higher concentrations of **ATX-ABP** (Fig. 2A). Increasing the incubation time (at a fixed probe concentration) also resulted in more labeling (Fig. 2B). Importantly, **ATX-ABP** did not label BSA, which is present at high concentrations in the circulation where it functions as a lipid carrier and scavenger of electrophiles. When probe was added to a mixture of BSA and ATX (Fig. 2C) or BSA alone (Fig. 2D) no significant BSA labeling was observed. Furthermore, **ATX-ABP** did not label alkaline phosphatase (AP; Fig. 2E), and the catalytically dead mutant ATX-T210A was resistant to reaction compared to active ATX (Fig. 3, lane 1). These results confirm that **ATX-ABP** specifically labels ATX in an activity-dependent manner.

Activity labeling of ATX isoforms

Alternative splicing of the ATX-encoding gene, *ENPP2*, results in three distinct isoforms. The best studied isoform, ATXβ (863 amino acids), is identical to plasma lysoPLD. The original "melanoma-derived" isoform, ATXα (915 amino acids) contains a 52 residue polybasic insert of unknown function in the catalytic domain. A "brain-specific" isoform (ATXγ) contains a short insert in the C-terminal domain. All three isoforms exhibit the same catalytic activity in vitro (29). The recombinant ATX isoforms were incubated for 1 hour at 37°C with 50 μM of **ATX-ABP** (Fig. 3, lanes 2-4). As expected, all three ATX isoforms reacted with the probe. Labeling was equally efficient for ATXβ and ATXγ. The ATXα isoform however labeled less efficiently, which might be explained by the known proteolytic cleavage of ATXα in its polybasic insert (29). Indeed, we could detect a major band that corresponds to the N-terminal cleavage fragment of ATXα, which did show some labeling. We conclude that **ATX-ABP** labels all three isoforms of ATX in an activity-dependent manner.

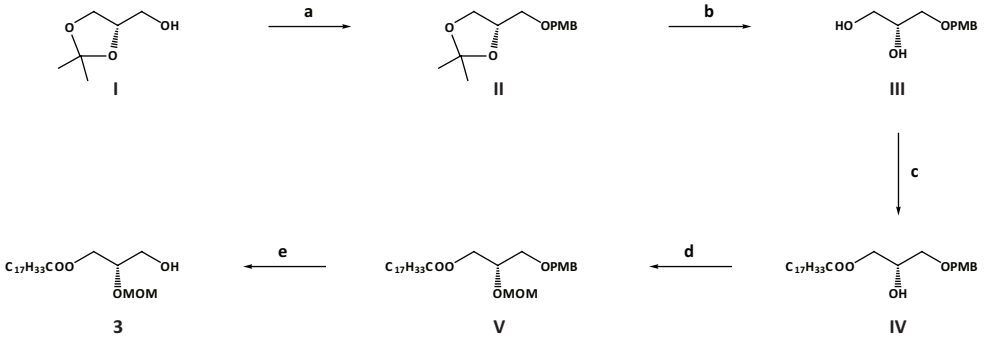

Scheme 3: Synthesis of building block 3. Reagents: (a) PMBCl, NaH, DMF, RT, 1 h; (b) 5% (wt) p-TsOH, MeOH, rt, 1 h, directly used in the next step; (c) oleic acid, DMAP, DCC, CH_2Cl_2, RT, overnight; (d) MOMCl, DiPEA, DMF, RT, overnight; (e) DDQ, wet CH_2Cl_2, RT, overnight.

ATX inhibitor profiling

Next, we used **ATX-ABP** in competition experiments with LPA (the product of ATX-mediated LPC hydrolysis) and the ATX inhibitor **HA130** (IC50 ~ 30 nM) (17), as shown in Fig. 4. Recombinant ATX was incubated with increasing concentrations of inhibitor for 1 hour at 37°C and subsequently with 50 µM of **ATX-ABP** for 15 minutes at 37°C. In-gel analysis showed that LPA did not compete with ATX-ABP, as demonstrated by unchanged fluorescence intensity of ATX incubated with increasing concentrations of LPA prior to labeling (Fig. 4A). In contrast, **HA130** caused a dose-dependent loss of fluorescence intensity, reflecting a decrease in catalytic activity (Fig. 4B). These experiments show that **ATX-ABP** is a useful tool for inhibitor profiling and suggest that the physiological product of ATX, namely LPA, does not interfere with ATX-mediated hydrolysis of our probe.

Labeling of ATX activity in whole serum

We determined the ability of **ATX-ABP** to monitor ATX activity in whole serum and plasma *ex vivo*. Measurements of enzymatic activity and function in serum are challenging due to high levels of interfering albumin, a lipid carrier and electrophile scavenger present in concentrations between 30-40 mg/ml, whereas ATX levels in serum or plasma are relatively low (ca. 0.5 µg/ml) (30). Incubation of fetal calf serum with 2 µM **ATX-ABP** did not reveal a detectable fluorescent signal (data not shown). We therefore purified serum samples by anion-exchange column chromatography (eluted with a linear gradient of 0-1 M NaCl). Active fractions were identified using the FS3 ATX-activity assay (31) and incubated with 2 µM **ATX-ABP**. Upon termination of the reaction, the samples were concentrated, and ATX activity was detected by SDS-PAGE. ATX labeling was observed in the active but not in the inactive fractions, although the observed labeling profile was weak (Fig. 5). Although a fluorescent signal could be detected, ATX levels were too low to be visualized by SYPRO or Coomassie Blue staining; this indicated the high sensitivity of our probe. To confirm specificity of the probe, labeled bands and controls were excised from the gel and analyzed by tandem mass spectrometry after trypsin digestion. Several tryptic ATX peptide fragments (CFELQEAGPPDCR, SYPEILTLK, GDCCTNYQVVCK and WWGGQPLWITATK) were found in the fluorescent bands but not in control lanes. These results show that **ATX-ABP** is able to label active ATX in serum, although a purification step is required.

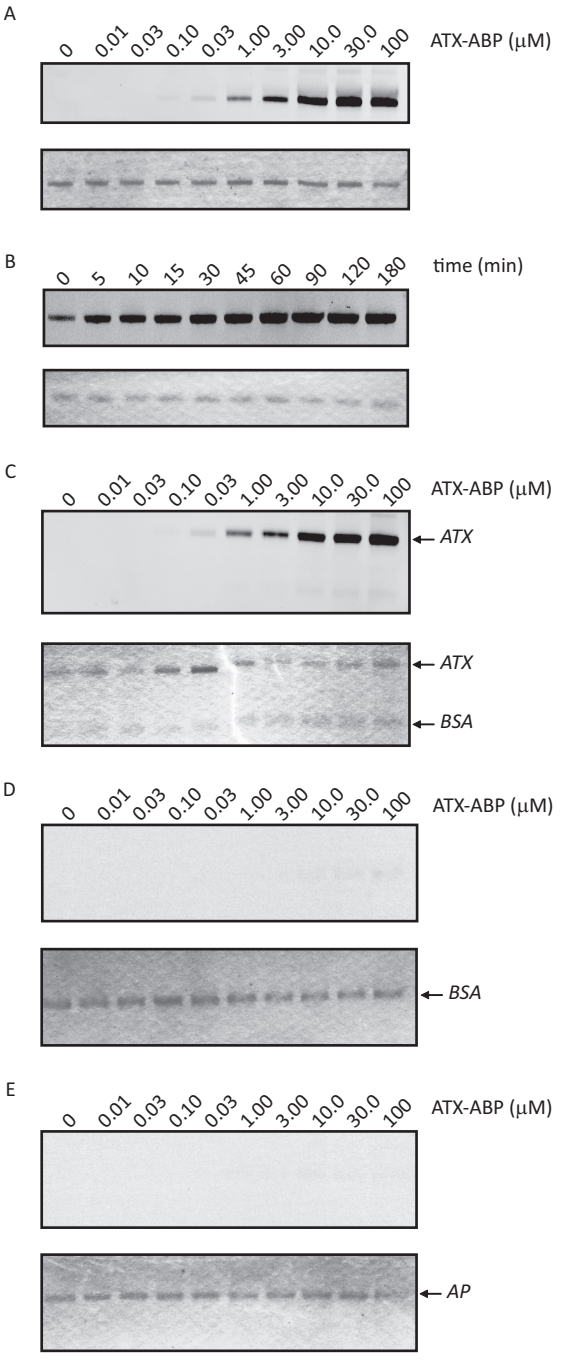

Figure 2: Validation of ATX-ABP labeling. (A) Labeling of recombinant ATX with increasing concentrations of **ATX-ABP**, showing a concentration-dependent increase of the amount of labeling. (B) Time range labeling of recombinant ATX, incubated with 50 μM **ATX-ABP** for different time points. (C) Labeling of ATX and BSA in equal amounts with increasing concentrations of **ATX-ABP**, indicating specific labeling of ATX. (D) Labeling of BSA for 1 hour at 37°C with increasing concentrations of **ATX-ABP**. (E) Labeling of AP for 1 hour at 37°C with increasing concentrations of **ATX-ABP**.
Upper panels: in-gel fluorescence scan, lower panels: Coomassie blue staining.

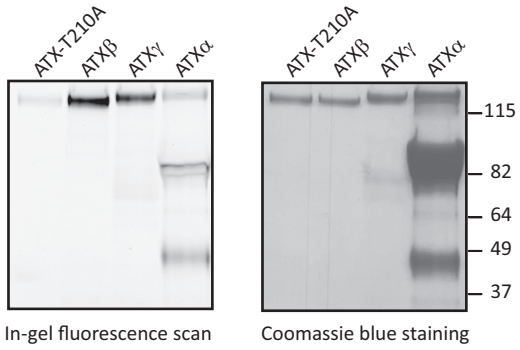

Figure 3: Labeling of recombinant ATX isoforms with ATX-ABP.
All three isoforms react with the probe, whereas the catalytically dead mutant ATX-T210A is resistant to reaction. Left panel: in-gel fluorescence scan, right panel: Coomassie blue staining. ATXβ: ATX teratocarcinoma isoform (plasma lysoPLD), ATXγ: brain-specific isoform, ATXα: melanoma isoform.

Immunoprecipitation of labeled ATX from human plasma

In order to obtain a more efficient activity-based profiling procedure, we investigated a combination of active-site labeling and immunoprecipitation. Plasma samples were incubated with 10 µM of **ATX-ABP** for 1 hour at 37°C and subsequently immunoprecipitated with anti-ATX antibody 5E5 immobilized onto sepharose beads (30). ATX activity in human plasma was estimated by comparing the fluorescent signal of immunoprecipitated plasma ATX to that of recombinant ATX. Analysis of the fluorescence intensity indicated that the ATX activity in 1 ml of human plasma is equivalent to that of 0.5 µg recombinant ATX (Fig. 5), which is in agreement with the reported plasma ATX concentration of about 0.5 µg/ml (30). Thus, when combined with immunoprecipitation, **ATX-ABP** is a convenient tool to monitor ATX activity in plasma.

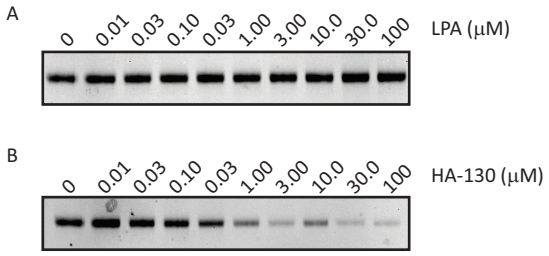

Figure 4: ATX inhibitor profiling.
(A) **ATX-ABP** labeling of recombinant ATX is not inhibited by LPA, in-gel fluorescence scan (B) ATX inhibitor **HA130** is able to compete with **ATX-ABP** in a dose-dependent manner, in-gel fluorescence scan.

DISCUSSION

We describe a convergent synthetic approach of an ATX active site-directed probe (**ATX-ABP**) that efficiently labels recombinant ATX in a specific and activity-dependent manner. We have shown that **ATX-ABP** labels all three isoforms of ATX and that it can be used in inhibitor competition experiments. The inactive mutant ATX-T210A showed hardly any labeling, consistent with **ATX-ABP** labeling in an activity-dependent manner.

Furthermore, we examined the labeling efficiency in more complex biological fluids. Recent studies have suggested that the serum ATX protein level is a promising marker for follicular lymphoma. The plasma ATX level in healthy individuals is about 0.5 µg/ml, whereas follicular lymphoma patients consistently show threefold higher ATX levels (19). Direct labeling of serum ATX with **ATX-ABP** proved difficult due to the high concentrations of serum albumin. Purification of serum ATX by anion exchange chromatography prior to labeling resulted in a weak signal, the specificity of which was confirmed by tandem mass spectrometry. To increase signal strength, we developed an affinity-purification protocol using ATX immunoprecipitation after labeling. In this way ATX activity in human plasma was readily detectable. We showed that **ATX-ABP** did not cross-react with albumin *in vitro*, yet it remains challenging to measure enzyme activity in complex biological samples. ATX activity-based probes could provide new insights into ATX biochemistry, and could also serve as a diagnostic reagent and a tool for inhibitor profiling studies.

In summary, we have synthesized and characterized a first-generation ATX-directed activity probe that labels active ATX specifically and efficiently. Affinity-purification after labeling enabled us to use **ATX-ABP** for activity profiling of biological fluids. Such probes may be useful to monitor ATX activity under normal and pathological conditions, and to profile ATX inhibitors in complex biological samples.

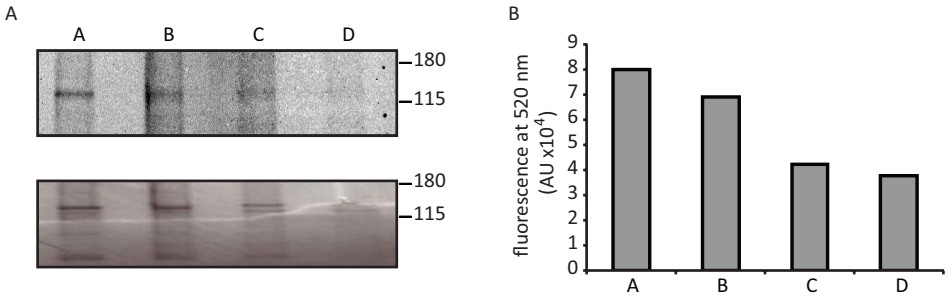

Figure 5: Activity labeling of serum ATX. (A) Active pooled anion exchange fractions of fetal calf serum (lanes A-D) were incubated for 1 hour at 37°C with 2 µM **ATX-ABP**. Upper panel: in-gel fluorescence scan, lower panel: Coomassie Blue staining. (B) FS3 activity assay of the anion exchange fractions shown in panel A.

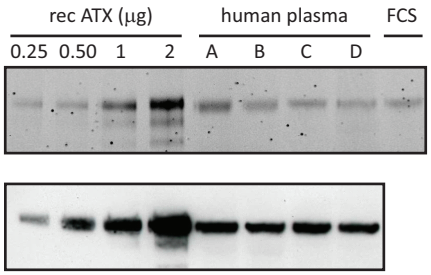

Figure 6: Screening of ATX activity in human plasma.
Human plasma samples from healthy volunteers (1 ml) and FCS (1 ml) were first incubated with **ATX-ABP** and subsequently affinity-purified with an anti-ATX monoclonal antibody. Recombinant ATX, also labeled but not affinity-purified, is included as a standard. A, B: healthy female volunteers; C, D: healthy male volunteers. Upper panel: in-gel fluorescence scan, lower panel: Western blot. The blot was incubated with an anti-ATX antibody (Cayman Chemical, Ann Arbor MI).

CONCLUSIONS

We have developed a fluorescent activity-based probe that can detect and quantify ATX activity in human plasma. Upon cleavage of the phosphodiester bond, a highly reactive species forms that cross-links nearby active-site residues. This approach allows the separation of labeled ATX prior to analysis and enables ATX activity readouts by SDS-PAGE followed by fluorescence scanning. This reagent is the first ATX activity reporter developed so far and it could, in principle, be developed into a diagnostic reagent to monitor ATX activity in body fluids. Moreover, **ATX-ABP** can be used in competition format with ATX inhibitors to guide their pharmacology, allowing *ex vivo* detection of ATX activity in body fluids after treatment with inhibitors.

EXPERIMENTAL PROCEDURES

Chemical synthesis

All reagents and starting materials were obtained from commercial suppliers at the highest grade available (Acros, Aldrich, and Merck) and used without further purification. ^{1}H, ^{13}C and ^{31}P NMR were recorded by using a Bruker ARX 400 spectrometer. ^{1}H NMR spectra in $CDCl_3$ were referenced to residual $CHCl_3$ at 7.24 ppm and ^{13}C NMR spectra to the central peak of $CDCl_3$ at 77.0 ppm. 85% H_3PO_4 was used as external standard for ^{31}P NMR spectroscopy. ESI-MS spectra were recorded on a LCT micromass/Waters mass spectrometer. Analytical TLC was performed with silica gel supported on aluminium sheets (silica gel, 60F254, 20x20 cm, Merck) and spots were visualized under UV light by staining with a solution of ammonium molybdate or a solution of ninhydrin, followed by charring at ~150°C. Column chromatography was performed with silica gel for chromatography Acros Organics (0.035-0.070 mm, 60 Å).

Synthesis of the fluorescent probe

Compounds **2** and **3** were synthesized by using modified published procedures (Scheme 2) (27;28).

*Compound **2***. A preactivated mixture of 4-hydroxylmandelic acid (893 mg, 4.8 mmol), EDC (922 mg, 4.8 mmol) and HOBt (648 mg, 4.8 mmol) was added to a solution of **1** (1 g, 4 mmol) in DMF (20 mL), and the reaction was stirred overnight at RT. The reaction mixture was evaporated to dryness. The product was purified by FCC (7% MeOH in CH_2Cl_2). Yield: 1.45 g (90%). R_f = 0.23 (10% MeOH in CH_2Cl_2); ^{1}H NMR ($CDCl_3$, 400 MHz): δ = 7.12 (d, 2H; Ar), 6.63 (d, 2H; Ar), 5.3 (s, 1H; benzylic CH), 5.16 (br s, 1H; OH), 4.94 (br s, 1H; OH) 3.55-3.25 (m, 10H; linker), 3.26 (m, 2H; linker), 1.42 ppm (s, 9H; Boc); ^{13}C NMR ($CDCl_3$, 101 MHz): δ = 173.59, 157.12, 156.53, 130.82, 128.55, 115.99, 80.06, 74.19, 70.43, 70.27, 69.66, 40.54, 39.31, 28.58 ppm; MS (ESI): *m/z*: 399.20 [*M*+H]$^+$, *m/z*: 421.09 [*M*+Na]$^+$, *m/z*: 365.07 [*M*-*t*Bu+Na]$^+$, *m/z*: 321.09 [*M*-Boc+Na]$^+$, *m/z*: 437.15 [*M*+K]$^+$.

*Compound **3**. **3-(4-methoxybenzyl)-sn-glycerol (III)**.* To a solution of **1,2-O-isopropylidene-sn-glycerol I** (2.12 g, 16.06 mmol) in 100 mL of dry DMF was added NaH (1.09 g, 60%, 19.27 mmol), followed by addition of p-methoxybenzyl chloride (2.6 ml, 19.27 mmol). The mixture was stirred at RT for 2 h (TLC, **II** Rf = 0.71, 33% ethyl acetate/hexane). Excess NaH was destroyed by dropwise addition of MeOH. Solvent was evaporated and CH_2Cl_2 was added to extract. The CH_2Cl_2 layer was washed with brine and dried over $MgSO_4$. After concentration, an oil was obtained and redissolved in 40 mL of MeOH containing p-toluenesulfonic acid monohydrate (153 mg, 0.05 equiv, 0.8 mmol). The mixture was stirred at RT for 2 h (TLC, **III** Rf = 0.25, 75% ethyl acetate/hexane). Next, $NaHCO_3$ (100 mg) was added, and the solvent was evaporated. The residue was purified by flash chromatography on silica gel with 80% ethyl acetate in n-hexane to give 2.986 g of **3-(4-methoxybenzyl)-sn-glycerol** (**III**) (83% yield from **I**): 1H-NMR ($CDCl_3$, 400 MHz) d: 7.16 (d, 2H, phenyl), 6.79 (d, 2H, phenyl), 4.38 (s, 2H, $PMBCH_2O$), 3.79-2.79 (m, 5H, CH_2 and CH glycerol), 3.72 (s, 3H, MeO) ppm. 13C-NMR ($CDCl_3$, 101 MHz) d: 129.67, 129.41, 113.79, 73.11, 71.31, 70.68, 63.94, 55.20 ppm. MS (ESI): m/z = 235.40 [M+Na]+.

***1-O-Oleoyl-3-(4-methoxybenzyl)-sn-glycerol (IV)**.* To a solution of **3-(4-Methoxybenzyl)-sn-glycerol III** (2.93 g, 13.81 mmol) and oleic acid (4.68 mL, 16.57 mmol) in dry CH_2Cl_2 (100 mL) was added a solution of DCC (3.42 g, 16.57 mmol) and DMAP (844 mg, 6.91 mmol) in dry CH_2Cl_2 (50 mL). The solution was stirred for 16 h at RT, filtered, and concentrated in vacuo, and the residue was purified by flash chromatography on silica gel with 40% ethyl acetate in n-hexane to afford 4.45 g of **IV** (67%) as a colorless oil: Rf = 0.32 (ethyl acetate/hexane, 1/20, v/v); 1H-NMR ($CDCl_3$, 400 MHz) d: 7.18 (d, 2H, phenyl), 6.82 (d, 2H, phenyl), 5.23 (m, 2H, CH= oleoyl), 4.95 (m, 1H, CH glycerol), 4.42 (s, 2H, $PMBCH_2O$), 4.12-3.37 (m, 4H, CH_2 glycerol), 3.74 (s, 3H, MeO), 2.24 (m, 2H, CH_2CO oleoyl), 1.93 (m, 4H, CH_2CH= oleoyl), 1.54 (m, 2H, CH_2CH_2CO oleoyl), 1.18 (m, 20H, CH_2 oleoyl), 0.82 (m, 3H, CH_3 oleoyl) ppm. 13C-NMR ($CDCl_3$, 101 MHz) d: 173.90, 159.34, 130.20, 129.98, 129.70, 129.40, 113.77, 73.15, 70.53, 68.71, 65.35, 55.25, 34.12, 31.88, 29.75, 29.68, 29.63, 29.50, 29.30, 29.14, 29.08, 27.20, 27.15, 24.88, 22.62, 14.10 ppm. MS (ESI): m/z = 499.71 [M+Na]+.

***1-O-Oleoyl-2-O-methoxymethyl-3-(4-methoxybenzyl)-sn-glycerol (V)**.* Chloromethyl methyl ether (0.75 mL, 10 mmol) was added to a stirred solution of **IV** (498 mg, 1 mmol) and DiPEA (1.74 mL, 10 mmol) in dry CH_2Cl_2 (50 mL) under N_2 at 0 °C. The mixture was stirred at 0 °C for 2 h and overnight at RT. The organic layer was washed with water, brine and then dried. Product **V** (496 mg, 95% yield) was obtained after removal of the solvent and purification by chromatography (hexane/EtOAc 4/1). Rf = 0.61 (8/2 Hex/EtOAc). 1H-NMR ($CDCl_3$, 400 MHz) d: 7.23 (d, 2H, phenyl), 6.87 (d, 2H, phenyl), 5.33 (m, 2H, CH= oleoyl), 4.71 (m, 2H, CH_2

MOM), 4.45 (s, 2H, $PMBCH_2O$), 4.24-3.96 (m, 3H, CH and CH_2 glycerol), 3.80 (s, 3H, MeO), 3.53 (m, 2H, CH_2 glycerol), 3.40 (s, 3H, MeO MOM), 2.30 (m, 2H, CH_2CO oleoyl), 1.98 (m, 4H, CH_2CH= oleoyl), 1.58 (m, 2H, CH_2CH_2CO oleoyl), 1.25 (m, 20H, CH_2 oleoyl), 0.86 (m, 3H, CH_3 oleoyl) ppm. 13C-NMR ($CDCl_3$, 101 MHz) d: 173.79, 159.44, 130.43, 130.21, 129.94, 129.48, 128.26, 128.10, 113.98, 96.24, 74.02, 73.29, 70.53, 69.55, 64.24, 55.70, 55.47, 34.40, 31.88, 29.74, 29.39, 27.38, 27.10, 14.33 ppm. MS (ESI): m/z = 542.65 [M+Na]+.

1-O-Oleoyl-2-O-methoxymethyl-sn-glycerol (3). DDQ (258.8 mg, 1.14 mmol) was added to a solution of **V** (298.2 mg, 0.57 mmol) in CH_2Cl_2 (40 mL) and H_2O (0.4 mL) and the reaction was stirred overnight at RT. The reaction mixture was diluted with CH_2Cl_2, washed with saturated $NaHCO_3$, water, and then brine, dried ($MgSO_4$), and evaporated. The product was purified by FCC (40% EtOAc in n-Hexane). Yield: 193.2 mg (84%). Rf = 0.41 (40% EtOAc in n-Hexan). 1H-NMR ($CDCl_3$, 400 MHz) d: 5.34 (m, 2H, CH= oleoyl), 4.74 (s, 2H, CH_2 MOM), 4.20-3. 60 (m, 5H, CH and CH_2 glycerol), 3.43 (s, 3H, MeO MOM), 2.31 (m, 2H, CH_2CO oleoyl), 2.01 (m, 4H, CH_2CH= oleoyl), 1.60 (m, 2H, CH_2CH_2CO oleoyl), 1.25 (m, 20H, CH_2 oleoyl), 0.85 (m, 3H, CH_3 oleoyl) ppm. 13C-NMR ($CDCl_3$, 101 MHz) d: 173.95, 130.22, 129.92, 96.85, 77.94, 62.83, 62.61, 55.95, 34.36, 29.53, 29.33, 27.42, 25.10, 14.32 ppm. MS (ESI): m/z = 422.87 [M+Na]+.

*Compound **4***. 1-*O*-Oleoyl-2-*O*-methoxymethyl-*sn*-glycerol **3** (40.1 mg, 0.1 mmol) was co-evaporated with MeCN (3x) and dissolved in anhyd. CH_2Cl_2 (5 mL) under an argon atmosphere. iPr_2EtN (0.02 ml, 0.11 mmol) and chloro(diisopropylamino)methoxyphosphine (0.02 ml, 0.11 mmol) were added to this solution, and the reaction was stirred for 1 h at RT. 1*H*-Tetrazole (0.5 ml, 0.2 mmol of a 0.45 M stock solution in MeCN) was added to this stirring solution. Meanwhile compound **2** (39.8 mg, 0.1 mmol) was co-evaporated with MeCN (3x), diluted in anhyd. CH_2Cl_2 (10 ml) and added to the reaction mixture. The solution was stirred overnight at RT and cooled to −70°C, while *tert*-butyl hydroperoxide (0.02 ml, 0.13 mmol of 70 wt % in H_2O) was added dropwise. After stirring the reaction at −70°C for 10 min, the reaction was allowed to come to RT over 2 h, diluted with CH_2Cl_2 (10 mL) and washed with a sat. Na_2SO_3 solution (20 mL). The organic layer was extracted with H_2O (2×20 mL), brine (20 mL), then dried over anhyd. Na_2SO_4, filtered, and concentrated under vacuum to yield a colorless syrup. The residue was purified on a silica gel column (3% MeOH in CH_2Cl_2). Yield: 32.6 mg (37% over three steps). R_f = 0.35 (5% MeOH in CH_2Cl_2); ^{1}H NMR ($CDCl_3$, 400 MHz): δ = 7.69 (br s, 1 H; NH), 7.44 (d, 2H; Ar), 7.19 (d, 2H; Ar), 7.10 (br s, 1 H; NH), 5.34 (m, 2H; CH= oleoyl), 5.15-5.00 (br s, 1H; benzylic C*H*OH), 4.69 (s, 2H; CH_2MOM), 4.30-3.95 (m, 5H; CH, CH_2 glycerol), 3.87 (s, 3H; CH_3OP isomer 1), 3.84 (s, 3H; CH_3OP isomer 2), 3.68-3.48 (m, 10H; linker), 3.37 (s, 3H; CH_3O MOM), 3.34-3.24 (m, 2H; linker), 2.32 (m, 2H, CH_2CO oleoyl), 2.01 (m, 4H, C*H*$_2$CH= oleoyl), 1.61 (m, 2H; C*H*$_2$CH$_2$CO oleoyl), 1.42 (s, 9H; Boc), 1.28 (m, 20H; CH_2 oleoyl), 0.88 ppm (m, 3H; CH_3 oleoyl). ^{13}C NMR ($CDCl_3$, 101 MHz): δ = 173.43, 129.97, 129.67, 128.26, 119.99, 96.10, 96.06, 73.30, 73.22, 73.16, 70.29, 70.23, 70.20, 70.12, 69.50, 67.17, 67.11, 62.77, 62.75, 55.63, 40.42, 40.37, 39.04, 34.03, 31.86, 29.72, 29.66, 29.61, 29.57, 29.48, 29.43, 29.28, 29.22, 29.14, 29.07, 29.06, 28.34, 27.18, 27.13, 24.80, 22.64 ppm; ^{31}P NMR ($CDCl_3$ 162 MHz): δ = -5.282 ppm. MS (ESI): *m/z*: 897.14 [*M*+Na]$^+$, *m/z*: 841.16 [*M*-*t*Bu+Na]$^+$, *m/z*: 797.20 [*M*-Boc+Na]$^+$.

ATX-ABP. Dimethylaminosulfur trifluoride (0.01 ml, 0.08 mmol) was added to a solution of **4** (15 mg, 0.02 mmol) in CH_2Cl_2 (5 mL) under argon at -78°C, and the reaction mixture was stirred for 3 h. When TLC monitoring (2% methanol in CH_2Cl_2) showed complete consump-

tion of **4**, CH_2Cl_2 was added to the reaction, and the organic layer was washed with a sat. solution of $NaHCO_3$ (3x) and brine. The organic extracts were dried over $MgSO_4$, filtered, and evaporated. The remaining colorless solid was purified by column chromatography over silica gel (2% MeOH in CH_2Cl_2) to afford **5** as colorless oil (10.3 mg, yield 68%). Compound **5** (30 mg, 34.21 µmol) was co-evaporated with MeCN (3x), diluted in anhyd. CH_2Cl_2 (2 mL) and placed under an argon atmosphere. The solution was cooled to 0°C and trimethylsilyl bromide (0.04 ml, 0.342 mmol) was added under argon, and the reaction mixture was first stirred for 4 h at 0°C and then for 1 h at RT. The reaction mixture was poured into a sat. solution of $NaHCO_3$, acidified and then extracted with CH_2Cl_2 (3x) and washed with brine. The organic extracts were dried over $MgSO_4$, filtered, and evaporated. Product **6** was directly used for the following reaction without further purification. MS (ESI): *m/z*: 836.71 $[M+18]^+$. Crude product **6** was dissolved in TFA/CH_2Cl_2 (1:1, *v/v*, 2 ml). After 1 h the reaction mixture was evaporated, and the remaining amorphous TFA salt was dissolved in a minimal amount of H_2O/MeCN and freeze-dried. MS (ESI): *m/z*: 741.55 $[M+Na]^+$. The resulting product **7** was directly used in the following reaction without further purification. To a solution of **7** in DMF (1 ml) was added iPr_2EtN (6 µl, 34.21 µmol) and Cy5 NHS ester (26 mg, 34.21 µmol). The reaction mixture was stirred overnight at RT and solvents were then removed under reduced pressure to give a blue film, which was purified by reversed-phase HPLC on a semi-preparative Vydac C8 column by using a linear gradient (20-95% MeCN) to afford 4 mg of pure fluorescent **ATX-ABP** (8% after HPLC purification). ^{1}H NMR ($CDCl_3$, 400 MHz): δ = 7.70 (br s, 1 H; NH), 7.48 (d, 2H; Ar), 7.23 (d, 2H; Ar), 6.90-6.83 (br s, 1 H; NH), 5.77 (d, *J* = 48.3 Hz, 1H; benzylic CHF), 5.34 (m, 2H; CH= oleoyl), 5.18 (m, 1H; CH glycerol), 4.40-3.30 (m, 16H, CH_2 glycerol and linker), 2.34 (m, 2H; C*H*$_2$CO oleoyl), 2.00 (m, 4H; C*H*$_2$CH= oleoyl), 1.62 (m, 2H; C*H*$_2$CH$_2$CO oleoyl), 1.25 (m, 20H; CH_2 oleoyl), 0.88 ppm (m, 3H; CH_3 oleoyl); ^{31}P NMR ($CDCl_3$ 162 MHz): δ = -5.656 ppm. MS (ESI): *m/z* 1434.55 $[M+2K-H]^+$.

Activity profiling: covalent labeling with ATX-ABP

The indicated amount of purified recombinant ATX was incubated with **ATX-ABP** in reaction buffer (containing 140 mM NaCl, 5 mM KCl, 1 mM $CaCl_2$, 1 mM $MgCl_2$, 50 mM Tris pH 7.8) at 37°C for 1 h. A range of concentrations of **ATX-ABP** was prepared by dilution in reaction buffer of a stock solution (10 mM) of probe in MeOH containing 10% DMSO. The reactions were quenched by the addition of an equal amount of reducing sample buffer followed by heating at 70°C for 10 min. Protein was separated by 4-12% SDS polyacrylamide gel electrophoresis (SDS-PAGE). The fluorescent signal was detected using a PerkinElmer scanner (625-680 nm). Proteins were then visualized by staining with Coomassie Blue or SYPRO.

ATX inhibitor profiling

Purified recombinant ATX was incubated with LPA and ATX inhibitor **HA130** in reaction buffer (containing 140 mM NaCl, 5 mM KCl, 1 mM $CaCl_2$, 1 mM $MgCl_2$, 50 mM Tris pH 7.8) at 37°C for 1 h. A range of concentrations of the LPA and ATX inhibitor **HA130** was obtained by dilution in reaction buffer from a stock solution (10 mM) in DMSO. Subsequently, samples were incubated with **ATX-ABP** (50 µM) at 37°C for 15 min as described above.

ATX enrichment from fetal bovine serum

Fetal bovine serum (FBS) was purified with anion-exchange chromatography (SP Sepharose TM Fast Flow). FBS was diluted with 50 mM TRIS buffer (pH8) and loaded onto the column. The column was eluted with a linear gradient of NaCl (0-1 M). Active fractions (100 mM

NaCl) were identified by using a commercially available FS3 ATX-activity assay (Echelon) (31). Active fractions were incubated with 2 µM probe for 1 h at 37°C as described above.

FS3 ATX-activity assay

FS3 was obtained from Echelon Bioscience and maintained as a 1 mM stock solution in Tris-buffered saline. Purified fractions collected from the anion exchange chromatography were diluted with Tris-buffered saline (140 mM NaCl, 5 mM KCl, 1 mM $CaCl_2$, 1 mM $MgCl_2$, 50 mM Tris, pH 7.8) containing 0.2 µg/µl fatty acid free BSA (BSA-FAF) and 2.5 µM FS3 at a concentration of 100 µM and incubated in a dark flat-bottom 96-well plate overnight at 37°C. The increase in fluorescence was measured in a Victor Wallac 96-well plate reader (485/535 nm).

MS analysis and in-gel digestion of proteins

Selected Coomassie-blue-stained gel bands were excised and digested with trypsin using a Proteineer DP digestion robot (Bruker, Bremen, Germany), by following the protocol supplied by the manufacturer. This protocol includes destaining, reduction and alkylation, followed by overnight digestion with trypsin. After digestion tryptic fragments were extracted with 50:50:1 H_20/MeCN/formic acid. Extracts were pooled and lyophilized.

Mass spectrometry and database searching

Lyophilized preparations were dissolved in H_20/MeCNl/formic acid (95:3:0.1, *v/v/v*) and subsequently sequenced by tandem mass spectrometry. Peptides were analyzed by nanoflow liquid chromatography using an Agilent 1100 HPLC system (Agilent Technologies) coupled on line to a 7-tesla LTQ-FT mass spectrometer (Thermo Electron, Bremen, Germany). The chromatographic system consisted of the following components. ReproSil-Pur C18-AQ, 3 µm (Dr. Maisch GmbH, Ammerbuch, Germany) was used as a resin for the analytical nanocolumn and AQUA-C18 5 µm was used as a resin for the trapping column. Columns were prepared in house. The end of the nanocolumn was drawn to a tip (ID approximately 5 µm), from which the eluent was sprayed into the mass spectrometer. Peptides were trapped at 5 µl/min on a 1 cm column (100 µm internal diameter, packed in house) and eluted to a 15 cm column (50 µm internal diameter, packed in house) at 150 nl/min in a 60 min gradient from 0 to 50% MeCN (0.1% formic acid). The mass spectrometer was operated in data-dependent mode, automatically switching between MS and MS/MS acquisition. Full-scan MS spectra were acquired in the FT-ICR with a resolution of 25 000 at a target value of 5 000 000. The two most intense ions were then isolated for accurate mass measurements by a selected ion-monitoring scan in FT-ICR with a resolution of 50 000 at a target accumulation value of 50 000. The selected ions were then fragmented in the linear ion trap by using collision-induced dissociation at a target value of 10 000. In a post-analysis process, raw data were converted to peak lists using Bioworks Browser software, version 3.1. For protein identification, MS/MS data were submitted to the Swiss Prot database (version 51.6; 257964 entries) using Mascot version 2.1 (Matrix Science) with the following settings: 2 ppm and 0.8 Da deviation for precursor and fragment masses, respectively, and trypsin was the enzyme specified.

IP and antibody coupling to CNBr activated sepharose 4B

For the purification of ATX from plasma samples using an immunoprecipitation (IP) strategy the samples were first incubated with the fluorescent probe at a final concentration of 10 µM. After incubation at 37°C for 2 h the samples were immediately incubated with the

precipitating monoclonal 5E5 antibody in PBS/10% $NaHCO_3$ (30) coupled to CNBr activated sepharose 4B beads for 5 h tumbling at 4°C. Proteins were eluted by boiling for 10 min at 70°C in reducing loading buffer, separated by SDS-PAGE and scanned for fluorescence. Subsequently, proteins were transferred to nitrocellulose filters and probed with an anti-ATX antibody (Cayman Chemical, Ann Arbor MI) and HRP-conjugated secondary antibody (Amersham).

ACKNOWLEDGEMENTS

This work was supported by grants from the Netherlands Foundation for Scientific Research (NWO chemical sciences; ECHO; to H.O. and W.H.M), the Netherlands Proteomics Centre (to H.O) and by the Dutch Cancer Society (to W.H.M. and H.O). We thank Laurens van Meeteren, Adrian Rzadkowski and John de Widt for their support.

REFERENCES

1. Tokumura, A., Majima, E., Kariya, Y., Tominaga, K., Kogure, K., Yasuda, K., and Fukuzawa, K. (2002) *J. Biol. Chem.* **277,** 39436-39442
2. Umezu-Goto, M., Kishi, Y., Taira, A., Hama, K., Dohmae, N., Takio, K., Yamori, T., Mills, G. B., Inoue, K., Aoki, J., and Arai, H. (2002) *J. Cell Biol.* **158,** 227-233
3. van Meeteren, L. A. and Moolenaar, W. H. (2007) *Prog. Lipid Res.* **46,** 145-160
4. Stefan, C., Jansen, S., and Bollen, M. (2005) *Trends Biochem. Sci.* **30,** 542-550
5. Stracke, M. L., Krutzsch, H. C., Unsworth, E. J., Arestad, A., Cioce, V., Schiffmann, E., and Liotta, L. A. (1992) *J. Biol. Chem.* **267,** 2524-2529
6. Nam, S. W., Clair, T., Campo, C. K., Lee, H. Y., Liotta, L. A., and Stracke, M. L. (2000) *Oncogene* **19,** 241-247
7. David, M., Wannecq, E., Descotes, F., Jansen, S., Deux, B., Ribeiro, J., Serre, C. M., Gres, S., driss-Vermare, N., Bollen, M., Saez, S., Aoki, J., Saulnier-Blache, J. S., Clezardin, P., and Peyruchaud, O. (2010) *PLoS. One.* **5,** e9741
8. Jonkers, J. and Moolenaar, W. H. (2009) *Cancer Cell* **15,** 457-459
9. Mills, G. B. and Moolenaar, W. H. (2003) *Nat. Rev. Cancer* **3,** 582-591
10. Tanaka, M., Okudaira, S., Kishi, Y., Ohkawa, R., Iseki, S., Ota, M., Noji, S., Yatomi, Y., Aoki, J., and Arai, H. (2006) *J. Biol. Chem.* **281,** 25822-25830
11. van Meeteren, L. A., Ruurs, P., Stortelers, C., Bouwman, P., van Rooijen, M. A., Pradere, J. P., Pettit, T. R., Wakelam, M. J., Saulnier-Blache, J. S., Mummery, C. L., Moolenaar, W. H., and Jonkers, J. (2006) *Mol. Cell Biol.* **26,** 5015-5022
12. Kanda, H., Newton, R., Klein, R., Morita, Y., Gunn, M. D., and Rosen, S. D. (2008) *Nat. Immunol.* **9,** 415-423
13. Tager, A. M., LaCamera, P., Shea, B. S., Campanella, G. S., Selman, M., Zhao, Z., Polosukhin, V., Wain, J., Karimi-Shah, B. A., Kim, N. D., Hart, W. K., Pardo, A., Blackwell, T. S., Xu, Y., Chun, J., and Luster, A. D. (2008) *Nat. Med.* **14,** 45-54
14. Inoue, M., Rashid, M. H., Fujita, R., Contos, J. J., Chun, J., and Ueda, H. (2004) *Nat. Med.* **10,** 712-718
15. Inoue, M., Xie, W., Matsushita, Y., Chun, J., Aoki, J., and Ueda, H. (2008) *Neuroscience* **152,** 296-298
16. Albers, H. M., van Meeteren, L. A., Egan, D. A., van Tilburg, E. W., Moolenaar, W. H., and Ovaa, H. (2010) *J. Med. Chem.* **53,** 4958-4967
17. Albers, H. M., Dong, A., van Meeteren, L. A., Egan, D. A., Sunkara, M., van Tilburg, E. W., Schuurman, K., van, T. O., Morris, A. J., Smyth, S. S., Moolenaar, W. H., and Ovaa, H. (2010) *Proc. Natl. Acad. Sci. U. S. A* **107,** 7257-7262
18. Gierse, J., Thorarensen, A., Beltey, K., Bradshaw-Pierce, E., Cortes-Burgos, L., Hall, T., Johnston, A., Murphy, M., Nemirovskiy, O., Ogawa, S., Pegg, L., Pelc, M., Prinsen, M., Schnute, M., Wendling, J., Wene, S., Weinberg, R., Wittwer, A., Zweifel, B., and Masferrer, J. (2010) *J. Pharmacol. Exp. Ther.* **334,** 310-317
19. Masuda, A., Nakamura, K., Izutsu, K., Igarashi, K., Ohkawa, R., Jona, M., Higashi, K., Yokota, H., Okudaira, S., Kishimoto, T., Watanabe, T., Koike, Y., Ikeda, H., Kozai, Y., Kurokawa, M., Aoki, J., and Yatomi, Y. (2008) *Br. J. Haematol.* **143,** 60-70
20. Nakamura, K., Igarashi, K., Ide, K., Ohkawa, R., Okubo, S., Yokota, H., Masuda, A., Oshima, N., Takeuchi, T., Nangaku, M., Okudaira, S., Arai, H., Ikeda, H., Aoki, J., and Yatomi, Y. (2008) *Clin. Chim. Acta* **388,** 51-58
21. Barglow, K. T. and Cravatt, B. F. (2007) *Nat. Methods* **4,** 822-827
22. Ovaa, H. (2007) *Nat. Rev. Cancer* **7,** 613-620
23. Kumar, S., Zhou, B., Liang, F., Wang, W. Q., Huang, Z., and Zhang, Z. Y. (2004) *Proc. Natl. Acad. Sci. U. S. A* **101,** 7943-7948
24. Kumar, S., Zhou, B., Liang, F., Yang, H., Wang, W. Q., and Zhang, Z. Y. (2006) *J. Proteome. Res.* **5,** 1898-1905
25. Lo, L. C., Pang, T. L., Kuo, C. H., Chiang, Y. L., Wang, H. Y., and Lin, J. J. (2002) *J. Proteome. Res.* **1,** 35-40
26. Lu, C. P., Ren, C. T., Wu, S. H., Chu, C. Y., and Lo, L. C. (2007) *Chembiochem.* **8,** 2187-2190
27. Q.Zhu, X.Huang, G.Chen, and S.Yao (2003) Activity-based fluorescent probes that target phosphatases. Tetrahedron Letters,
28. Jiang, G., Xu, Y., Falguieres, T., Gruenberg, J., and Prestwich, G. D. (2005) *Org. Lett.* **7,** 3837-3840
29. Giganti, A., Rodriguez, M., Fould, B., Moulharat, N., Coge, F., Chomarat, P., Galizzi, J. P., Valet, P., Saulnier-Blache, J. S., Boutin, J. A., and Ferry, G. (2008) *J. Biol. Chem.* **283,** 7776-7789
30. Nakasaki, T., Tanaka, T., Okudaira, S., Hirosawa, M., Umemoto, E., Otani, K., Jin, S., Bai, Z., Hayasaka, H., Fukui, Y., Aozasa, K., Fujita, N., Tsuruo, T., Ozono, K., Aoki, J., and Miyasaka, M. (2008) *Am. J. Pathol.* **173,** 1566-1576
31. Ferguson, C. G., Bigman, C. S., Richardson, R. D., van Meeteren, L. A., Moolenaar, W. H., and Prestwich, G. D. (2006) *Org. Lett.* **8,** 2023-2026

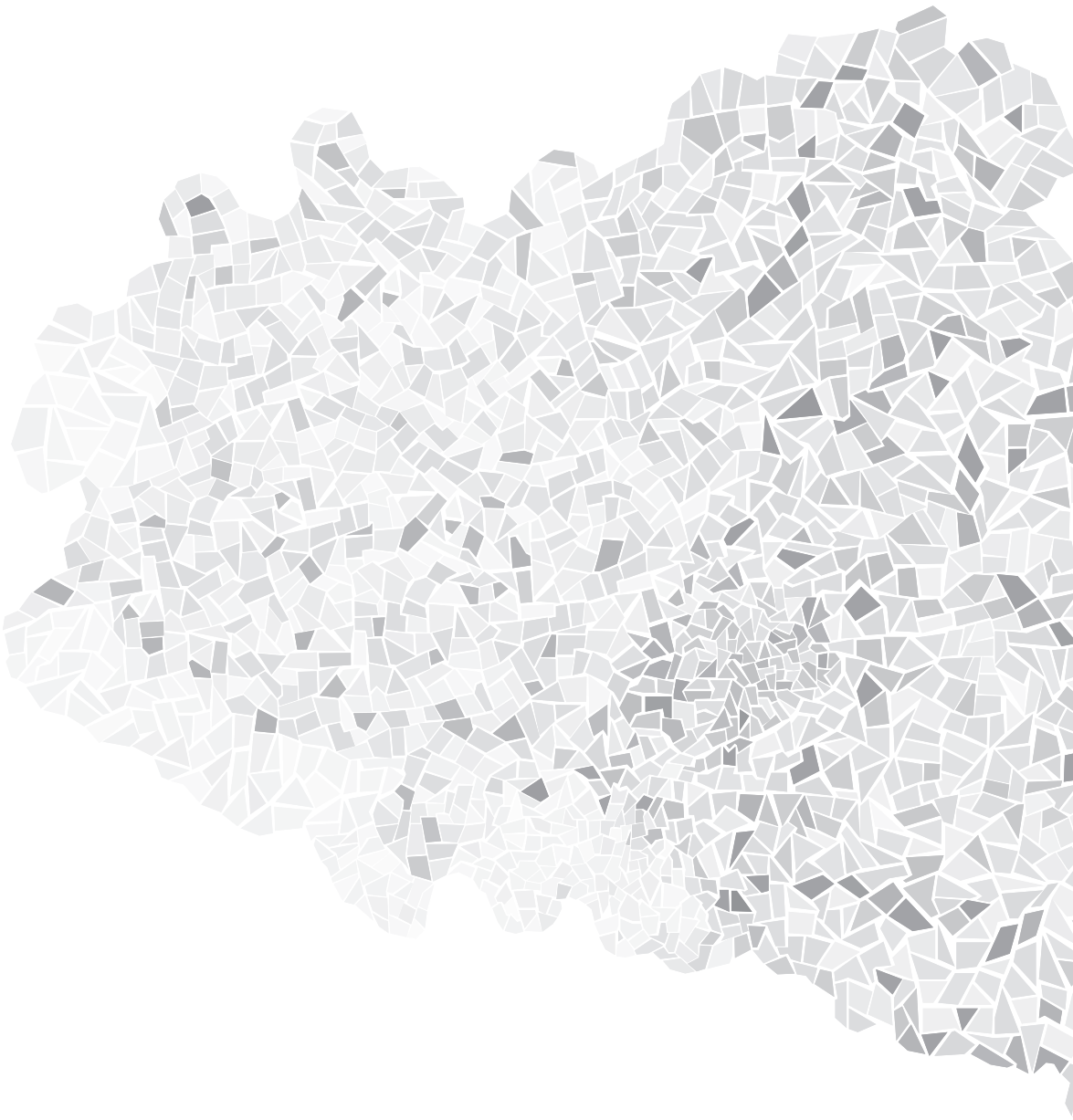

CHAPTER 5

The long isoform of autotaxin (ATXα) undergoes intradomain cleavage by furin and binds to heparin with high affinity

Submitted 2012

The long isoform of autotaxin (ATXα) undergoes intradomain cleavage by furin and binds to heparin with high affinity

Anna J.S. Houben[1] *,
Laurens A. van Meeteren[1,4] *,
Xander M.R. van Wijk[2],
Leonie van Zeijl[3],
Els M.A. van de Westerlo[2],
Jens Hausmann[3],
Alexander Fish[3],
Anastassis Perrakis[3],
Toin H. van Kuppevelt[2]
and Wouter H. Moolenaar[1]

[1]Division of Cell Biology,
The Netherlands Cancer Institute,
Amsterdam, The Netherlands
[2]Department of Biochemistry,
Nijmegen Centre for Molecular Life
Sciences, Radboud University
Nijmegen Medical Centre,
Nijmegen, The Netherlands
[3]Division of Biochemistry,
The Netherlands Cancer Institute,
Amsterdam, The Netherlands
[4]Present address: Department of
Molecular Cell Biology,
Leiden University Medical Center,
Leiden, The Netherlands

* These authors contributed equally
to this work

ABSTRACT

Autotaxin (ATX) is a secreted lysophospholipase D that converts lysophosphatidylcholine (LPC) into the lipid mediator lysophosphatidic acid (LPA), playing a key role in diverse physiological and pathophysiological processes. ATX exists in distinct isoforms, but isoform-specific functions are still largely uncharacterized. The ATXα isoform, first identified as a motility factor for melanoma cells, differs from the canonical form ATXβ by having a 52-residue polybasic insert in the catalytic domain, containing a furin cleavage site and putative heparin-binding motifs. Here we report that secreted ATXα is cleaved by furin after residue R340, yet remains structurally and functionally intact due to strong interactions within the catalytic domain. ATXα and ATXβ show similar catalytic efficiency towards LPC and are equally effective in stimulating cell migration. Through ELISA and surface plasmon resonance assays, we show that ATXα binds specifically and saturably to heparin with high affinity (K_d ~10^{-8} M), whereas ATXβ does not. Furthermore, heparin enhanced the lysophospholipase D activity of ATXα up to two-fold, but did not affect ATXβ activity. These findings suggest that, owing to its basic insert, ATXα may preferentially bind to cell-surface heparan sulfate proteoglycans to promote localized LPA production and signaling.

INTRODUCTION

Autotaxin (ATX), or ecto-nucleotide pyrophosphatase/phosphodiesterase 2 (ENPP2), is a secreted lysophospholipase D (lysoPLD) that converts lysophosphatidylcholine (LPC) into the multifunctional lipid mediator lysophosphatidic acid (LPA). LPA signals through six distinct G protein-coupled receptors (1) and stimulates migration, proliferation and other functions in many cell types, both normal and malignant (2;3). However, anti-migratory effects of ATX-LPA signaling have also been observed, depending on receptor expression profile and cell type (4). Studies in mice have uncovered key roles for ATX and LPA in a remarkable variety of physiological and pathophysiological processes, ranging from vascular development (5-7) and lymphocyte homing (8) to cancer (9;10), neuropathic pain (11) and pulmonary fibrosis (12), making the ATX-LPA signaling axis an attractive drug target.

Full-length ATX is synthesized as a pre-proenzyme. Upon removal of its N-terminal signal peptide followed by N-glycosylation, ATX is further processed by proprotein convertases and secreted via the classical secretory pathway as an active glycoprotein of 110-120 kDa (13;14). Mature ATX consists of two N-terminal somatomedin B-like (SMB) domains, a central catalytic phosphodiester domain (PDE) and a C-terminal nuclease-like (NUC) domain. Recent structural studies show that ATX has evolved a deep lysophospholipid-binding pocket at the active site and a nearby open tunnel that could function as an LPA exit channel (15;16). The NUC domain serves to maintain the rigidity of the PDE domain, while the N-terminal SMB domains mediate binding of ATX to activated integrins (15;17). Integrin binding localizes ATX to the cell surface, providing a mechanism to generate and deliver LPA close to its cognate receptors (8;17-19). Whether ATX uses additional or alternative mechanisms for spatially and temporally restricted LPA production is unknown.

Alternative splicing gives rise to distinct ATX isoforms (20), yet isoform-specific functions of ATX are still largely uncharacterized. The canonical isoform, termed ATXβ, was originally cloned from teratocarcinoma cells (21) and later shown to be identical to plasma lysoPLD, accounting for LPA production in plasma and serum (22;23). Virtually all our current understanding of ATX is derived from studies on ATXβ. The original α-isoform was first isolated as an 'autocrine motility factor' from melanoma cells (24) and is characterized by a 52-residue polybasic insert of unknown function in the catalytic domain (3;25). Conceivably, the ATXα insert could confer different catalytic activity, (sub)cellular localization, processing or binding-partner preference. It was previously reported that the insert is subject to proteolytic cleavage, leading to inactivation and degradation of ATXα (20); however, the latter notion remains to be substantiated.

In this study, we set out to examine the properties of ATXα relative to those of ATXβ, guided by the identification of a consensus furin cleavage site, putative heparin-binding motifs in the ATXα insert and by the crystal structure of ATXβ. Here we report two new findings. First, the ATXα insert is proteolytically cleaved by furin (or a furin-like endoprotease) at or near the cell surface, yet cleaved ATXα remains structurally and functionally intact. Second, the ATXα insert confers high-affinity binding to heparin and furthermore, heparin stimulates ATXα lysoPLD activity. On the basis of these findings, we suggest that ATXα may preferentially interact with cell-surface heparan sulfate proteoglycans to promote localized LPA production and signaling.

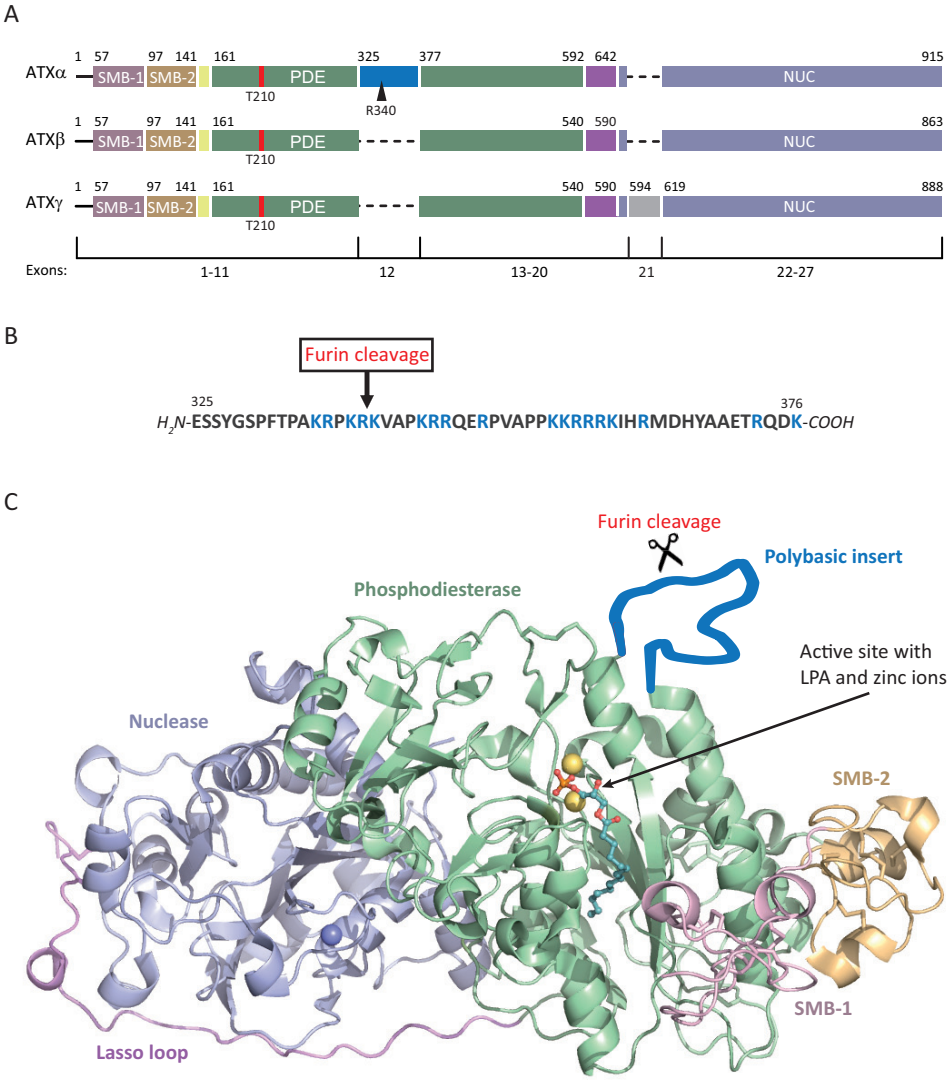

Figure 1. ATX isoforms: domain architecture and structure. (A) The α, β and γ isoforms of ATX differ by the absence or presence of exon 12 or 21. All isoforms share the same domain architecture of two N-terminal somatomedin B-like domains (SMB-1 and SMB-2), a central phosphodiester domain (PDE) with the catalytic residue T210, a C-terminal nuclease-like domain (NUC) and a 'lasso loop' connecting the PDE and NUC domains. ATXβ is the canonical isoform. ATXα contains a 52-residue insertion (amino acids 325-376) in the catalytic domain containing a proteolytic site at R340 (see Fig. 1B). ATXγ contains a 25-residue insertion (amino acids 594-618), encoded by exon 21, in the NUC domain. Transcript ID: ENST00000259486 (ATXα), ENST00000075322 (ATXβ), ENST00000522826 (ATXγ). (B) Amino acid sequence of the ATXα insert. Basic residues are indicated in blue. A consensus furin cleavage site (R-x-K/R-R) is located between residues R340 and K341 (arrow). (C) The crystal structure of rat ATXβ (ref. (15)), with the ATXα-specific insert shown as a flexible loop protruding out of the PDE domain. Domain colors are the same as in Fig. 1A, with LPA (blue-green), the phosphate (orange), the zinc ions (yellow spheres) bound to the active site, and the EF hand-bound calcium ion (blue sphere) shown in stick-and-sphere representation. The figure was prepared using Pymol (www.pymol.org).

RESULTS AND DISCUSSION

ATXα: structure and expression

The human and murine ATX gene is organized in 27 exons. The best known splice variants, termed α, β and γ, differ by the presence or absence of sequences encoded by exons 12 and 21 (Fig. 1A). ATXα contains an exon 12-encoded region of 52 residues in the catalytic domain. The canonical ATXβ isoform lacks exons 12 and 21, while the 'brain-specific' ATXγ isoform (formerly PD-1α) contains a 25-residue insert encoded by exon 21 in the NUC domain (26;27). A recently identified fourth isoform (ATXδ) has a four-residue deletion in the linker region ('lasso loop') between the PDE and NUC domain, but otherwise is identical to ATXβ (ref. (28) and AJH, unpublished results).

Here we focus on the properties of ATXα relative to those of ATXβ. The ATXα insert is highly basic with a calculated pI ~11.5. Sequence inspection revealed a consensus cleavage site for the endoprotease furin (target sequence R-x-K/R-R; ref. (29)) between R340 and K341, as well as putative heparin-binding motifs which are commonly characterized by clusters of basic residues (Fig. 1B). The recently determined crystal structure of ATXβ allowed us to understand the localization of the insert in ATXα. The insert, which is predicted to be unstructured and solvent-exposed, starts right in front of an α-helix in the PDE domain. In Fig.1C, it is depicted as a flexible, hydrophilic loop that protrudes out of the PDE domain, relatively far away from the catalytic site and the lysophospholipid-binding pocket. Given its location and hydrophilic nature, the insert is unlikely to affect the tertiary structure of the ATXα catalytic domain.

We examined ATX expression in various tissues and cell lines. In agreement with previous studies (8;10;20) and publicly available microarray data (30), highest ATX expression (all isoforms) was found in brain, kidney, spleen and lung, and somewhat lower expression in liver, skin and adipose tissue (Fig. 2A). Previous studies detected ATXα in kidney and liver (20) as well as in melanoma (24) and non-small-cell lung cancer cells (31). Using RT-PCR analysis, we detected ATXα in human skin fibroblasts (HF cells) and glioblastoma cells (SNB-78 and U-138). Analysis of mouse tissues shows that ATXα expression is much less widespread than ATXβ (Fig. 2B). ATXα mRNA was detected in skin, presumably reflecting expression in dermal fibroblasts since skin-derived keratinocytes lacked detectable ATXα (data not shown). ATXα-specific antibodies raised against sequences in the insert recognized overexpressed ATXα in HEK293 cells, but unfortunately could not detect endogenous ATXα (LvM, unpublished results). It is of note that ATXα was consistently found co-expressed with ATXβ in the cell lines and tissues examined. We therefore examined whether both isoforms might interact, but co-immunoprecipitation studies using HEK293 cells did not support this hypothesis (AJH, unpublished results). Using confocal microscopy, we found that ATXα and ATXβ show a very similar localization pattern in intracellular vesicles, consistent with both isoforms following the same vesicular trafficking route prior to secretion (Fig. 2C).

Secreted ATXα undergoes furin processing at R340

Furin cleavage of ATXα at R340 is predicted to result in an N-terminal part of 340 amino acids and a C-terminal fragment of 575 amino acids. When expressed in HEK293 cells, secreted ATXα was consistently detected not only as a ~120 kDa band but also as two prominent fragments of about 40 and 70 kDa, as shown by using antibodies against the N-terminal and C-terminal parts of ATX, respectively (Fig. 3A, lane 2). Three lines of evidence confirm

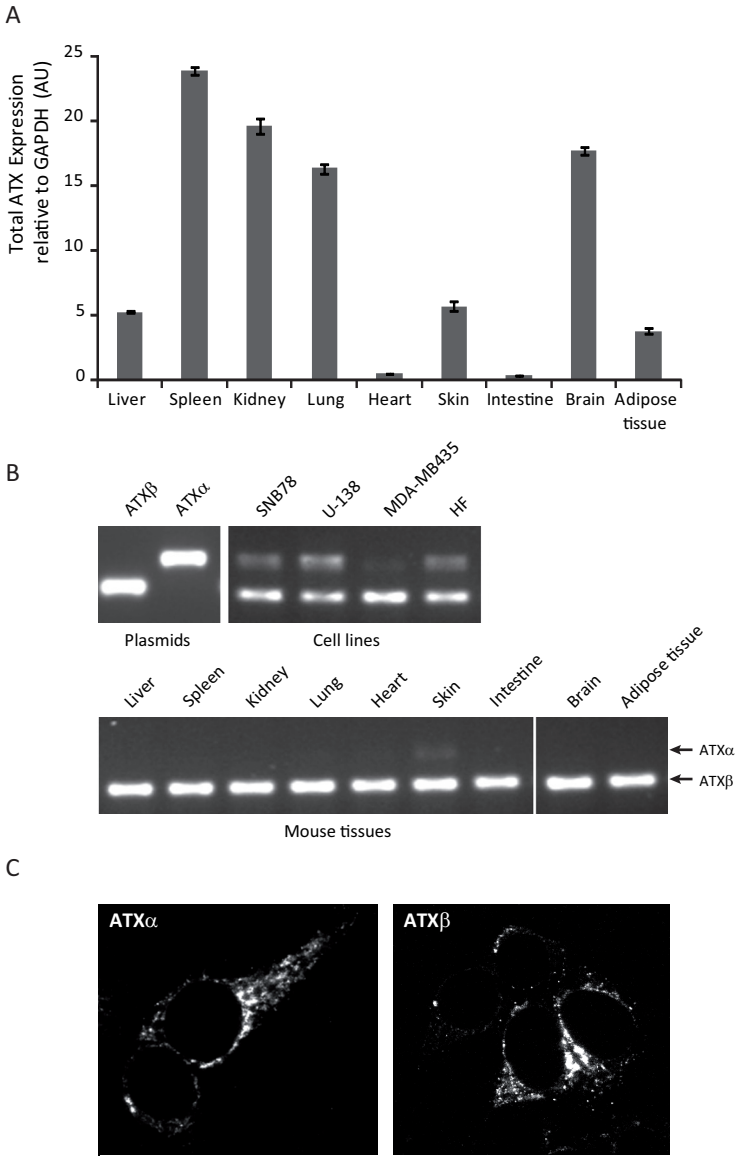

Figure 2. ATX isoform expression. (A) Quantitative PCR analysis of total ATX mRNA (all isoforms) relative to GAPDH in various mouse tissues. (B) RT-PCR analysis of ATXα and ATXβ expression in human cell lines and mouse tissues. Plasmid DNA analysis confirms specificity of the primers. Cell lines used: SNB78 and U138, glioblastoma; MDA-MB-435, melanoma; HF, foreskin fibroblasts. PCR primers were designed based on sequences around the ATXα-specific insert, resulting in an isoform-discriminative PCR. (C) Subcellular localization of ATXα and ATXβ (C-terminally Myc-tagged) in transfected HEK293 cells.

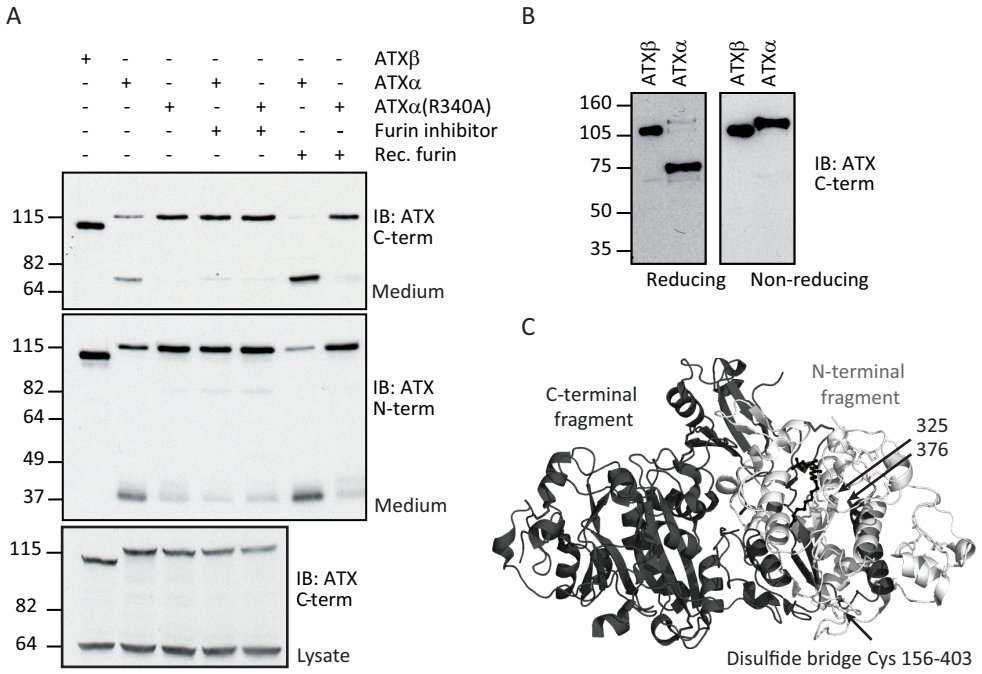

Figure 3. Cleavage of the ATXα insert by furin. (A) Western blot analysis of conditioned media from HEK293 cells expressing ATXβ (lane 1), ATXα (lanes 2, 4, 6) or mutant ATXα-R340A (lanes 3, 5, 7). Cleaved ATXα was detected in the medium (upper two panels), but not in cell lysates (lower panel). Cells were treated with 10 μM Dec-RVKR-CMK furin inhibitor overnight (lanes 4 and 5). Conditioned medium was treated with recombinant furin for 1 hour at 37°C (lanes 6 and 7). Antibodies used: ATX C-term (polyclonal; Cayman) and ATX N-term (monoclonal; 4F1). The residual faint bands observed in lanes 3, 4, 5 and 7 may be attributable to ATXα cleavage at non-optimal cleavage sites present in the insert. (B) Detection of HEK293 cell-conditioned media containing ATXα or ATXβ under reducing and non-reducing SDS-PAGE conditions. Note that ATXα cleavage is not observed under non-reducing conditions. Antibody: polyclonal anti-ATX C-term (Cayman). (C) The crystal structure of ATXβ with the ATXα insert superimposed. The N-terminal cleavage fragment is depicted in light grey, the C-terminal fragment in dark grey. The lysophopholipid binding pocket is composed by residues in both halves. LPA is depicted in the binding pocket. The disulfide bridge C157-C403 (arrow) connects the two fragments. The model was tilted 90°C on the x-axis compared to Fig. 1C to emphasize the extended interface between the two cleavage fragments. The polybasic insert of ATXα protrudes into the direction of the viewing plane, depicted by its first and last amino acid (325 and 376, respectively). See text for further details about intramolecular interactions.

that ATXα is cleaved after R340 by furin or a furin-like endoprotease. First, mutant ATXα-R340A was resistant to proteolysis (Fig. 3A, lane 3). Second, treatment of ATXα-expressing cells with decanoyl-Arg-Val-Lys-Arg-chloromethylketone (dec-RVKR-CMK), an inhibitor of furin-family endoproteases (32), prevented ATXα proteolysis (Fig. 3A, lanes 4-5). Third, addition of recombinant furin to HEK293-conditioned medium resulted in nearly complete cleavage of wild-type ATXα, but left ATXα-R340A intact (Fig. 3A, lanes 6-7).

Importantly, the two ATXα fragments were detected only in the medium but not in cell lysates (Fig. 3A, lower panel), indicating that ATXα cleavage occurs at or near the cell surface rather than along the intracellular trafficking route. Indeed, although furin resides predominantly in the trans-Golgi network (TGN), furin (and related proteases) can also traffic to the cell surface and can be secreted to act in a paracrine manner (33;34). Thus, furin exerts a dual action on ATXα: first, it releases mature ATX from its precursor in the TGN and, second, it cleaves the ATXα insert at or near the cell surface.

What could be the structural and functional consequences of the observed intradomain cleavage? When ATXα was examined under non-reducing conditions, there was no sign of proteolytic fragmentation indicating that ATXα remains intact (Fig. 3B). As can be inferred from the crystal structure (Fig. 3C), cleavage of ATXα at R340 leaves the N- and C-terminal parts tightly together due to an extended interaction surface area between both parts (10,980 Å^2, as calculated by PISA (35)). An analysis using FoldX (36) indicates that van der Waals interactions are primarily responsible for the stability of the interface (-76 kcal/mol). Stability is further re-enforced by numerous hydrogen bonds (-69 kcal/mol), ionic interactions (-12 kcal/mol) and a disulfide linkage between Cys157 and Cys403 (-3 kcal/mol). Thus, the N- and C-terminal parts of ATXα normally form a very stable structure (calculated free energy of dissociation >100 kcal/mol) that can only be separated under reducing SDS-PAGE conditions. This refutes the previously held notion that ATXα undergoes rapid proteolytic fragmentation *in vivo*, being a new way of terminating catalytic activity (20).

ATX activity

It was previously reported that ATXα and ATXβ show similar LPC substrate preferences, but enzyme kinetics were not examined (20). We measured lysoPLD activity of both isoforms by using LPC(18:1) as a substrate and monitoring the release of free choline. As shown in Fig. 4A, we find that the catalytic efficiency (V_{max}/K_m) of ATXα towards LPC is about 70% of that

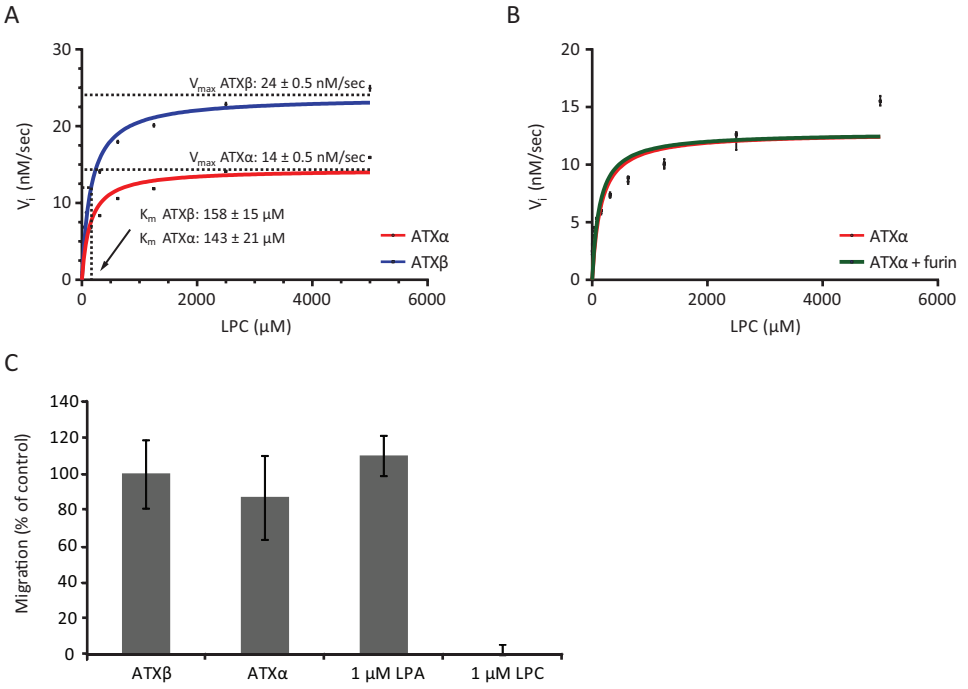

Figure 4. LysoPLD activity of ATXα relative to ATXβ. (A) LysoPLD activity of ATXα (red) and ATXβ (blue) at increasing concentrations of LPC(18:1). (B) LysoPLD activity of ATXα before (red) and after (green) treatment with recombinant furin. Data in (A) and (B) are expressed as means ± SD of three replicates and are representative of two independent experiments. (C) Chemotactic activity of ATXα and ATXβ, as measured by the transwell migration of A2058 melanoma cells using 2 nM recombinant ATX in the presence of 2 µM LPC. LPA (1 µM) was used as a positive control and LPC (1 µM) as a negative control.

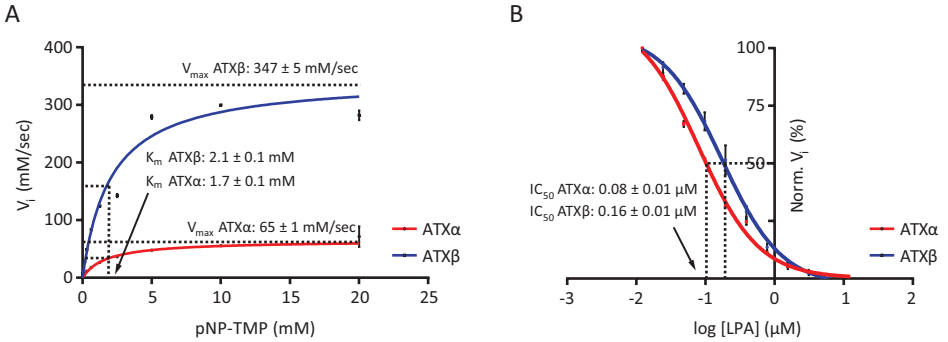

Figure 5. Nucleotide phosphodiesterase activity of ATXα relative to ATXβ. (A) Phosphodiesterase activity of ATXα and ATXβ at increasing concentrations of pNP-TMP. (B) LPA-induced inhibition of ATX activity towards 1 mM pNP-TMP. Based on the indicated IC_{50} values, the K_i values were calculated as 50 nM and 110 nM for ATXα and ATXβ, respectively. Data are expressed as means ± SD of three replicates and are representative of two independent experiments.

of ATXβ, primarily due to a lower V_{max} value. Treatment of ATXα with recombinant furin (in order to ensure full cleavage of the insert) did not affect its lysoPLD activity (Fig. 4B). Furthermore, ATXα and ATXβ were equally effective in stimulating the transwell migration of A2058 melanoma cells in the presence of LPC (Fig. 4C).

In addition to lysophospholipids, nucleotides can also serve as substrates for ATX, although the *in vivo* relevance of the latter reaction is unclear. We found that the catalytic efficiency of ATXα towards pNP-TMP is >4-fold lower than that of ATXβ, mainly due to a lower V_{max} (Fig. 5A). We have currently no structural data that can explain this observation.

The nucleotide phosphodiesterase activity of ATXβ is inhibited by LPA (37). As shown in Fig. 5B, LPA(18:1) inhibited pNP-TMP hydrolysis by ATXα and ATXβ with K_i values of 50 nM and 110 nM, respectively, suggesting that the ATXα insert may exert a small positive effect on LPA binding affinity.

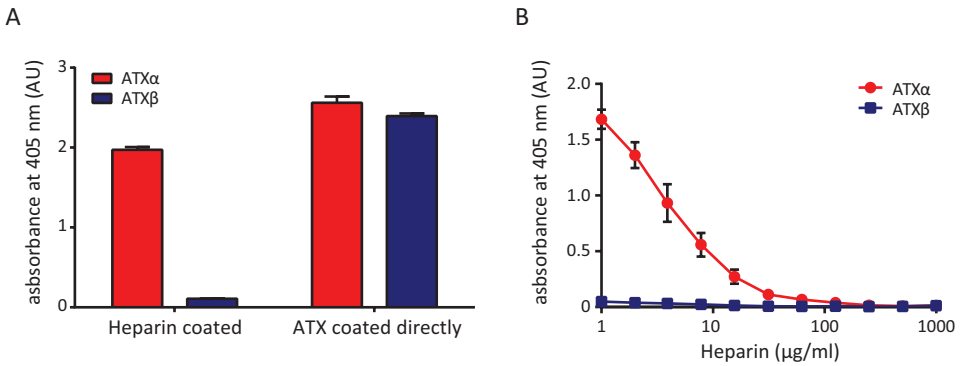

Figure 6. ATX binding to immobilized heparin measured by ELISA. (A) ATXα and ATXβ were applied to heparin-coated wells. Left panel: ATXα binds strongly to heparin, whereas ATXβ does not. Right panel: control experiments in which ATXα and ATXβ were directly immobilized to the wells (without heparin), giving similar readings for both isoforms. (B) Competition ELISA in which ATXα and ATXβ were pre-incubated with various amounts of heparin prior to application to heparin-coated wells. Binding of ATXα to immobilized heparin was inhibited by pre-incubation with heparin in a dose-dependent manner.

ATXα binds specifically to heparin

Given the presence of positively charged K/R clusters, we reasoned that the ATXα insert could confer high-affinity binding to heparin. Heparin is structurally very similar to heparan sulfate (HS), which is ubiquitously expressed as proteoglycans on cell surfaces and in extracellular matrices, where it recruits growth factors, chemokines and other molecules to fine-tune signaling events under both physiological and pathophysiological conditions (38-40). Although heparin/HS-binding domains are characterized by clusters of basic residues, absolute consensus motifs cannot be defined from sequence data (41;42). High-affinity binding of ATX to heparin *in vitro* would point to a new mechanism for localized LPA production and signaling *in vivo*.

We first determined the binding of ATXα and ATXβ to unfractionated heparin using ELISA, in which recombinant ATX was added to heparin-coated wells. We found that ATXα binds strongly to immobilized heparin, whereas ATXβ hardly did (Fig. 6A). As a positive control,

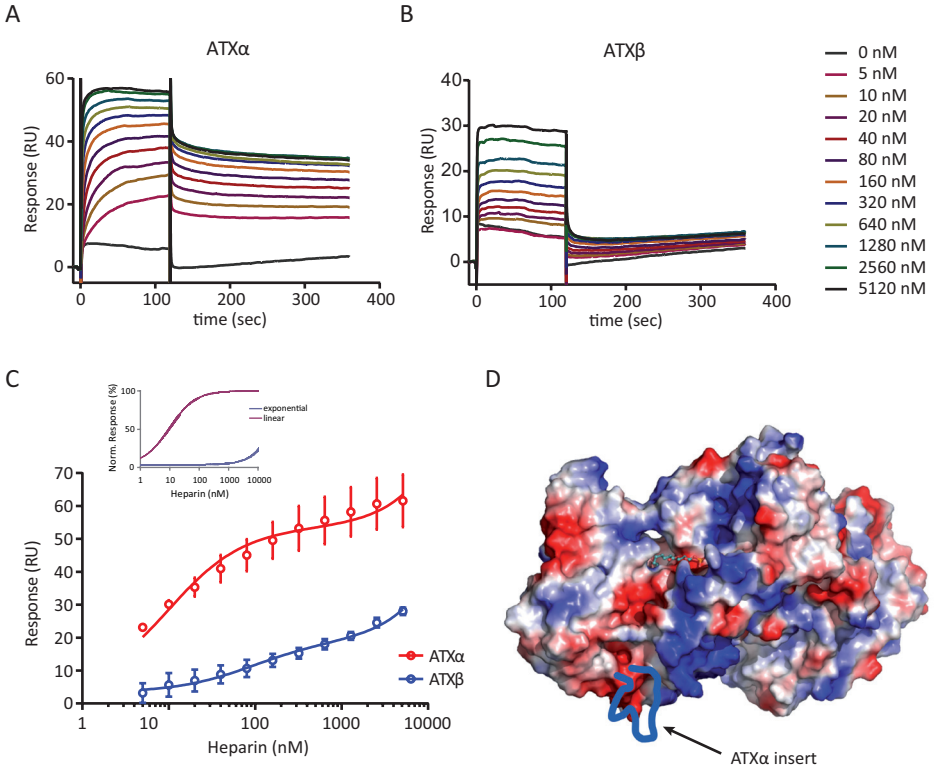

Figure 7. ATX binding to heparin measured by surface plasmon resonance. (A), (B). Surface plasmon resonance analysis of ATX binding to heparin, showing sensorgrams of heparin binding to immobilized ATXα and ATXβ, respectively. Heparin concentrations are based on a MW of unfractionated heparin of 15 kDa. (C) Heparin saturation binding plot of ATXα (red) and ATXβ (blue). The inset shows the exponential, saturable heparin-binding curve (red) and a linear component (blue; non-specific binding). The data were fit as described in the Experimental Procedures. Error bars correspond to the SD for a duplicate experiment. (D) Surface representation of ATXα indicating the electrostatic potential (-65 to +65 kT; positive charges in blue, negative charges in red). The polybasic insert of ATXα may cover a negative patch and might even extend the long positive patch running vertically over the protein. The figure was prepared using Pymol (www.pymol.org).

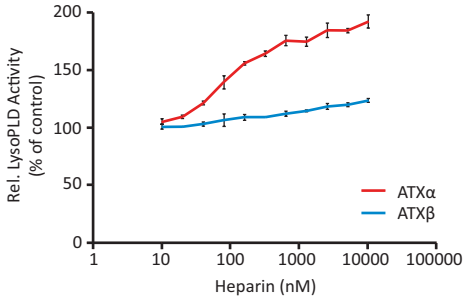

Figure 8. Effect of heparin on ATX lysoPLD activity. LysoPLD activity of ATXα (red) and ATXβ (blue) using LPC (150 μM) as a substrate and increasing concentrations of heparin. Half-maximal effect was observed at ~35 nM (based on a MW of heparin of 15 kDa). Data are expressed as means ± SD of three replicates and are representative of two independent experiments.

both isoforms were immobilized directly to the wells (without prior heparin coating), which gave similar readings for both isoforms. We also used a competition ELISA, in which ATX was pre-incubated with various amounts of soluble heparin prior to addition to heparin-coated wells. In these experiments, we observed a dose-dependent inhibition of ATXα binding to immobilized heparin, confirming that the observed ATXα-heparin interaction is specific (Fig. 6B).

We next examined ATX-heparin binding using surface plasmon resonance, in which recombinant ATX was immobilized and heparin was used as the analyte (Fig. 7A-C). Again, we found that ATXα binds heparin much stronger than does ATXβ. As can been seen in Fig. 7A, heparin binds ATXα rapidly and dissociates slowly, consistent with specific binding. In contrast, ATXβ showed very fast heparin binding and dissociation kinetics **(Fig. 7B), suggestive of non-specific binding.** Based on an average MW of heparin of 15 kDa, we determined the apparent K_d of ATXα for heparin to be approximately 10 nM. The K_d of ATXβ could not reliably be determined since heparin binding did not reach a plateau; however, it is at least 10-fold lower than that of ATXα (Fig. 7C). We conclude that the basic insert of ATXα confers stable, high-affinity binding to heparin with a slow dissociation rate.

An electrostatic surface charge representation of ATX sheds some light on how and where heparin may bind (Fig. 7D). The model shows several positively charged patches, representing potential heparin/HS-binding regions common to both isoforms. It is seen that the basic insert of **ATXα is located close to one of those patches in the catalytic domain, suggesting** that the insert and the positively charged surface patch may act in a cooperative manner to enhance binding to heparin/HS. Co-crystallization studies using defined heparin/HS fragments should help to test this scenario and, furthermore, uncover to what extent proteolytic cleavage at R340 may affect the heparin/HS interactions.

Interestingly, heparin enhanced the lysoPLD activity of ATXα towards LPC(18:1) up to two-fold in a concentration-dependent manner (EC_{50} ~35 nM), whereas heparin had little or no effect on the activity of ATXβ (Fig. 8). This raises the possibility that interaction of ATXα with cell-associated HS proteoglycans may serve not only to generate and deliver LPA close to its receptors, but also to increase the catalytic efficiency of this particular isoform.

CONCLUSIONS

We have shown that the polybasic insert of ATXα is susceptible to proteolytic cleavage by furin and confers high-affinity binding to heparin. It is noteworthy that ATXα cleavage occurs extracellularly, as it is not detectable in cell lysates, and leaves ATXα structure, stability and activity virtually unaltered. Although furin is the major proprotein convertase in the TGN, it is also found at the cell surface (34;43), where it can process secreted proteins such as, for example, the ADAMTS exo-enzymes (44)**.** Thus there is precedent for cleavage of secreted proteins by cell surface-associated furin. Furthermore, soluble furin and the furin-like PACE4 endoprotease can be secreted to act in a paracrine fashion over several cell diameters (33). *In vivo*, furin and PACE4 show distinct spatiotemporal distribution and delivery routes (33). Future studies should address whether secreted ATXα normally is processed by furin or PACE4, or whether both enzymes complement each other. The physiological consequences of ATXα cleavage are currently not clear, but it is tempting to speculate that proteolytic processing of secreted ATXα may serve to fine-tune its heparin/HS-binding properties *in vivo*, a scenario that warrants further investigation.

The finding that ATXα has nanomolar affinity for heparin strongly suggests that this isoform may preferentially localize to HS proteoglycans at the cell surface and/or in extracellular matrices. HS proteoglycans interact with numerous proteins, including growth factors and morphogens, and can facilitate the formation of growth factor gradients. Furthermore, our finding that heparin increases ATXα activity may point to a catalytic regulatory mechanism of this particular isoform. Previous studies have shown that ATXβ binds to activated integrins via its SMB domains, which provides one mechanism for localized production of LPA close to its cognate receptors (8;15;17;19). Binding of ATXα to heparin/HS proteoglycans may represent an additional, isoform-specifc mechanism for spatially and temporally restricted LPA production (18). It will be interesting to explore whether ATXα, HS and furin/PACE4 can be detected as a ternary complex at the cell surface or in extracellular matrices.

EXPERIMENTAL PROCEDURES

Cells and materials

HEK293T cells were grown in Dulbecco's modified Eagle's medium (DMEM) containing 10% fetal calf serum. The furin inhibitor decanoyl-Arg-Val-Lys-Arg-chloromethylketone (Dec-RVKR-CMK) was obtained from Biomol International, recombinant furin from New England Biolabs, LPC(18:1) and LPA(18:1) from Avanti Polar Lipids Inc. (Alabaster, AL), and heparin (from porcine intestinal mucosa; sodium salt) from Sigma-Aldrich (cat. no. H4784). Antibodies used: anti-Myc (9E10, home made); polyclonal anti-ATX against the C-terminal part of ATX (residues 573-588) (Cayman Chemical, Ann Arbor, USA); goat anti-ATX IgG (R&D systems, Minneapolis, USA); monoclonal anti-ATX, 4F1, against an N-terminal polypeptide of ATX (residues 58-182) (ref. (45); kindly provided by J. Aoki).

ATX constructs and recombinant protein

For ATX overexpression studies, human ATXβ was ligated in the pcDNA3 vector with a 3' Myc tag as previously described (37). Human ATXα, ligated in pcDNA3 containing a 3' Myc/His tag was a generous gift from Dr. Andree Blaukat (Merck-Serono, Darmstadt, Germany). Mutant ATXα-R340A was generated using the Stratagene site-directed mutagenesis kit, with

the following primers: p686-forward (GGCTAAGAGACCTAAGGCGAAAGTTGCCCC) and p687-reverse (GGGGCAACTTTCGCCTTAGGTCTCTTA GCC). For production of recombinant protein, ATXα and ATXβ were ligated in pcDNA5-FRT (Invitrogen) with a C-terminal Myc-tag and a 6xHis-tag. HEK293 cells stably expressing ATXα or ATXβ were generated using the FLPin system (Invitrogen). Recombinant His-tagged ATX was purified from conditioned HEK293 medium using POROS-20 MC columns pre-loaded with Ni^{2+}, as previously described (46). The column was washed with eight to ten column volumes of buffer *A* (20 mM Tris-HCl pH 8.0, 150 mM NaCl and 20 mM imidazole). ATX protein was eluted with a linear gradient of buffer *A* containing 750 mM imidazole.

Expression analysis

Cells were grown to confluency and total RNA was extracted using the RNeasy mini kit and column DNase treatment (Qiagen). First strand cDNA synthesis was performed using 2 µg total RNA, 0.5 µg oligo-dT primers (Promega), 500 nM dNTPs (Roche), 40 units RNAsin (Promega), 10 mM DTT (Invitrogen) and 200 units Superscript II RT. Quantitative ATX expression was measured using the TaqMan gene expression probe Hs00196470_m1 in an ABI 7500 Fast Sequence Detection System (Applied Biosystems). Cycling parameters were: 10 min. at 95°C followed by 40 cycles of 15 sec. at 95°C and 1 min. at 60°C. The relative product levels were quantified using the ddCt method and were normalized to GAPDH expression. Expression of the ATXα and ATXβ isoforms was measured by RT-PCR using primers (forward 5'-ATTACAGCCACCAAGCAAGG-3' and reverse 5'-TCCCTCAGAGGATTTGTCAT-'3) located around the insertion of the ATXα-specific insert, resulting in a 209 bp fragment for ATXβ and a 366 bp fragment for ATXα. Human plasmid DNA was used to confirm the specificity of the primers, which were species-independent.

Transfection and western blotting

HEK293 cells were transfected with ATX constructs using the calcium phosphate method. At 24 hrs after transfection, cells were incubated in serum-free DMEM for 48 hrs. Conditioned medium was centrifuged (5000 rpm for 30 min.) to remove cell debris. Samples were analyzed by gel electrophoresis using NuPAGE 4-12% Bis-Tris gels (Invitrogen) under either reducing or non-reducing conditions. For Western blot analysis, nitrocellulose filters were blocked using 5% non-fat powdered milk and probed with primary antibodies, followed by HRP-conjugated secondary antibodies (Dako, Glostrup, Denmark) and proteins were visualized using ECL detection (Amersham, Arlington Heights, IL).

Cell migration

Chemotactic migration of human A2058 melanoma cells was measured in 48-wells Boyden chambers (Neuroprobe) as described previously (47). Filters (8 µm pores) were coated with gelatin and cells were serum starved overnight, trypsinized and seeded in the upper chamber. ATX (2 ng/ml) was added to the bottom chamber in the presence of 2 µM LPC(18:1) and 1 mg/ml fatty-acid free BSA. After 4 hrs, cells at the top side were removed and migrated cells at the bottom side of the filter were fixed, stained and quantified.

Immunofluorescence

HEK293 cells were transfected with C-terminally Myc-tagged ATXα or ATXβ. At 24 hrs after transfection, cells were fixed with ice-cold ethanol and ATX was visualized by confocal microscopy using anti-Myc antibody (9E10) and anti-mouse Alexa488.

ATX activity assays

To measure lysoPLD activity, LPC(18:1) was used as substrate in 50 mM Tris (pH 7.4), 0.01% Triton X-100, 25 mM $CaCl_2$, containing 2.5 mM homovanillic acid, 2 units/ml horseradish peroxidase, 2 units/ml choline oxidase. After addition of recombinant ATX, the increase in fluorescence was monitored at 37°C (excitation/emission: 355/460 nm), as previously described (48). Nucleotide phosphodiesterase activity was measured using pNP-TMP (Sigma-Aldrich) as substrate in 50 mM Tris (pH 7.8), 140 mM NaCl, 5 mM KCl, 1 mM $CaCl_2$, 1 mM $MgCl_2$, 1 mg/ml fatty-acid free BSA**.** After addition of recombinant ATX, the amount of liberated *para*-nitrophenolate (pNP) was determined by the absorbance at 405 nm, as described (37). Michaelis-Menten kinetic parameters were determined using GraphPad Prism software.

ELISA

Binding of ATX (α or β) to heparin was evaluated by ELISA in two ways: (a) application of ATX to heparin-coated wells of microtiter plates, and (b) competition assays in which ATX was first incubated with heparin and then transferred to a heparin-coated plate. A 96-well flat-bottom plate was incubated for 16 h with 100 µl of 10 µg/ml heparin in coating buffer. As a control, wells were coated for 16 h with 1 µg/ml ATX in 0.05 M carbonate- bicarbonate buffer (Sigma-Aldrich, St Louis, MO). After blocking with PBS containing 2% BSA (w/v) for 1 h, 1 µg/ml ATX (in PBS containing 2% BSA) was added and incubated for 2 hrs. Plates were washed six times with PBS and bound ATX was detected using goat anti-ATX IgG (1:200; R&D systems), followed by incubation with alkaline phosphatase-conjugated rabbit anti-goat IgG (1:2000; Sigma-Aldrich), both for 1 h. Plates were washed six times with PBS, and enzyme activity was detected using 100 µl of a *p*-nitrophenyl phosphate solution (1 mg/ml) containing 1 M diethanolamine and 0.5 mM $MgCl_2$ (pH 9.8). Absorbance was measured at 405 nm. For the competition assay, 0.1 µg/ml ATX was incubated with an increasing content of heparin (0-1 mg/ml) for 1 h in 100 µl and transferred to a 96-well plate previously coated with heparin. Plates were washed six times with PBS before measuring bound ATX, as described above.

Surface plasmon resonance

ATX binding to heparin was measured by surface plasmon resonance spectroscopy using a Biacore T100 machine (Biacore, GE Healthcare). Recombinant ATXα and ATXβ were covalently coupled to separate flow cells of a CM5 sensor chip at pH 4.0 at roughly equal amounts (about 10,000 response units). Increasing concentration of unfractionated heparin in running buffer (150 mM NaCl, 20 mM Hepes pH 7.6) were injected across the chip at flow rate of 50 µl/min. Injection of 1 M NaCl was used to regenerate the chip surface at the end of each cycle. The response units (RUs) for the binding of heparin were evaluated after subtraction of the signal in a flow cell of the same sensor chip which has been left uncoated. To determine the apparent dissociation constant (K_d), the background-subtracted data were fit using a model in which the total binding results from specific binding plus a linear nonspecific component and a concentration-independent background according to the equation:

$$R_c = \frac{B_{\max} c}{K_d + c} + ac + b$$

where c is the protein concentration, R_c the observed response for that specific concentration, $B_{\max}$ the estimated maximal response, a the slope of the linear nonspecific components and b the estimated background. The values for non-specific binding and the back-

ground (a and b) were kept the same for both ATXα and ATXβ binding, and only the K_d value was fit individually for each protein. The model used was judged to be 99.9% more probable than a model assuming only specific binding, according to the Akaike information criterion (AIC). Analysis was performed with GraphPad software, using an average MW value for heparin of 15 kDa.

ACKNOWLEDGEMENTS

We thank John de Widt, Paula Ruurs, Debbie Roffers and Adrian Rzadkowski for invaluable technical assistance, and Junken Aoki for anti-ATX antibodies. This work was supported by the Dutch Cancer Society (KWF) and the Netherlands Organization for Scientific Research (NWO).

REFERENCES

1. Chun, J., Hla, T., Lynch, K. R., Spiegel, S., and Moolenaar, W. H. (2010) *Pharmacol. Rev.* **62,** 579-587
2. Choi, J. W., Herr, D. R., Noguchi, K., Yung, Y. C., Lee, C. W., Mutoh, T., Lin, M. E., Teo, S. T., Park, K. E., Mosley, A. N., and Chun, J. (2010) *Annu. Rev. Pharmacol. Toxicol.* **50,** 157-186
3. van Meeteren, L. A. and Moolenaar, W. H. (2007) *Prog Lipid Res* **46,** 145-160
4. Jongsma, M., Matas-Rico, E., Rzadkowski, A., Jalink, K., and Moolenaar, W. H. (2011) *PLoS. One.* **6,** e29260
5. Fotopoulou, S., Oikonomou, N., Grigorieva, E., Nikitopoulou, I., Paparountas, T., Thanassopoulou, A., Zhao, Z., Xu, Y., Kontoyiannis, D. L., Remboutsika, E., and Aidinis, V. (2010) *Dev. Biol.* **339,** 451-464
6. Tanaka, M., Okudaira, S., Kishi, Y., Ohkawa, R., Iseki, S., Ota, M., Noji, S., Yatomi, Y., Aoki, J., and Arai, H. (2006) *J Biol Chem* **281,** 25822-25830
7. van Meeteren, L. A., Ruurs, P., Stortelers, C., Bouwman, P., van Rooijen, M. A., Pradere, J. P., Pettit, T. R., Wakelam, M. J., Saulnier-Blache, J. S., Mummery, C. L., Moolenaar, W. H., and Jonkers, J. (2006) *Mol Cell Biol* **26,** 5015-5022
8. Kanda, H., Newton, R., Klein, R., Morita, Y., Gunn, M. D., and Rosen, S. D. (2008) *Nat Immunol* **9,** 415-423
9. Houben, A. J. and Moolenaar, W. H. (2011) *Cancer Metastasis Rev.* **30,** 557-565
10. Mills, G. B. and Moolenaar, W. H. (2003) *Nat. Rev. Cancer* **3,** 582-591
11. Inoue, M., Rashid, M. H., Fujita, R., Contos, J. J., Chun, J., and Ueda, H. (2004) *Nat. Med.* **10,** 712-718
12. Tager, A. M., LaCamera, P., Shea, B. S., Campanella, G. S., Selman, M., Zhao, Z., Polosukhin, V., Wain, J., Karimi-Shah, B. A., Kim, N. D., Hart, W. K., Pardo, A., Blackwell, T. S., Xu, Y., Chun, J., and Luster, A. D. (2008) *Nat. Med.* **14,** 45-54
13. Jansen, S., Stefan, C., Creemers, J. W., Waelkens, E., Van Eynde, A., Stalmans, W., and Bollen, M. (2005) *J Cell Sci* **118,** 3081-3089
14. Koike, S., Keino-Masu, K., Ohto, T., and Masu, M. (2006) *Genes Cells* **11,** 133-142
15. Hausmann, J., Kamtekar, S., Christodoulou, E., Day, J. E., Wu, T., Fulkerson, Z., Albers, H. M., van Meeteren, L. A., Houben, A. J., van Zeijl, L., Jansen, S., Andries, M., Hall, T., Pegg, L. E., Benson, T. E., Kasiem, M., Harlos, K., Kooi, C. W., Smyth, S. S., Ovaa, H., Bollen, M., Morris, A. J., Moolenaar, W. H., and Perrakis, A. (2011) *Nat Struct Mol Biol* **18,** 198-204
16. Nishimasu, H., Okudaira, S., Hama, K., Mihara, E., Dohmae, N., Inoue, A., Ishitani, R., Takagi, J., Aoki, J., and Nureki, O. (2011) *Nat Struct Mol Biol* **18,** 205-212
17. Fulkerson, Z., Wu, T., Sunkara, M., Kooi, C. V., Morris, A. J., and Smyth, S. S. (2011) *J. Biol. Chem.* **286,** 34654-34663
18. Moolenaar, W. H. and Perrakis, A. (2011) *Nat. Rev. Mol. Cell Biol.* **12,** 674-679
19. Pamuklar, Z., Federico, L., Liu, S., Umezu-Goto, M., Dong, A., Panchatcharam, M., Fulkerson, Z., Berdyshev, E., Natarajan, V., Fang, X., van Meeteren, L. A., Moolenaar, W. H., Mills, G. B., Morris, A. J., and Smyth, S. S. (2009) *J. Biol. Chem.* **284,** 7385-7394
20. Giganti, A., Rodriguez, M., Fould, B., Moulharat, N., Coge, F., Chomarat, P., Galizzi, J. P., Valet, P., Saulnier-Blache, J. S., Boutin, J. A., and Ferry, G. (2008) *J Biol Chem* **283,** 7776-7789
21. Lee, H. Y., Murata, J., Clair, T., Polymeropoulos, M. H., Torres, R., Manrow, R. E., Liotta, L. A., and Stracke, M. L. (1996) *Biochem Biophys Res Commun* **218,** 714-719
22. Tokumura, A., Majima, E., Kariya, Y., Tominaga, K., Kogure, K., Yasuda, K., and Fukuzawa, K. (2002) *J Biol Chem* **277,** 39436-39442
23. Umezu-Goto, M., Kishi, Y., Taira, A., Hama, K., Dohmae, N., Takio, K., Yamori, T., Mills, G. B., Inoue, K., Aoki, J., and Arai, H. (2002) *J Cell Biol* **158,** 227-233
24. Stracke, M. L., Krutzsch, H. C., Unsworth, E. J., Arestad, A., Cioce, V., Schiffmann, E., and Liotta, L. A. (1992) *J Biol Chem* **267,** 2524-2529
25. Murata, J., Lee, H. Y., Clair, T., Krutzsch, H. C., Arestad, A. A., Sobel, M. E., Liotta, L. A., and Stracke, M. L. (1994) *J Biol Chem* **269,** 30479-30484
26. Fuss, B., Baba, H., Phan, T., Tuohy, V. K., and Macklin, W. B. (1997) *J Neurosci* **17,** 9095-9103
27. Kawagoe, H., Stracke, M. L., Nakamura, H., and Sano, K. (1997) *Cancer Res.* **57,** 2516-2521
28. Hashimoto, T., Okudaira, S., Igarashi, K., Hama, K., Yatomi, Y., and Aoki, J. (2012) *J. Biochem.* **151,** 89-97
29. Nakayama, K. (1997) *Biochem. J.* **327 (Pt 3),** 625-635
30. Wu, C., Orozco, C., Boyer, J., Leglise, M., Goodale, J., Batalov, S., Hodge, C. L., Haase, J., Janes, J., Huss, J. W., III, and Su, A. I. (2009) *Genome Biol.* **10,** R130
31. Yang, Y., Mou, L., Liu, N., and Tsao, M. S. (1999) *Am J Respir Cell Mol Biol* **21,** 216-222
32. Tian, S. and Jianhua, W. (2010) *Int. J. Biol. Sci.* **6,** 89-95
33. Mesnard, D., Donnison, M., Fuerer, C., Pfeffer,

P. L., and Constam, D. B. (2011) *Genes Dev.* **25,** 1871-1880
34. Thomas, G. (2002) *Nat Rev Mol Cell Biol* **3,** 753-766
35. Krissinel, E. and Henrick, K. (2007) *J Mol Biol* **372,** 774-797
36. Van, D. J., Delgado, J., Stricher, F., Serrano, L., Schymkowitz, J., and Rousseau, F. (2011) *Bioinformatics.* **27,** 1711-1712
37. van Meeteren, L. A., Ruurs, P., Christodoulou, E., Goding, J. W., Takakusa, H., Kikuchi, K., Perrakis, A., Nagano, T., and Moolenaar, W. H. (2005) *J Biol Chem* **280,** 21155-21161
38. Hacker, U., Nybakken, K., and Perrimon, N. (2005) *Nat Rev Mol Cell Biol* **6,** 530-541
39. Kreuger, J., Spillmann, D., Li, J. P., and Lindahl, U. (2006) *J Cell Biol* **174,** 323-327
40. Sasisekharan, R., Shriver, Z., Venkataraman, G., and Narayanasami, U. (2002) *Nat Rev Cancer* **2,** 521-528
41. Capila, I. and Linhardt, R. J. (2002) *Angew Chem Int Ed Engl* **41,** 391-412
42. Munoz, E. M. and Linhardt, R. J. (2004) *Arterioscler Thromb Vasc Biol* **24,** 1549-1557
43. Mayer, G., Boileau, G., and Bendayan, M. (2004) *J. Histochem. Cytochem.* **52,** 567-579
44. Koo, B. H., Longpre, J. M., Somerville, R. P., Alexander, J. P., Leduc, R., and Apte, S. S. (2006) *J Biol Chem* **281,** 12485-12494
45. Tanaka, M., Kishi, Y., Takanezawa, Y., Kakehi, Y., Aoki, J., and Arai, H. (2004) *FEBS Lett* **571,** 197-204
46. Hausmann, J., Christodoulou, E., Kasiem, M., De, M., V, van Meeteren, L. A., Moolenaar, W. H., Axford, D., Owen, R. L., Evans, G., and Perrakis, A. (2010) *Acta Crystallogr. Sect. F. Struct. Biol. Cryst. Commun.* **66,** 1130-1135
47. Clair, T., Aoki, J., Koh, E., Bandle, R. W., Nam, S. W., Ptaszynska, M. M., Mills, G. B., Schiffmann, E., Liotta, L. A., and Stracke, M. L. (2003) *Cancer Res* **63,** 5446-5453
48. Albers, H. M., Dong, A., van Meeteren, L. A., Egan, D. A., Sunkara, M., van Tilburg, E. W., Schuurman, K., van Tellingen, O., Morris, A. J., Smyth, S. S., Moolenaar, W. H., and Ovaa, H. (2010) *Proc Natl Acad Sci U S A* **107,** 7257-7262

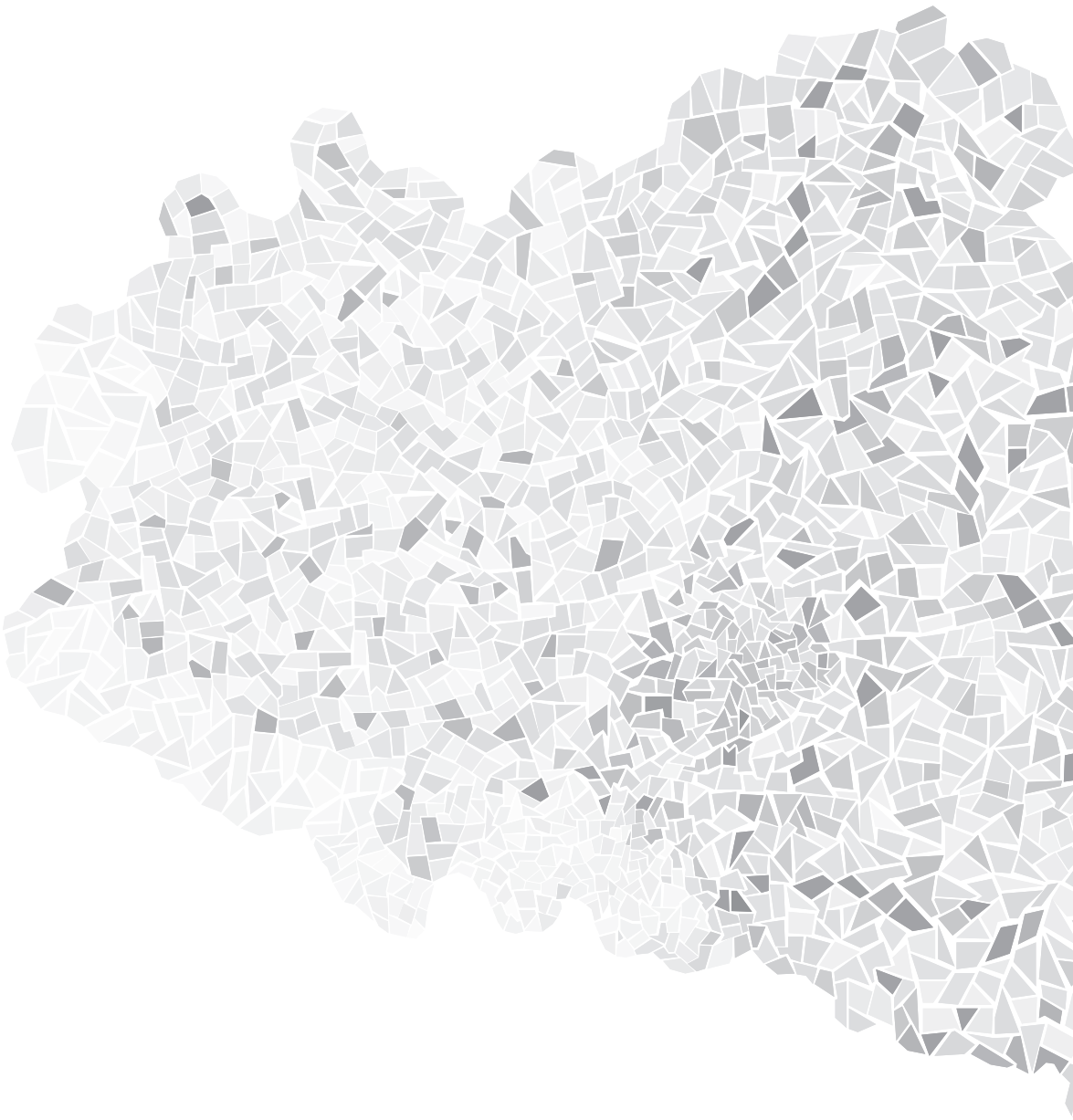

CHAPTER 6

SH3 domain-mediated protein interactions of the ATXα isoform

SH3 domain-mediated protein interactions of the ATXα isoform

Anna J.S. Houben[1]
and Wouter H. Moolenaar[1]

[1]Division of Cell Biology,
The Netherlands Cancer Institute,
Amsterdam, The Netherlands

PREFACE

The proline-rich nature of the polybasic insert of ATXα hints at the presence of potential SH3-domain binding motifs. SH3-domains are protein modules that mediate protein-protein interactions by binding to proline-rich sequences (1;2). We hypothesized that the polybasic insert could mediate protein-protein interaction(s) of ATXα with yet unknown binding partner(s). Here we explored the potential of ATX to interact with secreted, SH3 domain-containing proteins, which could function to modulate ATX localization, activity or binding to integrins and heparan sulphate (HS) proteoglycans.

Literature search for secreted proteins - containing an SH3 domain - revealed melanoma-inhibitory activity (MIA) as a single candidate. MIA, or cartilage-derived retinoic acid-sensitive protein (CD-RAP) is a 12 kDa melanoma-derived growth-regulatory protein that is expressed in cartilage as well as produced by malignant melanoma cells (3). MIA is the first secreted protein containing an SH3 domain and represents a serum marker for systemic malignant melanoma cells (4-6). MIA has been reported to promote melanoma invasion by binding to fibronectin and thereby masking the binding site of integrins to these extracellular matrix components (7). We therefore set out to examine whether ATXα may bind to MIA.

.

RESULTS

Detailed sequence analysis using SH3 hunter software (8) predicted two potential binding motifs (consensus sequence P-x-x-P(-P)) in the polybasic insert of ATXα at residues 331-334 and 351-354 (Fig. 1A). This suggests that the ATXα insert might indeed function as a docking place for SH3-domain based interaction candidates. Moreover, two additional motifs are present in the ATXβ sequence; one upstream (residues 204-207) of the polybasic insert and one downstream (residues 849-852). However, structural analysis shows that the SH3-domain binding motifs of ATXβ are not exposed at the surface of the protein (Fig. 1B). This argues against the functionality of these domains, making it unlikely that they mediate in protein-protein interactions.

We tested whether ATXα could interact with MIA by overexpression in HEK293 cells followed by immunoprecipitation. As shown in Fig. 2A, ectopically expressed ATXα and MIA could be precipitated as a complex. The interaction could only be detected in the cell lysate, but not in conditioned medium (data not shown). However, the interaction was not specific for ATXα as we detected co-immunoprecipitation between ATXβ and MIA as well. This suggests that the interaction is not mediated by the polybasic insert of ATXα. As our structural analysis excludes an SH3 domain-based interaction mediated by the potential binding motifs beyond the polybasic insert, the interaction between MIA and ATX is likely mediated via a different, yet unidentified motif.

Specificity of the ATX-MIA interaction was further tested in MDA-MB-435 cells, which endogenously express both ATX (predominantly ATXβ) and MIA (data not shown). Despite many efforts, we were unable to detect an interaction between endogenous ATX and MIA (Fig. 2B). Next, we tried to verify the interaction *in vitro* by using recombinant proteins. Again, interaction between ATX and MIA could not be detected; neither in a co-immunoprecipitation assay (Fig. 2C) nor by using surface plasmon resonance (data not shown). Furthermore, MIA did not affect ATX activity (Fig. 2D). Together, these results argue against MIA as physiological binding partner of ATX *in vivo*.

DISCUSSION

The polybasic insert of ATXα contains potential SH3-domain binding motifs, which are exposed at the surface of the protein. We hypothesized that the insert could function as a docking platform for binding partners and studied the ability of ATX to form a complex with MIA, the only secreted SH3-domain containing protein known thus far. Although ATXα and MIA were found to interact, ATXβ was found to interact with MIA as well, arguing against the involvement of the polybasic insert of ATXα as basis for the interaction. Sequence analysis revealed the presence of two potential binding motifs outside the polybasic insert. However, the ATXβ crystal structure shows that these motifs are not exposed, suggesting that the ATX-MIA interaction should be mediated by other, yet unidentified, motifs.

Although ATX-MIA complexes could be detected when co-expressed, we could not verify the ATX-MIA interaction with endogenous or recombinant proteins. This could mean that either the interaction occurs only under specific physiological conditions, or might be indirect or very transient and thus hard to detect. However, our results strongly argue against

a functional ATX-MIA interaction. Nevertheless, it is still possible that the binding motifs in the polybasic insert play a role in the interaction of ATX with other (secreted) proteins. MIA is a member of a recently identified protein family of extracellular SH3 domain containing proteins. The MIA homologous proteins TANGO, MIA-2 and OTOR, whose biological functions remain to be determined, are part of this family as well (9). It is possible that one of these family members or another binding partner is able to interact with ATXα, a hypothesis that is worth exploring. It is noteworthy that the furin cleavage site is located in the middle of both motifs, pointing to a possible role of furin cleavage in modulating the interaction of ATXα and putative binding partners.

A

```
  1 MARRSSFQSCQIISLFTFAVGVNICLGFTAHRIKRAEGWEEGPPTVLSDSPWTNISGSCK  60
 61 GRCFELQEAGPPDCRCDNLCKSYTSCCHDFDELCLKTARGWECTKDRCGEVRNEENACHC 120
121 SEDCLARGDCCTNYQVVCKGESHWVDDDCEEIKAAECPAGFVRPPLIIFSVDGFRASYMK 180
181 KGSKVMPNIEKLRSCGTHSPYMRPVYPTKTFPNLYTLATGLYPESHGIVGNSMYDPVFDA 240
241 TFHLRGREKFNHRWWGGQPLWITATKQGVKAGTFFWSVVIPHERRILTILQWLTLPDHER 300
301 PSVYAFYSEQPDFSGHKYGPFGPEESSYGSPFTPAKRPKRKVAPKRRQERPVAPPKKRRR 360
361 KIHRMDHYAAETRQDKMTNPLREIDKIVGQLMDGLKQLKLHRCVNVIFVGDHGMEDVTCD 420
421 RTEFLSNYLTNVDDITLVPGTLGRIRSKFSNNAKYDPKAIIANLTCKKPDQHFKPYLKQH 480
481 LPKRLHYANNRRIEDIHLLVERRWHVARKPLDVYKKPSGKCFFQGDHGFDNKVNSMQTVF 540
541 VGYGSTFKYKTKVPPFENIELYNVMCDLLGLKPAPNNGTHGSLNHLLRTNTFRPTMPEEV 600
601 TRPNYPGIMYLQSDFDLGCTCDDKVEPKNKLDELNKRLHTKGSTEERHLLYGRPAVLYRT 660
661 RYDILYHTDFESGYSEIFLMPLWTSYTVSKQAEVSSVPDHLTSCVRPDVRVSPSFSQNCL 720
721 AYKNDKQMSYGFLFPPYLSSSPEAKYDAFLVTNMVPMYPAFKRVWNYFQRVLVKKYASER 780
781 NGVNVISGPIFDYDYDGLHDTEDKIKQYVEGSSIPVPTHYYSIITSCLDFTQPADKCDGP 840
841 LSVSSFILPHRPDNEESCNSSEDESKWVEELMKMHTARVRDIEHLTSLDFFRKTSRSYPE 900
901 ILTLKTYLHTYESEI                                              915
```

B

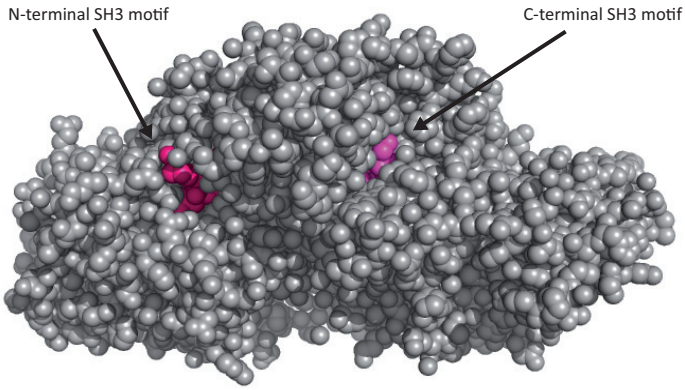

Figure 1: Potential SH3 domain-binding motifs in ATX. (A) Amino acid sequence of ATXα with the 52-residue polybasic insert of ATXα underlined. The potential SH3 domain-binding motifs are depicted in bold. Note the presence of four motifs (two motifs in the ATXα specific insert, one motif upstream of the insert and one motif downstream of the insert) and the presence of an R-R-R-K motif in the polybasic insert at residues 358-361 (a consensus site of R-x-x-K has been described as a novel mode of ligand recognition by SH3 domains (15)). ATXα transcript ID: ENSP00000259486. (B) Space-filling model of the ATXβ crystal structure, showing the N-terminal SH3 domain-binding motif (PVYPTK) in pink and the C-terminal motif (FILPHRP) in purple. Both motifs are not exposed to the surface, making it very unlikely that they will serve as interaction motifs. See ref. (13) for more details about the ATXβ crystal structure.

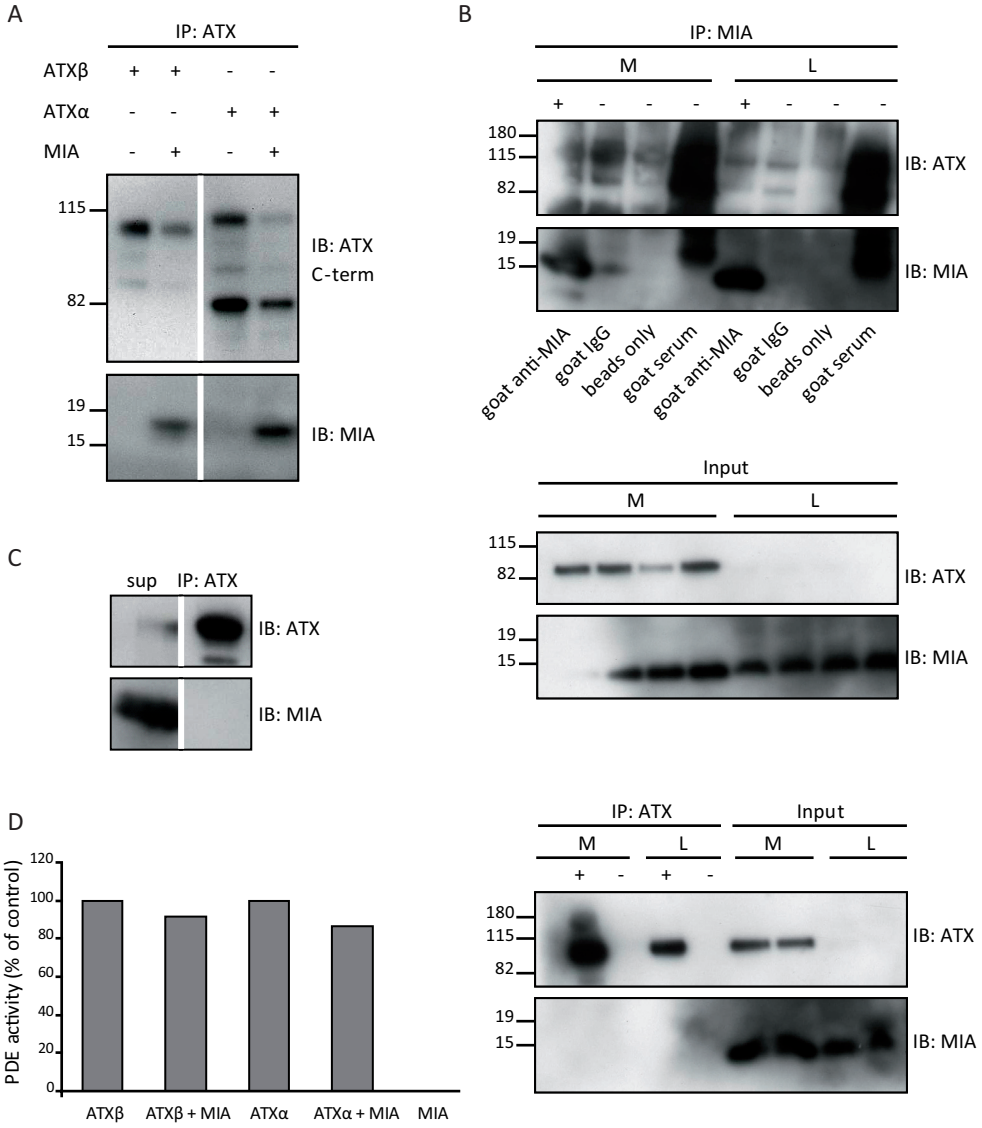

Figure 2: Analysis of the interaction between ATX and MIA. (A) Ectopic expression of MIA and ATXα or ATXβ in HEK293 cells. Pull down of ATXα or ATXβ from cell lysates results in co-immunoprecipitation of MIA. (B) Endogenous expression of ATX and MIA in MDA-MB-435 cells. Pull down of MIA or ATX does not result in co-immunoprecipitation of respectively ATX or MIA. Upper and middle panel: anti-MIA pull down and input blot (negative control: goat IgG, beads only, goat serum). Lower panel: anti-ATX pull down (negative control: beads only). M: conditioned medium; L: lysate; + : antibody IP; - : negative control (IP without antibody). Note that MDA-MB-435 cells express MIA and ATX, predominantly ATXβ (data not shown). (C) Pull down of recombinant ATX or MIA does not result in the detection of a protein complex. Note the presence of MIA in the residual supernatant after ATX immunoprecipitation. (D) PDE activity, as measured by the hydrolysis of 1 mM bis-pNPP. The activity of ATXα and ATXβ is not affected by MIA. Pre-incubation of the proteins did not result in any additional effects (data not shown).

EXPERIMENTAL PROCEDURES

Materials

Anti-MIA polyclonal antibody was obtained from R&D Systems; anti-ATX C-term polyclonal antibody was homemade, raised against the C-terminus of zebrafish ATX epitope CEDESKWVEELMKTHTAR; anti-ATX monoclonal antibodies 3D1 (10) and 5E5 (11) were a generous gift from Dr. J. Aoki. HRP-conjugated secondary antibodies were obtained from Dako, the ECL detection kit from Amersham and bis(p-nitrophenyl)phosphate (bis-pNPP) was obtained from Sigma.

Cells

HEK293 and MDA-MB-435 cells were grown in Dulbecco's modified Eagle's medium (DMEM) containing 10% fetal calf serum. For overexpression studies, HEK293 cells were transfected using the calcium phosphate transfection method.

Constructs

Human ATXβ was ligated in the pcDNA3 vector containing a 3' Myc tag, as previously described (12). Human ATXα, ligated in the pcDNA3 vector containing a 3' Myc-His tag, was a generous gift from Dr. Andree Blaukat (Merck-Serono, Darmstadt, Germany). MIA, ligated in the pCMX-PL1 vector, was a generous gift from Dr. Anja-Katrin Bosserhoff.

Recombinant proteins

Human ATXα and ATXβ were cloned in pcDNA5-FRT (Invitrogen) with a C-terminal Myc-tag and a 6xHis-tag. HEK293 cells stably expressing ATXα or ATXβ were generated using the FLPin system (Invitrogen). Recombinant His-tagged ATX was purified from conditioned HEK293 medium as previously described (13). Recombinant MIA was a generous gift from Dr. Anja-Katrin Bosserhoff.

Co-immunoprecipitation assay and Western Blotting

At 48 hrs after transfection, RIPA cell lysates and conditioned medium samples were collected and centrifuged (13,000 rpm for 30 min. at 4°C). For ATX IP, samples were incubated with the anti-ATX monoclonal antibody 5E5 coupled to sepharose 4B beads as described previously (14), and tumbled at 4°C for 5 hours. For MIA IP, samples were incubated with the anti-MIA polyclonal antibody and tumbled at 4°C for 4 hours. Subsequently, they were analyzed by gel electrophoresis using NuPAGE 4-12% Bis-Tris gels (Invitrogen) under reducing conditions. Proteins were transferred to nitrocellulose membranes, blocked using 5% non-fat powdered milk and probed with primary antibodies; anti-MIA polyclonal antibody, anti-ATX C-term polyclonal antibody, anti-ATX monoclonal antibody 3D1. Subsequently, the membranes were probed with HRP-conjugated secondary antibodies and proteins were visualized using ECL detection.

For immunoprecipitation studies using recombinant protein, 13.9 ug ATX was first incubated with anti-ATX antibody 5E5 coupled to beads and tumbled for 1 hour at 4°C. Subsequently, an equimolar amount of recombinant MIA was added for another 2 hours, tumbling at 4°C. Proteins were analyzed by gel electrophoresis as discussed above.

Phosphodiesterase activity assay

Phosphodiesterase activity was measured using 1 mM bis-pNPP in Tris-buffered saline (140 mM NaCl, 5 mM KCl, 1 mM $CaCl_2$, 1 mM $MgCl_2$, 50 mM Tris pH 8.0) containing 1 mg/ml fatty-acid free BSA. The amount of liberated *para*-nitrophenolate (pNP) was determined by reading the absorbance at 405 nm, as previously described (12).

ACKNOWLEDGEMENTS

We thank Anja-Katrin Bosserhoff (University of Regensburg, Germany) for providing MIA constructs and recombinant protein, Alex Fish (Netherlands Cancer Institute, Amsterdam) for performing surface plasmon resonance experiments, Winny Grernrum (Netherlands Cancer Institute, Amsterdam) for excellent technical assistance and Dr. J. Aoki (Tohoku University, Sendai, Japan) for providing the anti-ATX antibodies 3D1 and 5E5.

REFERENCES

1. Mayer, B. J. (2001) *J. Cell Sci.* **114,** 1253-1263
2. Ren, R., Mayer, B. J., Cicchetti, P., and Baltimore, D. (1993) *Science* **259,** 1157-1161
3. Blesch, A., Bosserhoff, A. K., Apfel, R., Behl, C., Hessdoerfer, B., Schmitt, A., Jachimczak, P., Lottspeich, F., Buettner, R., and Bogdahn, U. (1994) *Cancer Res* **54,** 5695-5701
4. Bosserhoff, A. K., Kaufmann, M., Kaluza, B., Bartke, I., Zirngibl, H., Hein, R., Stolz, W., and Buettner, R. (1997) *Cancer Res* **57,** 3149-3153
5. Dietz, U. H. and Sandell, L. J. (1996) *J Biol Chem* **271,** 3311-3316
6. Lougheed, J. C., Holton, J. M., Alber, T., Bazan, J. F., and Handel, T. M. (2001) *Proc Natl Acad Sci U S A* **98,** 5515-5520
7. Stoll, R., Renner, C., Zweckstetter, M., Bruggert, M., Ambrosius, D., Palme, S., Engh, R. A., Golob, M., Breibach, I., Buettner, R., Voelter, W., Holak, T. A., and Bosserhoff, A. K. (2001) *EMBO J* **20,** 340-349
8. Ferguson, C. G., Bigman, C. S., Richardson, R. D., van Meeteren, L. A., Moolenaar, W. H., and Prestwich, G. D. (2006) *Org Lett* **8,** 2023-2026
9. Stoll, R. and Bosserhoff, A. (2008) *Curr Protein Pept Sci* **9,** 221-226
10. Tanaka, M., Kishi, Y., Takanezawa, Y., Kakehi, Y., Aoki, J., and Arai, H. (2004) *FEBS Lett* **571,** 197-204
11. Nakasaki, T., Tanaka, T., Okudaira, S., Hirosawa, M., Umemoto, E., Otani, K., Jin, S., Bai, Z., Hayasaka, H., Fukui, Y., Aozasa, K., Fujita, N., Tsuruo, T., Ozono, K., Aoki, J., and Miyasaka, M. (2008) *Am J Pathol* **173,** 1566-1576
12. van Meeteren, L. A., Ruurs, P., Christodoulou, E., Goding, J. W., Takakusa, H., Kikuchi, K., Perrakis, A., Nagano, T., and Moolenaar, W. H. (2005) *J Biol Chem* **280,** 21155-21161
13. Hausmann, J., Kamtekar, S., Christodoulou, E., Day, J. E., Wu, T., Fulkerson, Z., Albers, H. M., van Meeteren, L. A., Houben, A. J., van Zeijl, L., Jansen, S., Andries, M., Hall, T., Pegg, L. E., Benson, T. E., Kasiem, M., Harlos, K., Kooi, C. W., Smyth, S. S., Ovaa, H., Bollen, M., Morris, A. J., Moolenaar, W. H., and Perrakis, A. (2011) *Nat Struct Mol Biol* **18,** 198-204
14. Cavalli, S., Houben, A. J., Albers, H. M., van Tilburg, E. W., de Ru, A., Aoki, J., van Veelen, P., Moolenaar, W. H., and Ovaa, H. (2010) *Chembiochem* **11,** 2311-2317
15. Liu, Q., Berry, D., Nash, P., Pawson, T., McGlade, C. J., and Li, S. S. (2003) *Mol Cell* **11,** 471-481

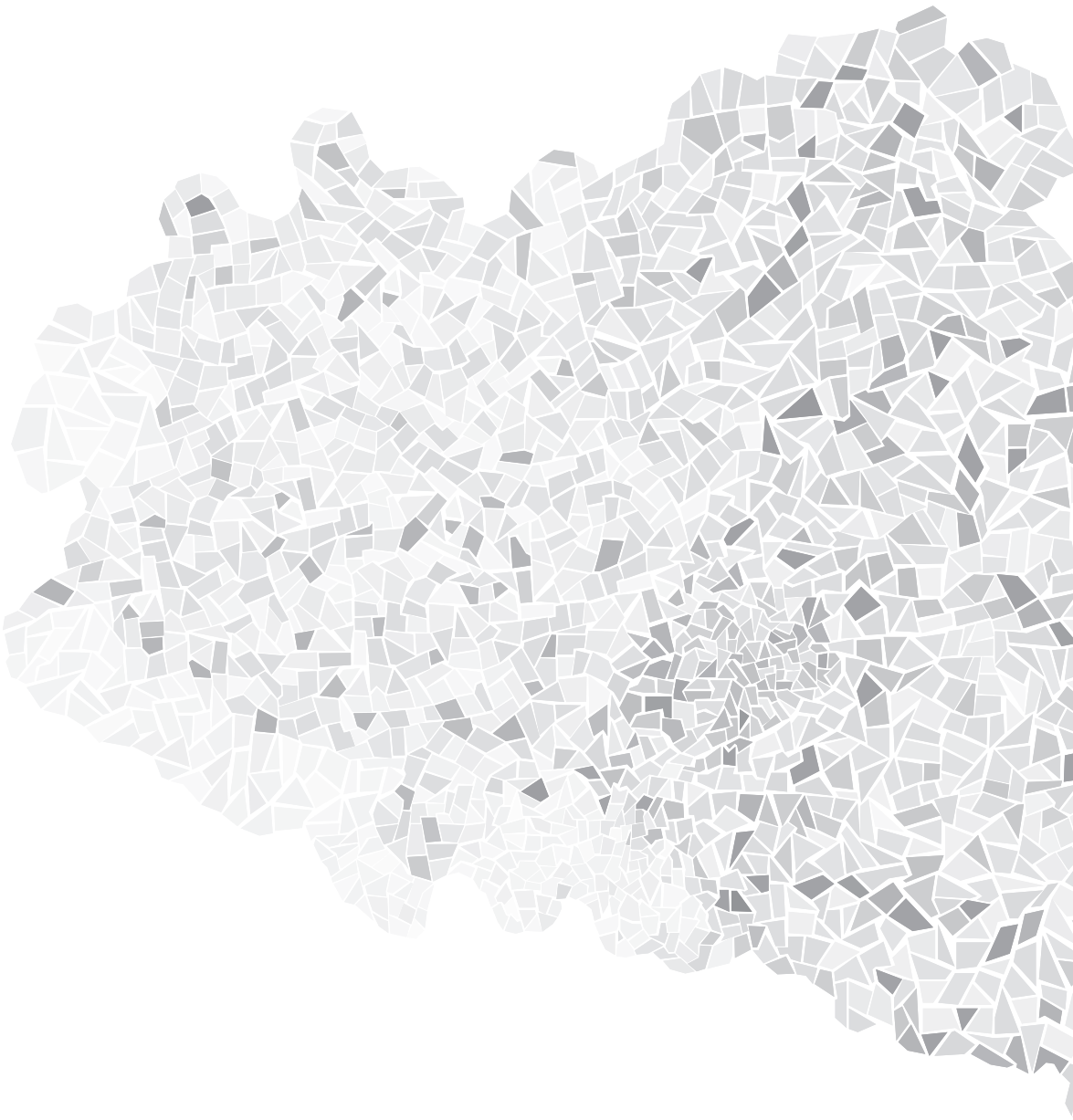

CHAPTER 7

Summary & Discussion

Summary & Discussion

Anna J.S. Houben[1]

[1]Division of Cell Biology,
The Netherlands Cancer Institute,
Amsterdam, The Netherlands

PREFACE

Autotaxin (ATX) is an extracellular multidomain protein that functions as a lysophospholipase D to produce lysophosphatidic acid (LPA) by hydrolyzing lysophosphatidylcholine (LPC). LPA is a small bioactive lipid that acts on specific receptors in the cell membrane and thereby elicits a great variety of cellular responses (1). LPA receptor signaling activates proliferation, migration and survival pathways and has been implicated in various physiological and pathological processes (2;3). ATX is the major LPA-producing enzyme and is essential for normal development (4;5). The studies described in this thesis aim at characterizing the biochemical and functional properties of ATX in order to advance our understanding of the molecular actions of ATX in (patho)physiology. Here, the findings of these studies are summarized and their implications for further research are discussed.

The ATX-LPA receptor axis in cancer

Since the discovery of ATX as an autocrine motility factor for melanoma cells (6), many subsequent studies have focused on ATX and LPA receptor signaling in cancer. In **chapter 2**, the evidence for a role of the ATX-LPA receptor axis in cancer is summarized. In short, elevated or aberrant expression of ATX is found in several human cancers (7-15), overexpression of ATX or LPA receptors in mouse tumor models stimulates tumor growth and invasion (16-23), while knockdown has the reverse effect (17;18;24;25). Moreover, ATX overexpression studies have shown an effect of ATX on tumor vascularization (21), consistent with a role for ATX-LPA receptor signaling in vascular development (4;5;26;27). Recently, ATX was shown to drive vascular development in zebrafish through LPA_1 and LPA_4 (28).

Emerging evidence indicates that LPA signaling needs to collaborate with other proto-oncogenic events to induce cell transformation (19;20;22;24;25). For example, transgenic overexpression of ATX and LPA receptors allows accumulation of secondary mutations, thereby increasing the probability of acquiring (pro-)oncogenic mutations and subsequent tumor development (19). On top of this, ATX can contribute to tumor growth and angiogenesis (16-23). This suggests that ATX-LPA receptor signaling plays an oncogenic role by affecting multiple hallmarks of cancer (29) and raises the question of whether aberrant ATX and/or LPA receptor expression is associated with clinical outcome in cancer.

ATX expression profiling in breast cancer

ATX-LPA receptor signaling in breast cancer has gained special interest since overexpression of ATX or individual EDG-family LPA receptors in mouse mammary glands promotes invasive and metastatic mammary cancer (19). Little is known, however, about ATX in human breast cancer. We have explored the prognostic value of ATX protein expression in human breast cancer in **chapter 3**. We find that virtually all tumors are ATX positive, although there is no significant correlation with clinico-pathological characteristics or patient outcome. Thus, ATX expression does not serve as a prognostic factor in breast cancer, despite the fact that studies in mice suggest a causal link between ATX-LPA receptor signaling and mammary cancer initiation (19) and progression (16;17).

Somewhat unexpectedly, analysis of a publicly available dataset of over 2400 human breast tumor samples (www.kmplot.com (30)) shows better survival for patients with high ATX expression, which differs from our findings. As discussed above, several studies suggest that LPA signaling needs to collaborate with other proto-oncogenic events (19;20;22;24;25), thus the intrinsic molecular features of the tumor cell and its microenvironment might influence the outcome of LPA signaling. Consequently, in this complex signaling network some of the cellular responses of ATX-LPA signaling may positively influence tumorigenesis (e.g. cell proliferation, migration and survival pathways), while others could have a negative effect (e.g. stimulation of immune responses). Recent evidence shows that, depending on the LPA receptor profile, LPA can exert inhibitory effects (31). In addition, breast cancer is a heterogeneous disease with different histological and molecular subtypes influencing clinical prognosis (32). Thus, the seemingly contradictory results may reflect the dual effects of ATX-LPA receptor signaling on tumorigenesis as well as the heterogeneity of breast tumors.

It is important to note that high ATX expression does not necessarily imply elevated LPA levels and enhanced receptor signaling. Upregulation of LPA_2 expression has been detected

in human invasive ductal breast carcinoma (33), pointing to the importance of LPA receptor expression profiles in determining the outcome of ATX-LPA signaling in breast cancer. To address this issue in future studies, a more comprehensive approach is required. Such an analysis should preferably focus on both LPA receptor and ATX expression profiles and, in addition, measure ATX activity levels in the tumor-stroma microenvironment.

ATX activity profiling

Aside from cancer, LPA receptor signaling has been implicated in various other pathological processes. These include obesity (34;35), cardiovascular disease (36;37), neuropathic pain (38), fibrosis (39;40), hydrocephalus (41) and cholestatic pruritus (42). Thus, measuring local ATX activity levels could have diagnostic potential in various diseases. Therefore, we developed a fluorescent ATX activity-based probe (ATX-ABP) to detect and quantify ATX activity in biological fluids. In **chapter 4** we describe the development and characterization of our first generation probe, designed to covalently react with the ATX active site upon recognition and activation. This allows the study of ATX based on catalytic activity instead of expression levels. We show that ATX-ABP labeling is specific as well as activity-, concentration- and time-dependent. Moreover, the probe can be used for inhibitor profiling and screening of ATX activity in human plasma, indicating the potential of ATX-ABP to be developed into a diagnostic reagent.

A drawback of our probe is the low *in vivo* labeling efficiency, which is circumvented by combining ATX-ABP labeling with an affinity-purification step. However, this method is time consuming and cannot be automated for high-throughput ATX activity screening of a large number of samples. As a result, there is a need for optimization to enable direct and efficient labeling of ATX in complex biological fluids. As the first ATX activity probe developed so far, ATX-ABP has the potential to evolve into second-generation probes. Making use of the recent insights into the ATX crystal structure (43;44), the challenge now is to develop activity reporters with increased sensitivity and efficiency. These efforts should lead the way to reagents that will be useful to proof the diagnostic potential and clinical application of ATX.

A second outstanding question is whether ATX acts in an autocrine or paracrine manner, or both. For instance in the tumor microenvironment: do tumor cells produce ATX to activate their own LPA receptors and/or LPA responsive stromal cells? Or is ATX predominantly produced by stromal cells to activate tumor cells? Most likely, there is extensive interplay between tumor cells and the microenvironment, combining both autocrine and paracrine signaling. To increase complexity even more, LPA signaling can stimulate fibroblasts to produce many mediators of tissue remodeling and inflammation. These include growth factors, chemokines, cytokines, proangiogenic factors and metalloproteases, that exert both autocrine and paracrine functions (45). In addition, ATX is implicated in immune responses by promoting lymphocyte-endothelial interactions and lymphocyte homing into secondary lymphoid organs (46;47). This shows that the effect of ATX-LPA receptor signaling is the result of a complex network of signaling events and the development of second-generation ATX activity probes is awaited to reveal the secrets of this largely unexplored field.

ATX isoforms and localized LPA signaling

Alternative splicing of the *ENPP2* gene results in distinct ATX isoforms (48-50). Whether these isoforms might display functional differences has long remained elusive. In **chapter**

5 we studied the biochemical properties of the ATXα isoform, which is of special interest since it harbors a 52-residue polybasic insert of unknown function in the heart of the PDE domain. We find that the ATXα insert contains a consensus cleavage site for the endoprotease furin as well as putative heparin-binding motifs and we show that secreted ATXα undergoes proteolytic cleavage by furin or a furin-like protease. Previously, cleavage of ATXα was suggested to induce rapid degradation (48). In contrast, our data show that cleaved ATXα remains structurally and functionally intact due to a strong and extended interaction surface between both cleavage fragments. ATXα cleavage seems to occur extracellulary, which suggests cleavage by a cell-surface or soluble protease. The furin-like protease PACE4 is of special interest, as it is known to bind heparin and to associate with the extracellular matrix (51). It is tempting to hypothesize that PACE4 is responsible for proteolytic processing of ATXα, which might serve to regulate the ATXα-heparin interaction. The low expression levels seem to contradict a functional role for ATXα. However, we show that ATXα is expressed at considerably high levels in several tumor cell lines. This might point to an isoform-specific role for ATXα in tumors, an interesting area for further research.

ATXα has a roughly ten-fold higher affinity for heparin than ATXβ, owing to the polybasic nature of the ATXα specific insert. Since heparin is structurally very similar to heparan sulphate (HS), ATX is expected to bind to cell membrane-bound HS proteoglycans. This suggests an isoform-specific recruitment of ATX to target cells, which subsequently could induce a local production and delivery of LPA to its receptors. Interaction of ATX with target cells, either via integrins or direct binding to the plasma membrane, is a mechanism that has recently attracted much interest (43;44;46;52). Our heparin-binding data suggest a third mechanism of ATX binding to target cells. Interestingly, heparin enhanced ATXα activity about two-fold, without affecting ATXβ. This may point to a catalytic regulatory mechanism and, in combination with an isoform-specific mechanism of localized LPA production and signaling, represents a functional difference between the ATXα and ATXβ isoforms.

CONCLUSIONS AND PERSPECTIVES

ATX-LPA receptor signaling plays a widespread role in physiological and pathological processes and therefore is of therapeutic interest. A comprehensive biochemical analysis of its mode of action is crucial to develop future therapeutic and clinical applications. Of special interest is the oncogenic potential of the ATX-LPA receptor axis (described in **chapter 2**), which has mainly emerged from studies in mice. The results from our ATX protein expression analysis in human breast cancer (**chapter 3**) indicate that we should primarily focus on LPA receptor levels, combined with ATX expression or activity profiling, to unravel the prognostic value of ATX-LPA receptor signaling in cancer. For the latter purpose, we developed an ATX activity-based probe (**chapter 4**), which holds promise for use in a clinical setting. The results described in **chapter 5** show increased affinity of ATXα for binding to heparin, suggesting isoform-specific localized LPA production and signaling via interaction of ATXα with target cells by binding to HS proteoglycans.

Both ATX, as an extracellular phosphodiesterase, and LPA receptors, belonging to the highly druggable GPCR superfamily, are attractive targets for therapeutic intervention. Small-molecule ATX inhibitors with *in vivo* efficacy have already been described (44;53;54) and major insights into the catalytic function of ATX have been provided by the recently determined ATX crystal structure (43;44). Studies focusing on both fundamental and clinical aspects should boost our understanding of the ATX-LPA receptor signaling axis. This will enable us to study the widespread diagnostic potential of ATX activity and/or LPA receptor expression level profiling, and the therapeutic application of ATX inhibitors.

REFERENCES

1. Moolenaar, W. H., van Meeteren, L. A., and Giepmans, B. N. (2004) *Bioessays* **26,** 870-881
2. Mills, G. B. and Moolenaar, W. H. (2003) *Nat Rev Cancer* **3,** 582-591
3. Moolenaar, W. H. and Perrakis, A. (2011) *Nat Rev Mol Cell Biol*
4. Tanaka, M., Okudaira, S., Kishi, Y., Ohkawa, R., Iseki, S., Ota, M., Noji, S., Yatomi, Y., Aoki, J., and Arai, H. (2006) *J Biol Chem* **281,** 25822-25830
5. van Meeteren, L. A., Ruurs, P., Stortelers, C., Bouwman, P., van Rooijen, M. A., Pradere, J. P., Pettit, T. R., Wakelam, M. J., Saulnier-Blache, J. S., Mummery, C. L., Moolenaar, W. H., and Jonkers, J. (2006) *Mol Cell Biol* **26,** 5015-5022
6. Stracke, M. L., Krutzsch, H. C., Unsworth, E. J., Arestad, A., Cioce, V., Schiffmann, E., and Liotta, L. A. (1992) *J Biol Chem* **267,** 2524-2529
7. Baumforth, K. R., Flavell, J. R., Reynolds, G. M., Davies, G., Pettit, T. R., Wei, W., Morgan, S., Stankovic, T., Kishi, Y., Arai, H., Nowakova, M., Pratt, G., Aoki, J., Wakelam, M. J., Young, L. S., and Murray, P. G. (2005) *Blood* **106,** 2138-2146
8. Hoelzinger, D. B., Mariani, L., Weis, J., Woyke, T., Berens, T. J., McDonough, W. S., Sloan, A., Coons, S. W., and Berens, M. E. (2005) *Neoplasia* **7,** 7-16
9. Kawagoe, H., Stracke, M. L., Nakamura, H., and Sano, K. (1997) *Cancer Res* **57,** 2516-2521
10. Kehlen, A., Englert, N., Seifert, A., Klonisch, T., Dralle, H., Langner, J., and Hoang-Vu, C. (2004) *Int J Cancer* **109,** 833-838
11. Masuda, A., Nakamura, K., Izutsu, K., Igarashi, K., Ohkawa, R., Jona, M., Higashi, K., Yokota, H., Okudaira, S., Kishimoto, T., Watanabe, T., Koike, Y., Ikeda, H., Kozai, Y., Kurokawa, M., Aoki, J., and Yatomi, Y. (2008) *Br J Haematol* **143,** 60-70
12. Stassar, M. J., Devitt, G., Brosius, M., Rinnab, L., Prang, J., Schradin, T., Simon, J., Petersen, S., Kopp-Schneider, A., and Zoller, M. (2001) *Br J Cancer* **85,** 1372-1382
13. Yang, S. Y., Lee, J., Park, C. G., Kim, S., Hong, S., Chung, H. C., Min, S. K., Han, J. W., Lee, H. W., and Lee, H. Y. (2002) *Clin Exp Metastasis* **19,** 603-608
14. Yang, Y., Mou, L., Liu, N., and Tsao, M. S. (1999) *Am J Respir Cell Mol Biol* **21,** 216-222
15. Zhang, G., Zhao, Z., Xu, S., Ni, L., and Wang, X. (1999) *Chin Med J (Engl)* **112,** 330-332
16. Boucharaba, A., Serre, C. M., Gres, S., Saulnier-Blache, J. S., Bordet, J. C., Guglielmi, J., Clezardin, P., and Peyruchaud, O. (2004) *J Clin Invest* **114,** 1714-1725
17. Boucharaba, A., Serre, C. M., Guglielmi, J., Bordet, J. C., Clezardin, P., and Peyruchaud, O. (2006) *Proc Natl Acad Sci U S A* **103,** 9643-9648
18. David, M., Wannecq, E., Descotes, F., Jansen, S., Deux, B., Ribeiro, J., Serre, C. M., Gres, S., Bendriss-Vermare, N., Bollen, M., Saez, S., Aoki, J., Saulnier-Blache, J. S., Clezardin, P., and Peyruchaud, O. (2010) *PLoS One* **5,** e9741
19. Liu, S., Umezu-Goto, M., Murph, M., Lu, Y., Liu, W., Zhang, F., Yu, S., Stephens, L. C., Cui, X., Murrow, G., Coombes, K., Muller, W., Hung, M. C., Perou, C. M., Lee, A. V., Fang, X., and Mills, G. B. (2009) *Cancer Cell* **15,** 539-550
20. Nam, S. W., Clair, T., Campo, C. K., Lee, H. Y., Liotta, L. A., and Stracke, M. L. (2000) *Oncogene* **19,** 241-247
21. Nam, S. W., Clair, T., Kim, Y. S., McMarlin, A., Schiffmann, E., Liotta, L. A., and Stracke, M. L. (2001) *Cancer Res* **61,** 6938-6944
22. Taghavi, P., Verhoeven, E., Jacobs, J. J., Lambooij, J. P., Stortelers, C., Tanger, E., Moolenaar, W. H., and van Lohuizen, M. (2008) *Oncogene* **27,** 6806-6816
23. Yu, S., Murph, M. M., Lu, Y., Liu, S., Hall, H. S., Liu, J., Stephens, C., Fang, X., and Mills, G. B. (2008) *J Natl Cancer Inst* **100,** 1630-1642
24. Lin, S., Wang, D., Iyer, S., Ghaleb, A. M., Shim, H., Yang, V. W., Chun, J., and Yun, C. C. (2009) *Gastroenterology* **136,** 1711-1720
25. Lin, S., Lee, S. J., Shim, H., Chun, J., and Yun, C. C. (2010) *Am J Physiol Gastrointest Liver Physiol* **299,** G1128-G1138
26. Koike, S., Keino-Masu, K., and Masu, M. (2010) *Biochem Biophys Res Commun* **400,** 66-71
27. Sumida, H., Noguchi, K., Kihara, Y., Abe, M., Yanagida, K., Hamano, F., Sato, S., Tamaki, K., Morishita, Y., Kano, M. R., Iwata, C., Miyazono, K., Sakimura, K., Shimizu, T., and Ishii, S. (2010) *Blood* **116,** 5060-5070
28. Yukiura, H., Hama, K., Nakanaga, K., Tanaka, M., Asaoka, Y., Okudaira, S., Arima, N., Inoue, A., Hashimoto, T., Arai, H., Kawahara, A., Nishina, H., and Aoki, J. (2011) *J. Biol. Chem.*
29. Hanahan, D. and Weinberg, R. A. (2000) *Cell* **100,** 57-70
30. Gyorffy, B., Lanczky, A., Eklund, A. C., Denkert, C., Budczies, J., Li, Q., and Szallasi, Z. (2010) *Breast Cancer Res. Treat.* **123,** 725-731
31. Jongsma, M., Matas-Rico, E., Rzadkowski, A., Jalink, K., and Moolenaar, W. H. (2011) *PLoS. One.* **6,** e29260
32. Polyak, K. (2011) *J. Clin. Invest* **121,** 3786-3788
33. Kitayama, J., Shida, D., Sako, A., Ishikawa, M., Hama, K., Aoki, J., Arai, H., and Nagawa, H. (2004) *Breast Cancer Res.* **6,** R640-R646
34. Dusaulcy, R., Rancoule, C., Gres, S., Wanecq,

E., Colom, A., Guigne, C., van Meeteren, L. A., Moolenaar, W. H., Valet, P., and Saulnier-Blache, J. S. (2011) *J Lipid Res*

35. Ferry, G., Tellier, E., Try, A., Gres, S., Naime, I., Simon, M. F., Rodriguez, M., Boucher, J., Tack, I., Gesta, S., Chomarat, P., Dieu, M., Raes, M., Galizzi, J. P., Valet, P., Boutin, J. A., and Saulnier-Blache, J. S. (2003) *J Biol Chem* **278,** 18162-18169
36. Panchatcharam, M., Miriyala, S., Yang, F., Rojas, M., End, C., Vallant, C., Dong, A., Lynch, K., Chun, J., Morris, A. J., and Smyth, S. S. (2008) *Circ. Res.* **103,** 662-670
37. Zhou, Z., Subramanian, P., Sevilmis, G., Globke, B., Soehnlein, O., Karshovska, E., Megens, R., Heyll, K., Chun, J., Saulnier-Blache, J. S., Reinholz, M., van, Z. M., Weber, C., and Schober, A. (2011) *Cell Metab* **13,** 592-600
38. Inoue, M., Ma, L., Aoki, J., Chun, J., and Ueda, H. (2008) *Mol. Pain* **4,** 6
39. Tager, A. M., LaCamera, P., Shea, B. S., Campanella, G. S., Selman, M., Zhao, Z., Polosukhin, V., Wain, J., Karimi-Shah, B. A., Kim, N. D., Hart, W. K., Pardo, A., Blackwell, T. S., Xu, Y., Chun, J., and Luster, A. D. (2008) *Nat Med* **14,** 45-54
40. Pradere, J. P., Klein, J., Gres, S., Guigne, C., Neau, E., Valet, P., Calise, D., Chun, J., Bascands, J. L., Saulnier-Blache, J. S., and Schanstra, J. P. (2007) *J. Am. Soc. Nephrol.* **18,** 3110-3118
41. Yung, Y. C., Mutoh, T., Lin, M. E., Noguchi, K., Rivera, R. R., Choi, J. W., Kingsbury, M. A., and Chun, J. (2011) *Sci Transl Med* **3,** 99ra87
42. Kremer, A. E., Martens, J. J., Kulik, W., Rueff, F., Kuiper, E. M., van Buuren, H. R., van Erpecum, K. J., Kondrackiene, J., Prieto, J., Rust, C., Geenes, V. L., Williamson, C., Moolenaar, W. H., Beuers, U., and Oude Elferink, R. P. (2010) *Gastroenterology* **139,** 1008-18, 1018
43. Hausmann, J., Kamtekar, S., Christodoulou, E., Day, J. E., Wu, T., Fulkerson, Z., Albers, H. M., van Meeteren, L. A., Houben, A. J., van Zeijl, L., Jansen, S., Andries, M., Hall, T., Pegg, L. E., Benson, T. E., Kasiem, M., Harlos, K., Kooi, C. W., Smyth, S. S., Ovaa, H., Bollen, M., Morris, A. J., Moolenaar, W. H., and Perrakis, A. (2011) *Nat Struct Mol Biol* **18,** 198-204
44. Nishimasu, H., Okudaira, S., Hama, K., Mihara, E., Dohmae, N., Inoue, A., Ishitani, R., Takagi, J., Aoki, J., and Nureki, O. (2011) *Nat Struct Mol Biol* **18,** 205-212
45. Stortelers, C., Kerkhoven, R., and Moolenaar, W. H. (2008) *BMC Genomics* **9,** 387
46. Kanda, H., Newton, R., Klein, R., Morita, Y., Gunn, M. D., and Rosen, S. D. (2008) *Nat Immunol* **9,** 415-423
47. Nakasaki, T., Tanaka, T., Okudaira, S., Hirosawa, M., Umemoto, E., Otani, K., Jin, S., Bai, Z., Hayasaka, H., Fukui, Y., Aozasa, K., Fujita, N., Tsuruo, T., Ozono, K., Aoki, J., and Miyasaka, M. (2008) *Am J Pathol* **173,** 1566-1576
48. Giganti, A., Rodriguez, M., Fould, B., Moulharat, N., Coge, F., Chomarat, P., Galizzi, J. P., Valet, P., Saulnier-Blache, J. S., Boutin, J. A., and Ferry, G. (2008) *J. Biol. Chem.* **283,** 7776-7789
49. Hashimoto, T., Okudaira, S., Igarashi, K., Hama, K., Yatomi, Y., and Aoki, J. (2011) *J. Biochem.*
50. van Meeteren, L. A. and Moolenaar, W. H. (2007) *Prog Lipid Res* **46,** 145-160
51. Tsuji, A., Sakurai, K., Kiyokage, E., Yamazaki, T., Koide, S., Toida, K., Ishimura, K., and Matsuda, Y. (2003) *Biochim. Biophys. Acta* **1645,** 95-104
52. Pamuklar, Z., Federico, L., Liu, S., Umezu-Goto, M., Dong, A., Panchatcharam, M., Fulkerson, Z., Berdyshev, E., Natarajan, V., Fang, X., van Meeteren, L. A., Moolenaar, W. H., Mills, G. B., Morris, A. J., and Smyth, S. S. (2009) *J Biol Chem* **284,** 7385-7394
53. Albers, H. M., Dong, A., van Meeteren, L. A., Egan, D. A., Sunkara, M., van Tilburg, E. W., Schuurman, K., van Tellingen, O., Morris, A. J., Smyth, S. S., Moolenaar, W. H., and Ovaa, H. (2010) *Proc Natl Acad Sci U S A* **107,** 7257-7262
54. Gierse, J., Thorarensen, A., Beltey, K., Bradshaw-Pierce, E., Cortes-Burgos, L., Hall, T., Johnston, A., Murphy, M., Nemirovskiy, O., Ogawa, S., Pegg, L., Pelc, M., Prinsen, M., Schnute, M., Wendling, J., Wene, S., Weinberg, R., Wittwer, A., Zweifel, B., and Masferrer, J. (2010) *J Pharmacol Exp Ther* **334,** 310-317

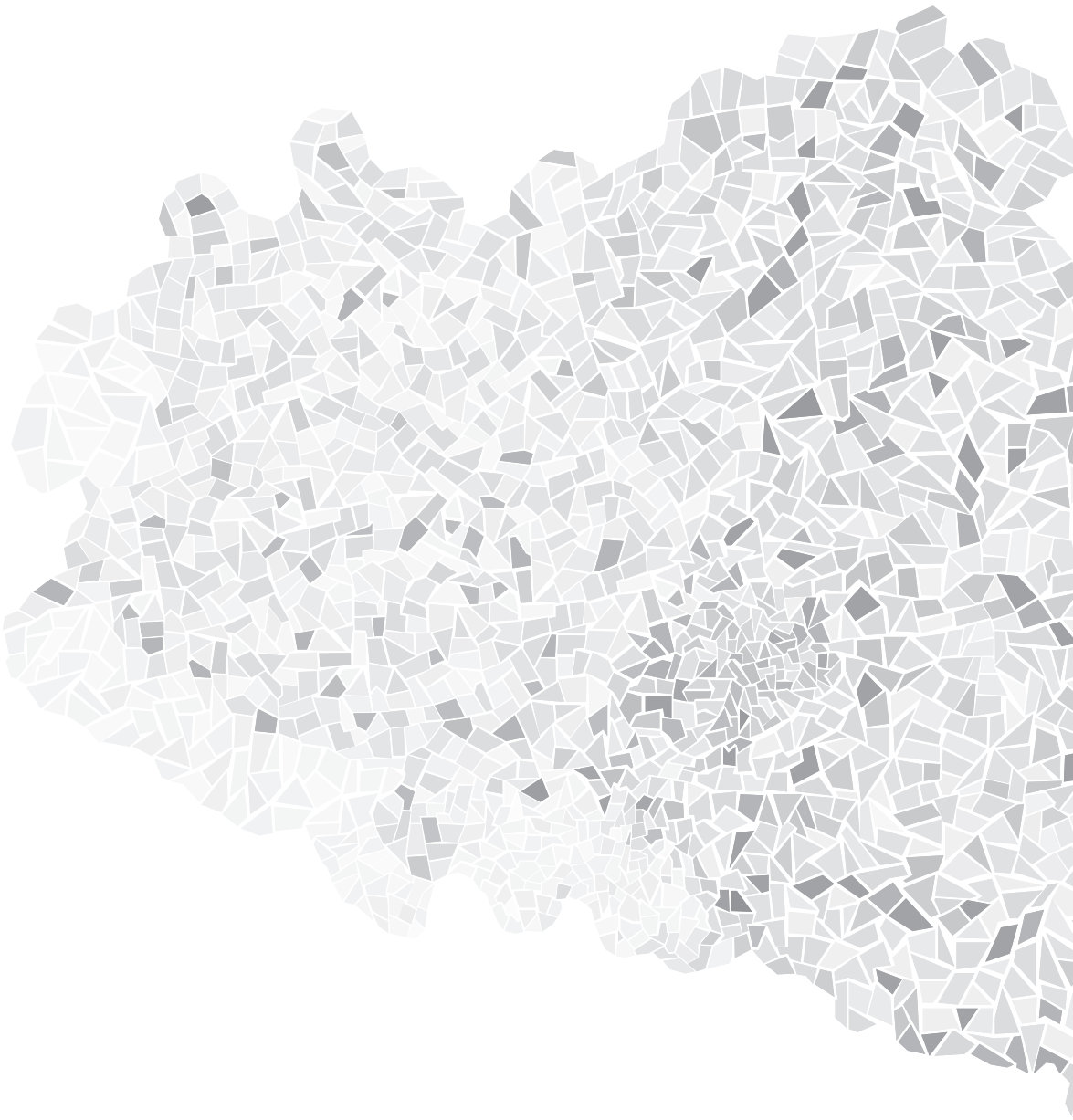

ADDENDUM &

NEDERLANDSE SAMENVATTING VOOR LEKEN

Een organisme bestaat uit vele cellen die voortdurend met elkaar communiceren en samenwerken. Hiervoor gebruiken cellen verschillende signaleringsmoleculen. Een voorbeeld hiervan is LPA (lysofosfatide-zuur), een vetachtig stofje dat wordt geproduceerd door het enzym autotaxine (ATX). LPA is belangrijk voor de communicatie tussen de cel en zijn omgeving. Door de binding van LPA aan LPA receptoren op de celmembraan worden processen in de cel geactiveerd, zoals proliferatie (het vermenigvuldigen van cellen), migratie (beweging van cellen) en overleving.

ATX wordt door cellen in het lichaam uitgescheiden in het extracellulaire milieu (lichaamsvloeistoffen, zoals bloed en hersenvocht). ATX is van kritisch belang gedurende de embryonale ontwikkeling en daarnaast speelt ATX een belangrijke rol in diverse ziektes zoals kanker, ontstekingen en overgewicht. Het is echter niet bekend wat de precieze functie is van ATX in zowel gezond als ziek weefsel. Het onderzoek beschreven in dit proefschrift heeft als doel het bestuderen van ATX op moleculair niveau, door middel van biochemische en functionele studies. Deze resultaten zullen bijdragen aan het vergroten van de algemene kennis over de werking van ATX en daarmee inzicht geven hoe ATX bijdraagt aan verschillende ziekteprocessen.

Hoofdstuk 1 van dit proefschrift geeft een algemene inleiding over ATX en LPA, met speciale aandacht voor de biologische functie, de enzymatische activiteit en biochemische aspecten van ATX en LPA, en de rol hiervan in gezonde en zieke weefsels. In **hoofdstuk 2** wordt een literatuuroverzicht gegeven over de specifieke rol van ATX en LPA in kanker. Studies in gekweekte cellen en muizen suggereren dat ATX en LPA de groei en progressie van tumoren positief beïnvloeden. Vervolgens wordt in **hoofdstuk 3** onderzocht of ATX een voorspellende factor is in de progressie van borstkanker in de mens. Omdat eerder onderzoek heeft laten zien dat excessieve ATX-LPA signalering in de muis de groei van tumoren en ontwikkeling van uitzaaiingen stimuleert, werd verwacht dat het meten van ATX niveaus in menselijke tumoren als een maat voor tumor agressiviteit zou kunnen functioneren. De resultaten van dit onderzoek laten zien dat het overgrote deel van de tumoren inderdaad verhoogde ATX niveaus heeft, maar dit correleert niet met de klinische en prognostische karakteristieken van de patiënt. Er moet dus geconcludeerd worden dat ATX niveaus niet gebruikt kunnen worden als voorspellende factor voor overlevingskansen van borstkanker-patiënten.

LPA receptor signalering wordt naast kanker in verband gebracht met meerdere ziektes, zoals bijvoorbeeld hart- en vaatziekten. Het meten van de ATX activiteit als maat voor LPA productie kan dus van groot belang zijn in verschillende ziektes. In **hoofdstuk 4** wordt de ontwikkeling en karakterisatie van een 'activiteitsprobe' als sensor voor ATX beschreven. De probe reageert met het enzymatische domein en dit heeft als voordeel dat in plaats van alleen de aanwezigheid, juist specifiek de activiteit van ATX gemeten kan worden. Onze studie laat zien dat deze eerste generatie probe gebruikt kan worden om ATX activiteit te meten in menselijk bloedplasma. De uitdaging voor de toekomst is om deze probe verder te ontwikkelen tot een diagnostische ATX sensor met een potentieel brede toepassing in verschillende ziektes.

In **hoofdstuk 5** wordt onderzoek verricht naar de specifieke aspecten van ATXα, een speciale variant (isovorm) van het ATX eiwit die oorspronkelijk is ontdekt in huidkanker cellen. Het interessante aan ATXα is de aanwezigheid van een unieke insertie van 52 aminozuren in het hart van het enzymatische domein. Onze resultaten tonen aan dat ATXα precies in deze insertie wordt geknipt door het enzym furine. Hierdoor zou men verwachten dat het ATXα eiwit uit elkaar valt en daardoor de enzymatische activiteit geremd wordt. Dit is echter niet het geval, wat verklaard kan worden door de zeer sterke intramoleculaire interacties in het enzymatische domein van ATXα. Ten tweede blijkt het ATXα eiwit een zeer sterke affiniteit te hebben voor heparine, een stofje dat sterke overeenkomsten vertoont met een bepaalde groep moleculen (de heparaansulfaat proteoglycanen) op de celmembraan. Dit suggereert dat de ATXα variant, in contrast met het 'normale' ATX, sterk aan de celmembraan kan binden. Bovendien stimuleert deze heparine binding de functie van ATXα, namelijk het produceren van LPA. Dit wijst op een isovorm-specifieke functie: het reguleren van de LPA productie op de celmembraan vlakbij de LPA receptoren.

In **hoofdstuk 6** wordt bestudeerd of de unieke insertie van de ATXα variant kan functioneren als bindingsplaats voor andere eiwitten. Zo'n interactie zou de functie en/of lokalisatie van ATXα kunnen beïnvloeden. Het aminozuur proline, dat in grote getale aanwezig is in de insertie van ATXα, kan functioneren als herkenningsplaats voor de binding van specifieke eiwitten die een zogenaamd SH3 domein bevatten. In het extracellulaire milieu, de plek waar ATX zijn functie uitoefent, is er maar een eiwit bekend met een SH3 domein, namelijk het eiwit 'MIA'. Hoewel we zien dat ATXα en MIA aan elkaar kunnen binden onder artificiële omstandigheden, hebben we dit niet kunnen aantonen in de 'normale' cellulaire omgeving. Dit suggereert dat ATXα en MIA waarschijnlijk niet als bindingspartners functioneren, maar het sluit echter niet uit dat ATXα aan andere eiwitten kan binden.

De resultaten beschreven in dit proefschrift vergroten ons inzicht in het werkingsmechanisme van ATX. Dergelijke studies zullen een belangrijke bijdrage leveren aan het ontrafelen van de functie van ATX-LPA receptor signalering in zowel gezonde als zieke weefsels. Uiteindelijk zal deze kennis vertaald moeten worden naar de ontwikkeling van diagnostische en therapeutische toepassingen.

CURRICULUM VITAE

Anna Houben werd geboren op 7 februari 1982 in Roermond. In 2000 behaalde ze haar gymnasium diploma aan het Bisschoppelijk College Schöndeln te Roermond. In datzelfde jaar begon ze aan haar studie Biomedische Wetenschappen aan de Universiteit van Utrecht. Tijdens haar eerste stage in het laboratorium voor Moleculaire Immunopathologie aan het Universitair Medisch Centrum Utrecht, bestudeerde ze mutaties in HLA klasse I genen in leukemie onder leiding van Dr. Judith Reinders en Prof. Dr. Marcel Tilanus. De tweede stage werd verricht in het Laboratorium voor Experimentele Cardiologie van het Hart-Long Instituut Utrecht, waar ze neovascularisatie in atherosclerose bestudeerde onder begeleiding van Dennis Lamers, Dr. Aryan Vink and Prof. Dr. Gerard Pasterkamp. In oktober 2005 behaalde Anna haar Master's diploma, afstudeerrichting "Biology of Disease", met het judicium *cum laude*. Na een paar maanden reizen door Zuid-Amerika startte ze in maart 2006 aan haar promotie onderzoek onder begeleiding van Prof. Dr. Wouter Moolenaar in de vakgroep Celbiologie van het Nederlands Kanker Instituut. Het onderzoek werd gesubsidieerd door KWF Kankerbestrijding en de resultaten die behaald zijn in dit onderzoek worden beschreven in dit proefschrift. Momenteel is Anna werkzaam als postdoctoraal onderzoeker in het laboratorium van Prof. Dr. Xavier Estivill in het "Genes and Disease" programma aan het Centre for Genomic Regulation in Barcelona, Spanje.

Anna Houben was born on February 7th 1982 in Roermond, The Netherlands. In 2000, she completed secondary school at the Bisschoppelijk College Schöndeln in Roermond. That same year she started her Biomedical Sciences training at the Utrecht University. During her first internship at the Laboratory Molecular Immunopathology, University Medical Center Utrecht, she performed a mutation analysis of HLA class I genes in leukemia under supervision of Dr. Judith Reinders and Prof. Dr. Marcel Tilanus. The second internship was performed in the Laboratory Experimental Cardiology of the Heart-Lung Institute Utrecht, where she studied neovascularization in atherosclerosis under supervision of Dennis Lamers, Dr. Aryan Vink and Prof. Dr. Gerard Pasterkamp. In October 2005, Anna obtained her Master's degree in Science, Biology of Disease, with the qualification *cum laude*. After a few months of traveling through South America, she started her PhD project in March 2006 at the Division of Cell Biology in the Netherlands Cancer Institute under supervision of Prof. Dr. Wouter Moolenaar. The project was funded by the Dutch Cancer Society and the results of this research are described in this thesis. Currently, Anna is working as a postdoctoral scientist in the laboratory of Prof. Dr. Xavier Estivill at the "Genes and Disease" program of the Centre for Genomic Regulation in Barcelona, Spain.

PUBLICATION LIST

Moolenaar WH, **Houben AJS** and van Meeteren LA
Autotaxin in embryonic development
Biochem Biophys Acta 2012 (in press)

Houben AJS, van Meeteren LA, van Wijk XMR, van Zeijl L, van de Westerlo EMA, Hausmann J, Fish A, Perrakis A, van Kuppevelt TH and Moolenaar WH
The long isoform of autotaxin: intradomain cleavage by furin and high-affinity binding to heparin
Submitted 2012
(AJSH and LAM contributed equally to this work)

Lai SL, Yao WL, Tsao KC, **Houben AJS**, Albers HMHG, Ovaa H, Moolenaar WH and Lee SJ
Autotaxin-Lpar3 signaling regulates Kupffer's vesicle formation and left-right asymmetry in zebrafish
Submitted 2012

Houben AJS and Moolenaar WH
Autotaxin and LPA receptor signaling in cancer
Cancer Metast Rev. 2011; 30(3-4): 557-65

Hausmann J, Kamtekar S, Christodoulou E, Day JE, Wu T, Fulkerson Z, Albers H, van Meeteren LA, **Houben AJ**, van Zeijl L, Jansen S, Andries M, Hall T, Pegg LE, Benson TE, Kasiem M, Harlos K, Kooi CW, Smyth SS, Ovaa H, Bollen M, Morris AJ, Moolenaar WH and Perrakis A
Structural basis for substrate discrimination and integrin binding by autotaxin
Nat Struct Mol Biol. 2011; 18(2): 198-204

Houben AJ, Cavalli S, Albers HMHG, van Tilburg EW, de Ru A, Aoki J, van Veelen P, Moolenaar WH and Ovaa H
Development of an activity-based probe for autotaxin
Chembiochem. 2010; 11(16): 2311-2317
(AJH and SC contributed equally to this work)

Vink A, Schoneveld AH, Lamers D, **Houben AJ**, van der Groep P, van Diest PJ and Pasterkamp G
HIF-1 alpha expression is associated with an atheromatous inflammatory plaque phenotype and upregulated in activated macrophages
Atherosclerosis. 2007; 195(2): E69-75

Reinders J, Rozemuller EH, Otten HG, **Houben AJ**, Dormoy A, Mulder A, van den Tweel JG, Petersen EJ and Tilanus MG
*Identification of HLA-A*0111N: a synonymous substitution, introducing an alternative splice site in exon 3, silenced the expression of an HLA-A allele*
Hum Immunol. 2005; 66(8): 912-20
(EHR and HGO contributed equally to this work)

I WISH TO EXPRESS MY GRATITUDE TO ALL WHO HAVE
CONTRIBUTED TO THIS THESIS

MIJN DANK GAAT UIT NAAR ALLEN DIE HEBBEN BIJGEDRAGEN AAN
DE TOTSTANDKOMING VAN DIT PROEFSCHRIFT

STELLINGEN

Behorende bij het proefschrift
Autotaxin, biochemical and functional studies

1- Het enzym autotaxine (ATX) komt tot expressie in borstkankerweefsel, maar het expressieniveau van ATX is geen voorspeller van klinische uitkomst *(dit proefschrift)*

2- Activiteits-afhankelijke probes bieden een praktische methode om de activiteit van ATX in biologische vloeistoffen te meten *(dit proefschrift)*

3- De lange isovorm van ATX (ATXα) heeft een unieke insertie in het katalytisch domein. Klieving van deze insertie door furine resulteert niet in verlies van activiteit, maar zou kunnen dienen om de interactie tussen ATXα en heparaansulfaat proteoglycanen te reguleren *(dit proefschrift)*

4- De interactie tussen ATXα en heparine suggereert een nieuw mechanisme voor gelocaliseerde LPA productie en signalering door binding van ATXα aan heparaansulfaat proteoglycanen op de celmembraan *(dit proefschrift*)

5- Een deletie van 18 aminozuren in het katalytisch domein van ATX ten opzichte van zijn nucleotide pyrofosfatase/fosfodiestedase (NPP) familieleden veroorzaakt de vorming van een bindingsgroeve voor lysofosfolipiden. De aanwezigheid van deze aminozuren in de NPP1 en NPP3 familieleden van ATX verklaart waarom zij niet kunnen functioneren als een lysofosfolipase enzym *(Hausmann et al, Nat Struct Mol Biol 2011; 18(2): 198-204* en *Nishimasu et al, Nat Struct Mol Biol 2011; 18(2): 205-12)*

6- De sterke interactie tussen het inactieve nuclease domein en het actieve katalytische domein van ATX is een slimme evolutionaire oplossing om de stabiliteit van het katalytische domein te waarborgen *(Moolenaar & Perrakis, Nat Rev Mol Cell Biol 2011; 12(10): 674-79)*

7- Studies naar het gedrag van tumoren zou niet alleen de eigenschappen van de tumorcellen zelf moeten omvatten, maar moet tevens de bijdrage van de tumor omgeving behelzen *(Hanahan & Weinberg, Cell 2011; 144(5): 646-74)*

8- Afwezigheid van bewijs is niet hetzelfde als bewijs van afwezigheid (*Altman & Bland, B M J 1995; 311(7003): 485*)

9- In tegenstelling tot de verwachting dat wetenschap eenduidige antwoorden oplevert, zijn er meestal vele antwoorden en nog meer vragen waar men genoegen mee moet nemen

10- Het humane genoom kan worden gezien als een boek van 23 hoofdstukken (de “chromosomen”) met in totaal meer dan drie biljoen letters (de “nucleotiden”). Het feit dat we pas zo’n 2% van deze tekst begrijpen, geeft aan dat we nog lang niet klaar zijn met lezen

11- Als je niet leert van je fouten, doe je iets fout *(Johan Cruijff)*

12- De wereld is een boek en degenen die niet reizen, lezen maar één pagina *(Aurelius Augustinus, Romeins filosoof, 354-430)*

PROPOSITIONS

Belonging to the thesis
Autotaxin, biochemical and functional studies

1- The enzyme autotaxin (ATX) is expressed in breast cancer, but ATX expression levels are not a prognostic factor for clinical outcome *(this thesis)*

2- Activity-dependent probes are useful tools to monitor ATX activity in biological fluids *(this thesis)*

3- The long isoform of ATX (ATXα) contains a unique insertion in the catalytic domain. Cleavage of this insert by furin does not result in loss of activity, but could serve to regulate the interaction between ATXα and heparan sulfate proteoglycans *(this thesis)*

4- Binding of ATXα to heparin suggests a new mechanism for localized LPA production and signaling by binding of ATXα to heparan sulfate proteoglycans at the cell membrane *(this thesis*)

5- Deletion of an 18-amino acid stretch in the catalytic domain of ATX compared to its nucleotide pyrophosphatase/phosphodiesterase (NPP) family members allows the formation of a lysophospholipid binding pocket. The presence of this stretch explains why the NPP1 and NPP3 family members of ATX cannot function as a lysophospholipase *(Hausmann et al, Nat Struct Mol Biol 2011; 18(2): 198-204* and *Nishimasu et al, Nat Struct Mol Biol 2011; 18(2): 205-12)*

6- The rigid interaction between the inactive nuclease domain and the active catalytic domain in the ATX structure is a clever evolutionary solution to maintain stability of the catalytic domain *(Moolenaar & Perrakis, Nat Rev Mol Cell Biol 2011; 12(10): 674-79)*

7- Studies to understand the behavior of tumor cells should not solely focus on the traits of tumor cells, but instead must include the contributions of the tumor environment as well *(Hanahan & Weinberg, Cell 2011; 144(5): 646-74)*

8- Absence of evidence is not evidence of absence (*Altman & Bland, B M J 1995; 311(7003): 485*)

9- Contrary to the expectation that science will reveal one single clear answer, more often than not scientists have to be satisfied with several answers and even more questions as a result

10- The human genome is like a book of 23 chapters (the “chromosomes”) with in total over three billion letters (the “nucleotides”). The fact that we comprehend only around 2% of this text indicates that we have not finished reading yet

11- If you do not learn from your mistakes, you make a mistake *(Johan Cruijff)*

12- The world is a book, and those who do not travel read only one page *(Aurelius Augustine, Roman philosopher, 354-430))*